BIOLOGICAL FUNCTIONS OF DENTIN SIALOPHSPHOPROTEIN IN MINERALIZED TISSUES

A Dissertation

by

PRIYAM HIMANSHU JANI

Submitted to the Office of Graduate and Professional Studies of
Texas A&M University
in partial fulfillment of the requirements for the degree of

DOCTOR OF PHILOSOPHY

Chair of Committee,	Chunlin Qin
Committee Members,	Yongbo Lu
	L.Bruno Ruest
	Philip Kramer
	Peter Buschang
	Xiaofang Wang
Head of Department,	Larry Bellinger

December 2016

Major Subject: Oral Biology

ABSTRACT

Dentin and bone are composed of mineralized extracellular matrices (ECM) produced by their formative cells, odontoblasts and osteoblasts. A major component of their ECM is Collage Type 1, along with numerous non-collagenous proteins (NCPs). Dentin sialophosphoprotein (DSPP) is the major NCP of dentin. Belonging to the SIBLING (Small Integrin-binding ligand, N-linked Glycoprotein) family of proteins, DSPP is primarily associated with mineralized tissues. Expression of DSPP (protein and mRNA) has been reported in dentin, periodontium, alveolar bone, condylar cartilage and several non-mineralized tissues. Upon secretion, DSPP is cleaved into two fragments - dentin sialoprotein (DSP) from the N-terminal region and dentin phosphoprotein (DPP) from the C-terminal region. In humans, DSPP mutations have been linked to non-syndromic inherited dentin diseases, dentinogenesis imperfecta (DGI) and dentin dysplasia (DD). DSPP deletion in mice results in formation of hypomineralized dentin. The dentin defects in the *Dspp* null mice closely resemble the dentin defects of human DGI type III, with widened predentin and irregular dentin mineralization. Although the role of DSPP is critical for the formation of dentin, its role in other hard tissues of the periodontium like alveolar bone and cementum is yet to be studied. Also, previous studies showed that the expression level of DSPP in the rat long bone is approximately 1/400th of that in the rat dentin, however, its role in long bone is not known. This dissertation is a comprehensive effort to outline the function of this protein and its cleaved fragments in periodontium and long bone formation. In the first study, we hypothesized that the

proteolytic cleavage of DSPP into its two fragments is essential to periodontal hard tissue formation. Transgenic mice expressing the uncleavable full-length DSPP but lacking endogenous *Dspp* had severe defects in alveolar bone and cementum. These results indicate that the proteolytic processing of DSPP is crucial for periodontal integrity. Previous studies have demonstrated that the NH2-terminal fragment of DSPP inhibits the formation and mineralization of dentin, while the role of this fragment in periodontium is unclear. In the second study, expressing only the NH2-terminal fragment with the lack endogenous *Dspp* exacerbated the periodontal defects of *Dspp*-null mice. This study indicates that the NH2-terminal fragment of DSPP may exert an inhibitory role in the formation and mineralization of hard tissues in the periodontium. Previous reports showed that transgenic expression of DSPP completely rescued the dentin defects of *Dmp1*-null mice. To investigate if this is true for the long bone defects, we assessed the effects of transgenic DSPP overexpression on osteogenesis by analyzing the formation and mineralization of the long bones in *Dmp*1-null mice that expresses a transgene encoding full-length DSPP. The transgenic DSPP overexpression partially rescued the long bone phenotypic defects of *Dmp*1-null mice. Together, these studies shed new light on the significant function of DSPP in mineralized tissue formation.

DEDICATION

To my parents, family and friends for their love, understanding and support during this long journey and to Dr. Chunlin Qin for his amity and genius in mentorship.

ACKNOWLEDGEMENTS

I would like to thank my mentor Dr. Chunlin Qin. This dissertation could not have been written without his mentoring and direction. During my Ph.D. program, Dr. Qin not only served as my advisor, but he also set high standards in our lab by being an outstanding scientist in this field. I am proud to be one of his students, and I will try to emulate his spirit and persistent drive towards the advancement of science for the rest of my life. My deepest gratitude also to my committee members, Dr. Yongbu Lu, Dr. Philip Kramer, Dr. Bruno Ruest, Dr. Peter Buschang and Dr. Xiaofang Wang for their guidance and support throughout the course of this research.

I sincerely thank my former colleague and friend Dr. Monica Prasad Gibson for her help and encouragement towards my PhD. I was also fortunate to have been guided by Dr. Chao Liu and Dr. Hua Zhang routinely in the lab and throughout my projects. The staff at Baylor including, Nancy Anthony, Marge Palma, Jeanne Santacruz, Darla Benson, Connie Tillberg, Ying Liu, Priscilla Hooks and Gerald Hill have been incredibly patient and helpful to me. Thanks also go to my friends and colleagues and the department faculty for making my time at Texas A&M University College of Dentistry a great experience.

CONTRIBUTORS AND FUNDING SOURCES

This work was supported by a dissertation committee consisting of Professor Dr. Chunlin Qin and Dr. Yongbu Lu, Dr. Philip Kramer, Dr. Bruno Ruest, Dr. Xiaofang Wang of the Department of Biomedical Sciences and Dr. Peter Buschang of the Department of Orthodontics.

Sincere thanks to Dr. Larry Fisher of National Institute of Health for providing the anti-Biglycan antibody (LF-159). Also thanks to Dr. Xiaofang Wang for providing the anti-FGF23 antibody used in the study. All other work conducted for the dissertation was completed by the student independently.

This work was supported by Grant DE005092 and DE022549 from the National Institutes of Health.

NOMENCLATURE

ECM	Extracellular matrix
NCP	Non-collagenous proteins
PDL	Periodontal ligament
HERS	Hertwig's epithelial root sheath
HA	Hydroxyapatite
SIBLING	Small integrin-binding ligand N-linked glycoproteins
DSPP	Dentin Sialophosphoprotein
DMP1	Dentin matrix protein 1
BSP	Bone sialoprotein
MEPE	Matrix extracellular phosphoglycoprotein
OPN	Oetopontin
DGI	Dentinogenesis Imperfecta
DD	Dentin dysplasia
DSP	Dentin Sialoprotein
DSP-PG	Proteoglycan form of DSP
DPP	Dentin Phosphoprotein
μ-CT	Micro-computed tomography
SEM	Scanning electron microscopy
CEJ	Cemento-enamel junction
ARHR	Autosomal recessive hypophosphatemic rickets

FGF23	Fibroblast growth factor 23
RT-qPCR	Real-time quantitative polymerase chain reaction
BV/TV	Ratio of bone volume to the total volume
H&E	Hematoxylin and eosin
FITC	Fluorescein isothiocyanate
IHC	Immunohistochemistry
Tb.N	Trabecular number
Tb.Th	Trabecular thickness
Tb.Sp	Trabecular seperation
GAPDH	Glyceraldehyde-3-phosphate dehydrogenase
EDTA	Ethylenediaminetetraacetic acid
SPSS	Statistical Package for the Social Sciences

TABLE OF CONTENT

Page

LIST OF FIGURES

Page

LIST OF TABLES

Page

CHAPTER I

INTRODUCTION

Mineralization in biological organisms is defined as the process by which these organisms produce minerals. The minerals are formed by normal cellular mechanisms that produce precisely organized structures in organisms ranging from bacteria and algae to bones in vertebrate animals [1, 2]. These biominerals provide support, and play significant roles in defense and feeding mechanisms. The development of endoskeletons improved mobility and mechanical stability in vertebrates. Bones and teeth protect the internal organs, enhance mobility, enable mastication and help organisms perform other functions. They also harbor a multitude of cells and growth factors that, in turn, control tissue properties [3]. Due to their significance, mineralized tissues are central subject of research and numerous studies have tried to understand the mechanisms and fundamental principles governing their development and regulation, and alleviating the disease process affecting these hard tissues.

Mineralized tissues

Mineralized tissues are complex structures consisting of an inorganic mineral phase, an organic phase, and cells. The cells secrete various factors that regulate these structures after formation and control the initial production of these tissues. Much of the vertebrate skeleton is made up of bone. Dentin, enamel and cementum are the other mineralized tissues in vertebrates and form the tooth. Study of the structure and

composition of these tissues may offer a comprehensive understanding of the mineralization process.

Bone

Long bones are made up of an outer cylinder of cortical bone which surrounds a marrow cavity that includes rods of trabecular bone. The organic extracellular matrix (ECM) of bone consists predominantly of a collagen (mostly type I + type III, traces of V, XII, XIV), and lesser amounts of other non-collagenous proteins (NCPs). Three different embryonic cell lineages make up the vertebrate skeleton. The craniofacial bones develop from the cranial neural crest cells, mesodermal cells give rise to the axial skeleton, and the limb skeleton arises from the lateral plate mesodermal cells. In the developing embryo, these cells migrate to where skeletal elements will develop, and differentiate into osteoblasts or chondroblasts to form bone and cartilage respectively [4]. The craniofacial skeleton forms by a process called intramembranous ossification as the neural crest cells directly differentiate into osteoblasts, whereas the remaining skeleton is formed by differentiation of the mesodermal cells into chondrocytes that produces a framework of cartilage of the future bones. The cartilage is subsequently replaced by bone through the process of endochondral ossification [5].

Tooth

The tooth proper consists of a hard, inert, acellular enamel which is supported by the less mineralized, more resilient, and vital hard connective tissue dentin. Dentin is

formed from odontoblasts and supported by the dental pulp which, a soft connective tissue rich in blood vessels and nerve endings [6]. Tooth development starts with a local thickening of the oral ectoderm that induces condensation of the neural-crest-derived mesenchyme [7]. Tooth development progresses through a series of well-defined stages – epithelial thickening, bud, cap and bell and late bell stages. In mouse embryo, a thickening of the oral epithelium is first visible at around E11.5 (embryonic day 11.5). Further invagination of the oral epithelium into the underlying mesenchyme gives rise to the tooth bud. [8, 9]. During the cap stage, around E13.5, the mesenchyme surrounding the bud condenses and expresses a host of signaling molecules and transcription factors [10, 11]. At the tip of the bud, the dental mesenchyme signals and induces the formation of a structure known as the enamel knot. This knot of cells express a host of signaling molecules and are considered as an important signaling center for tooth development [12]. The enamel knot disappears during the transition to the bell stage with the tooth organ cells terminally differentiating. The inner enamel epithelial cells differentiate into ameloblasts and the dental pulp mesenchymal cells into odontoblasts. [13]. Starting at the cusp tips, differentiation of odontoblasts proceeds in a cervical direction [14]. At the onset of the late or advanced bell stage, signals from odontoblasts pass to the overlying epithelium, triggering the terminal differentiation of ameloblasts, an event termed as reciprocal induction [15]. The later stages of tooth development are distinguished by the formation of the mineralized structures: dentin, cementum and enamel. Enamel is the hardest tissue due to its high mineral content and is supported by dentin to compensate for its brittleness. Dentin is a mineralized, elastic, yellow-white, avascular tissue that forms

the bulk of the tooth and encloses the central pulp chamber. Cementum covers the dentin around the root portion of the tooth and provides support for attachment of the periodontal ligament fibers.

Periodontium

In mammals, to withstand the forces of mastication, teeth are attached to the jaw by tooth-supporting tissues consisting of the cementum, periodontal ligament (PDL), and alveolar bone. The periodontium develops following continuing epithelial-mesenchymal interactions between the oral ectoderm and the mesenchymal cells of neural crest origin [6]. The outermost mesenchymal layer of the tooth germ, the dental follicle, gives rise to periodontal structures: cementum, PDL, and alveolar bone [16]. Well-coordinated signaling interactions regulate proper development of the tooth periodontium complex [17]. Root development is initiated by the formation of Hertwig's epithelial root sheath (HERS), a dual membrane of epithelial cells that extends from the cervical loop of the tooth germ [18]. The HERS and dental follicle cells interactions result in the development of periodontium cementoblasts, osteoblasts, and fibroblasts [19, 20]. Fibroblasts give rise to periodontal ligament fibers which anchor into cementum and in alveolar bone [21]. Thus, the mesenchymal cells of the dental follicle give rise to different structures of the periodontium. Synchronization of distinctive differentiation events is crucial for the proper development of the periodontium.

Composition of mineralized tissues

In tooth, type I collagen is the major organic constituent of dentin and cementum, whereas enamel lacks collagen altogether [22]. Inorganic portion of bone and dentin matrices are abundant in hydroxyapatite (HA). HA is also the major constituent of enamel. HA crystals are deposited along the long axes of collagen fibril in the ECM of dentin, bone and cementum. Collagenous and non-collagenous proteins play an important role in regulating the growth and proliferation of these crystals. Many NCPs are phosphorylated, suggesting a role in mineralization process [23-31]. Type III, IV, V and VI collagens have been detected immunohistochemically in odontoblasts [32], but are negligible in dentin matrix [33].

Noncollagenous proteins (NCPs)

The dentin layer produced by odontoblasts has many similarities to bone produced by osteoblasts [34]. Dentin is mainly composed of Collagen type I, occupying 90% of the organic volume whereas NCPs make up the remaining 10%. In the course of conversion of predentin, osteoid, and cementoid into dentin, bone, and cementum, NCPs are believed to play a vital role in controlling the mineralization of collagen fibers and crystal growth. One group of NCPs is the Small Integrin-Binding Ligand N-linked Glycoproteins (SIBLING) family [35]. The SIBLING family consists of five extracellular matrix proteins: dentin sialophosphoprotein (DSPP), dentin matrix protein 1 (DMP-1), bone sialoprotein (BSP), matrix extracellular glycophosphoprotein (MEPE), and osteopontin (OPN). SIBLING family gene cluster is located on human chromosome 4 (mouse

chromosome 5) (4q21). The SIBLING family proteins share several common features [36]. These include multiple phosphorylation sites, a highly acidic nature, the presence of an arginine–glycine–aspartic acid (RGD) integrin binding site, and a proteolytic resistant acidic serine–aspartate-rich MEPE-associated (ASARM) motif [31, 35]. SIBLING proteins are secreted into ECM and are believed to play critical roles in the formation of mineralized tissues [27, 37].

Dentin Sialophosphoprotein

Dentin sialophosphoprotein (DSPP; OMIM*125485) is linked to inherited dentin defects, dentin dysplasia (DD) type II and dentinogenesis imperfecta (DGI) type II and type III [38-46]. DSPP was first cloned from a mouse odontoblast cDNA library and consists of 5 exons and 4 introns (Fig. 1-1). The first exon is non-coding. [47]. The DSPP gene was primarily thought to be expressed in odontoblasts only, but recently its expression has been reported in osteoblasts, salivary glands, sweat glands, lungs, kidneys, and nasal cartilage [48-56]. Animal studies revealed that *Dspp* knock-out (*Dspp*-KO) mice manifest hypomineralization defects in dentin. The dentin defects in the *Dspp*-KO mice closely resemble the dentin defects of human DGI type III, with widened predentin and irregular dentin mineralization [57]. These findings indicate that DSPP is critical for the formation and mineralization of dentin.

DSPP is proteolytically processed into the NH2-terminal and the COOH-terminal fragments [47, 58-60]. The 5′ portion of the DSPP transcript encodes NH2-terminal fragment of DSPP which exists in two forms: the core protein form known as “dentin

sialoprotein" (DSP) and the proteoglycan form referred to as "DSP-PG" [61-64]. The 3′ region of the DSPP transcript encodes the COOH-terminal fragment of DSPP which is referred to as "dentin phosphoprotein" (DPP). The N-terminal core protein form (DSP) accounts for 5–8% of the NCPs in the ECM of rat dentin [30], whereas the proteoglycan form (DSP-PG) appears to be more abundant than DSP [61, 65]. An *in vitro* study showed that matrix metalloproteinases (MMP-2 and MMP-20) cleaved the NH2-terminal portion of porcine DSPP at multiple sites, yielding several low molecular weight fragments [66]. The function of DSP is unclear since it has no significant effect on the formation and growth of HA crystals [67]. *In vivo* studies involving the expression of a transgene encoding the NH2-terminal fragment of DSPP into the *Dspp*-KO background indicate that this fragment might regulate the initiation of dentin mineralization but not the maturation of mineralized dentin [68].

DPP, accounts for as much as 50% of the NCPs in the ECM of rat dentin [69]. It contains large amounts of aspartic acid (Asp) and serine (Ser) residues, with the majority of Ser being phosphorylated (Pse) [24, 70]. The high levels of Asp and Pse make DPP a highly phosphorylated and very acidic protein with the isoelectric point estimated to be 1.1 for rat DPP [71]. DPP is reported to have a high affinity to calcium [26, 28] and is believed to have a direct role in controlling the rate and/or site of dentin mineralization [23, 25, 72]. DPP is an important initiator and modulator in the formation and growth of HA crystals [27, 73, 74].

Although derived from the same mRNA, the remarkable chemical differences between DSP and DPP suggest that these molecular variants may perform different

functions in biomineralization. While significant amounts of DSP, DSP-PG, and DPP are present in the ECM of dentin, the full-length form of DSPP is found in a very minute quantity [75]. The abundance of DSPP fragments, but the lack of full-length DSPP in the dentin, suggests that the individual fragments of DSPP may be the functional forms responsible for its role in mineralization.

Previous *in vitro* studies have shown that bone morphogenetic protein 1 (BMP1)/Tolloid-like metalloproteinases cleave mouse DSPP at the NH2 terminus of Aspartic acid at position 452 (Asp^{452}). Substitutions of Asp^{452} or two residues that are immediately NH2-terminal to Asp^{452}, block the processing of this protein partially or completely [75-77]. The astacin proteases have also been reported to cleave DSPP to generate DPP [78]. Transgenic mice expressing a mutant DSPP in which Asp^{452} was replaced by Alanine (Ala) has been generated; the transgene expressing this mutant DSPP (referred to as "D452A-DSPP") was driven by the 3.6-kb rat *Col1a1* promoter (Fig. 1-2), which allows the expression of this transgene in the bone and dentin. The majority of D452A-DSPP was not cleaved in the bone of the transgenic mice in the wild type background, indicating that the D452A substitution effectively blocked the proteolytic processing of DSPP in the mouse bone [77].

Mineralized tissue disorders associated with DSPP

The changes that may occur in a mineralized tissue in acquired or experimentally induced diseases, inheritable disorders, or in genetically modified animals, can extend our understanding of the role each matrix component plays in the mineralization process. This

is reflected in the studies of congenital diseases which occur mostly due to the absence or mutation of one or more genes.

Nonsyndromic inherited dentin defects have an incidence of one in every 6000 to 8000 individuals [79, 80]. The defects are divided into two groups: dentinogenesis imperfecta (DGI) and dentin dysplasia (DD) [81, 82]. Dentinogenesis imperfecta has an estimated incidence between 1/6000 and 1/8000, and dentin dysplasia 1/100000 [83]. Dentinogenesis imperfecta is classified into three types: one associated with a syndrome osteogenesis imperfecta (DGI type I) and two nonsyndromic (DGI type II and III); also two types of dentin dysplasia (DD type I and II) have been described [38]. Dentinogenesis imperfecta is an autosomal dominant inherited dental disease and is characterized by abnormal dentin production and calcification. DGI type I is seen in patients affected by osteogenesis imperfecta.

Osteogenesis imperfecta is characterized by brittle bones and frequent fractures [84] and is caused by mutations in the genes that code for collagen (COL1A1 and COL1A2).

Periodontitis is an inflammatory disease affecting the periodontium. It is caused by bacterial infection, mainly *Aggregatibacter actinomycetemcomitans* or *Porphyromonas gingivalis*. The main signs of periodontitis are inflammation of gums, loss of epithelial attachment, periodontal pocket formation and excessive alveolar bone resorption, followed by tooth loss [85]. Moreover, several forms of inherited periodontitis are known (aggressive periodontitis/ juvenile periodontitis) [86, 87]. So far, however,

DSPP mutations have not been linked to periodontitis and most of the investigation is typically focused on dentin defects.

Dentin Sialophosphoprotein and Dentin Matrix Protein 1

Dentin matrix protein 1 (DMP1) was initially identified in odontoblasts during embryonic and postnatal development. DMP1 is highly expressed by osteocytes, chondrocytes, and preosteoblasts, unlike DSPP, which is predominantly expressed in odontoblasts [88]. When transgenic DMP1 was expressed using the *Col1a1* promoter on the *Dmp*1 null background, it completely rescued the defects in mineralization, dentinal tubules, and third molar development seen in *Dmp*1 null mice. These defects were not completely rescued in molars when DMP1 was reintroduced using the DSPP promoter on the *Dmp*1 null background [89]. The lack of DMP1 in bone results in decreased mineralization and increased crystal size, suggesting that DMP1 is involved in bone formation and acts as a nucleator of mineralization [90-92]. Transgenic mice overexpressing either full-length DMP1 or a 57-kDa (C-terminal) fragment using the *Col1a1* promoter were generated to test the *in vivo* roles of the C-terminal fragment. Both of the transgenic mice rescued the bone phenotypes of *Dmp1* null mice, suggesting that the 57-kDa C-terminal fragment is able to reiterate the function of intact DMP1 *in vivo* [93]. DMP1 is also reported to regulate *Dspp* gene expression by binding to the *Dspp* promoter directly [94, 95]. Therefore, it is likely that the tooth phenotype of *Dmp*1 null mice is at least partially caused by diminished expression of *Dspp.*

DSPP is believed to have descended from DMP1 by a gene duplication event and share many similarities in both their gene and protein structures [96]. The creation of DSPP by DMP1 duplication event may be crucial to toothed animals to form special mineralized structures [97]. DSPP and DMP1 are both cleaved into two protein chains; the N-terminal regions are glycoslated that contain chondroitin sulfate chains, and the C-terminal regions are highly phosphorylated [63-65, 70, 98, 99]. DSPP and DMP1 both play vital roles in mineralized tissue development. The in *vivo* roles for hard tissue development and mineralization have been characterized by employing many knockout and transgenic mouse models [57, 90, 94, 100, 101].

Conclusion

Role of DSPP in the formation of dentin has been studied extensively, but its role in other hard tissues of the periodontium like alveolar bone and cementum is not yet studied. The expression level of DSPP in bone is much less than in dentin, however, its role in long bone is not known [48]. DSPP has been shown to play an essential role in periodontal tissues. *Dspp* deficient mice manifest severe alveolar bone loss with reduced cementum deposition and altered osteocyte morphology [102]. *In vivo* studies showed that proteolytic processing into fragments is vital for DSPP function in dentinogenesis [103]. It is still unclear whether the proteolytic processing of DSPP is also essential for its biological function in maintaining periodontal health. To evaluate this, transgenic mice expressing the uncleavable full-length DSPP in the *Dspp*-KO background were analyzed. In the first aim of this study, we characterized the alveolar bone and cementum of the mice

expressing the mutant DSPP transgene in comparison with wild-type (WT) mice, *Dspp*-KO mice, and mice expressing the normal DSPP transgene in the *Dspp*-KO background.

DPP is a strong initiator and regulator for the formation and growth of HA crystals [73, 74], while DSP has no significant effects on these crystals [67]. Overexpressing the NH2-terminal fragment of DSPP (including both DSP and DSP-PG) worsened the dentin defects in *Dspp*-KO mice[104], indicating that DSP and/or DSP-PG may inhibit the formation and mineralization of dentin. The second aim of this investigation focuses on the specific roles of the NH2-terminal fragments of DSPP in periodontium, by analyzing the alveolar bone, cementum and periodontal ligaments in the mutant mice overexpressing the NH2-terminal fragment of DSPP but lacking the endogenous *Dspp* gene.

The role of DMP1 in osteogenesis has been studied at length, but function of DSPP in long bones has been studied only to a limited extent. Transgenic expression of DSPP was able to completely reverse the dentin and alveolar bone defects of *Dmp1*-null mice [105]. In the third aim of this investigation, we assessed the effects of transgenic DSPP on bone formation by analyzing the development and mineralization of the long bones in *Dmp1*-null mice that expresses a transgene encoding full-length DSPP driven by a 3.6-kb rat *Col1a1* promoter. Together, these studies shed new light on the significant function of DSPP in mineralized tissue formation

CHAPTER II

FAILURE TO PROCESS DENTIN SIALOPHOSPHOPROTEIN (DSPP) INTO FRAGMENTS LEADS TO PERIODONTAL DEFECTS IN MICE

Synopsis

Dentin sialophosphoprotein (DSPP) is known to play a vital role in dentinogenesis. DSPP in dentin is processed into the NH_2-terminal and COOH-terminal fragments. This proteolytic processing is essential to normal dentinogenesis. Besides its role in tooth formation, recent studies from our laboratory showed that in addition to dentin, DSPP is also highly expressed in the alveolar bone and cementum and that DSPP plays an essential role in maintaining periodontal integrity. In *Dspp* deficient mice, severe periodontal defects were observed, which included alveolar bone loss, decreased cementum deposition, abnormal osteocyte morphology in the alveolar bone, as well as the apical migration of periodontal ligament. It is still unclear whether the proteolytic processing of DSPP is also essential for its biological function in maintaining periodontal health. To evaluate this, we analyzed transgenic mice expressing the uncleavable full-length DSPP in the *Dspp* knockout (*Dspp*-KO) background (referred to as "*Dspp*-KO/D452A-Tg"

---

*Reprinted with permission from "Failure to process dentin sialophosphoprotein into fragments leads to periodontal defects in mice" by MP Gibson, P Jani, Y Liu, X Wang, Y Lu, JQ Feng, C Qin, 2013. European Journal of Oral Science 2013; 121: 545–550, Copyright 2013 by European Journal of Oral Science.

mice). We characterized the alveolar bone and cementum of the Dspp-KO/D452A-Tg mice; in comparison with wild-type (WT) mice, Dspp-KO mice, and mice expressing the normal DSPP transgene in the *Dspp*-KO background (referred to as *Dspp*-KO/normal-Tg mice). Results from this study showed that the expression of the normal DSPP was able to rescue the periodontal defects of the *Dspp*-KO mice, whereas expressing *Dspp*-KO/D452A-Tg failed to do so. These results indicate that the proteolytic processing of DSPP is crucial for periodontal integrity.

Introduction

Dentin sialophosphoprotein (DSPP), first discovered by cDNA cloning in 1997, plays a crucial role in dentinogenesis [39]. It undergoes post-translational modification and is cleaved into the NH_2-terminal fragments [existing in two forms: dentin sialoprotein (DSP) and the proteoglycan form termed DSP-PG] and COOH-terminal fragment [dentin phosphoprotein (DPP) [47, 58, 59]. Genetic studies have shown the association of *DSPP* mutations with dentinogenesis imperfecta (DGI) in humans [41-44, 106-108]. In animal models, *Dspp*-knock out (*Dspp*-KO) exhibits severe dentin hypomineralization defects with widened predentin zone resembling the dentin defects observed in human DGI [57]. These findings strongly suggest the importance of DSPP in the formation and mineralization of dentin.

Besides its established role in tooth formation, DSPP was also discovered in bone, cementum and several non-mineralized tissues [48, 50-52, 54, 109-112]. Its expression in alveolar bone and cementum is remarkably higher than in the long bone [110, 112].

Recent work from our laboratory showed that DSPP plays an essential role in these periodontal tissues [113]. In *Dspp* deficient mice we observed severe alveolar bone loss with reduced cementum deposition and altered osteocyte morphology [113]. The reduction in interdental alveolar bone caused apical migration of periodontal ligaments (PDL) leading to periodontal pockets [113]. *In vivo* studies done by our group showed that proteolytic processing of DSPP is vital for its function in dentinogenesis [103]. However, whether the same mechanism applies in periodontal tissues still remains to be tested. For this purpose, we systematically characterized the alveolar bone and cementum of the following groups of mice: 1) mice expressing the uncleavable D452A-DSPP in the *Dspp*-KO background (named as *Dspp*-KO/D452A-Tg mice); 2) *Dspp*-KO mice; 3) Wild-type (WT) mice and; 4) mice expressing the normal DSPP transgene in the *Dspp*–KO background (referred as *Dspp*-KO/normal-Tg mice). The results from this study showed that expression of normal DSPP was successful in rescuing the periodontal defects of *Dspp*-KO mice. However the transgenic expression of D452A-DSPP was unable to rescue the *Dspp* deficient defects. The findings from from this study provide *in vivo* evidence that the proteolytic processing of DSPP is necessary for maintaining the health of periodontal tissues.

Materials and methods

Mouse generation

Detailed description for the generation of transgenic mice used in this study has been described in our recent reports [103, 114]. Briefly, the D452A-DSPP and the normal

DSPP constructs are downstream to the 3.6-kb rat Col 1a1 promoter. The mouse lines that were crossbred with *Dspp*-KO mice (strain name: B6; 129-Dspptm1Kul/Mmnc; MMRRC, UNC, Chapel Hill, NC) and characterized in our recent study by Zhu et al. [114] were used in this investigation. The mice expressing the D452A-DSPP transgene in the *Dspp*-KO background are referred to as *Dspp*-KO/D452A-Tg mice while those expressing the normal DSPP transgene in the *Dspp*-KO background are called *Dspp*-KO/normal-Tg mice. Primers used for genotyping the transgenic and *Dspp* knockout mice have been described previously [114]. The animal protocols used in this study were approved by the Animal Welfare Committee of Texas A&M Univerisity Baylor College of Dentistry (Dallas, TX). In this study we analyzed the alveolar bone and cementum of the following four groups of mice: *Dspp*-KO/D452A-Tg mice, WT (C57/BL6J) mice, *Dspp*-KO mice and *Dspp*-KO/normal-Tg mice.

Histology

Under anesthesia, 3- and 6-months-old *Dspp*-KO/ D452A-Tg, WT, *Dspp*-KO and *Dspp*- KO/normal-Tg mice were perfused from the ascending aorta with 4% paraformaldehyde in 0.1 M phosphate buffer. The dissected mandibles were then fixed in the same fixative for 24 h, and then decalcified for approximately 2 weeks using the protocols as we previously described [114]. The tissues were then embedded in paraffin, and serial sections of 5 μm were prepared and stained with hematoxylin & eosin (H&E).

Micro-computed tomography (μ-CT)

Samples from the above mentioned four groups of mice at 3- and 6-months of age were analyzed by micro-computed tomography (μ-CT) using a μ-CT35 imaging system (Scanco Medical, Bassersdorf, Switzerland). A high-resolution scan (3.5 μm slice increment) of the alveolar bone in the furcation of the first mandibular molar with a fixed dimension for all samples was performed. The data acquired from five samples per group were used for quantitative analyses using the Student's *t*-test. $p < 0.05$ was considered statistically significant, and the data are presented as mean ± SD.

Backscattered and resin-casted Scanning Electron Microscopy (SEM)

The mandibles from the four groups of mice at 3-months of age were dissected and prepared as we previously described [113]. For backscattered scanning electron microscopy (SEM), the specimens were coated with carbon and examined with a FEI/Philips XL30 Field emission environmental SEM (Philips, Hillsboro, OR, USA). Following this, the surface was acid etched [113], coated with gold and palladium, and examined with SEM.

Results

Failure to process DSPP into fragments leads to alveolar bone defects

Results from the histological analyses showed severe alveolar bone loss with marked increase in inflammatory cells in the furcation region of the first mandibular molar in *Dspp*-KO mice at 3- and 6-months of ages (Figs. 2-1 D and H), when compared to the WT samples of the same ages (Figs. 2-1 A and E). The transgenic expression of D452A-

DSPP was unable to rescue these alveolar bone defects (Figs. 2-1 B and F) and resembled those of the *Dspp*-KO mice (Figs. 2-1 D and H). However, the alveolar bone of *Dspp*-KO/ normal-Tg mice at both ages (Figs. 2-1 C and G) appeared similar to the WT samples (Figs. 2-1 A and E) and hence, the transgenic expression of the normal DSPP was able to reverse the *Dspp* deficient alveolar bone defects to normal.

Results from the μ-CT analyses (Figs. 2-2 A and B) also showed that the transgenic expression of normal DSPP was able to revert the bone volume fraction of *Dspp*-KO mice to a level comparable to the WT mice at both 3-months (Fig. 2-2 A) and 6-months (Fig. 2-2 B) of age, whereas, the expression of D452A-DSPP was unable to achieve the same result.

Failure to process DSPP into fragments leads to loss of epithelium attachment in the interdental region

In the interdental regions between the first and second mandibular molars, the WT (Figs. 2-3 A and E) and *Dspp*-KO/ normal-Tg mice (Figs. 2-3 C and G) showed epithelial attachment at the cemento-enamel junction (CEJ) with healthy interdental alveolar bone deposition at both 3- and 6-months of age. However, in the *Dspp*-KO (Figs. 2-3 D and H) and *Dspp*-KO/ D452A-Tg mice (Figs. 2-3 B and F), the H&E staining showed a remarkable loss of alveolar bone and disruption of periodontal ligaments interdentally, along with the apical migration of the junctional epithelium. The defects in the *Dspp*-KO (Fig. 2-3 H) and *Dspp*-KO/ D452A-Tg mice (Fig. 2-3 F) appeared worse at 6-months of age with the epithelial attachment recessing even more apically than at the age of 3

months.

Failure to process DSPP into fragments leads to decreased cementum deposition

Using backscattered and resin-casted SEM (Fig. 2-4), we observed an overall loss of cementum in the apical region of mandibular first molar in the 3-month-old *Dspp-KO* (Figs. 2-4 D and H) and *Dspp*-KO/ D452A-Tg mice (Figs. 2-4 B and F), when compared with the WT mice of the same ages (Figs. 2-4 A and E). The transgenic expression of normal DSPP in the *Dspp*-KO/ normal-Tg mice (Figs. 2-4 C and G) was able to rescue the loss of cementum to a great extent. The cementum deposition in the *Dspp*-KO/ normal-Tg mice (Figs. 2-4 C and G) still showed some differences from the WT sample (Figs. 2-4 A and E), but was markedly improved when compared with the *Dspp*-KO (Fig. 2-4 D and H) and *Dspp*-KO/ D452A-Tg mice (Fig. 2-4 B and F).

Discussion

Previous *in vivo* experiments showed that the proteolytically processed NH_2-terminal and COOH-terminal fragments (including DSP, DSP-PG, and DPP) of DSPP are the active forms essential for dentinogenesis [114]. In the present study, we analyzed the periodontium of the same mouse lines used in our previous study [114] to examine whether transgenic expression of D452A-DSPP (in which Asp^{452}, a key cleavage-site residue, was replaced by Ala^{452}) or normal-DSPP could rescue the phenotypes observed in alveolar bone and cementum of *Dspp* deficient mice. We found that transgenic expression of normal-DSPP (with no mutation at the cleavage site) was able to rescue the

alveolar and cementum phenotypes in *Dspp*-deficient mice to a level comparable to the WT mice, but the D452A-DSPP transgene failed to do so. These results support that similar to dentinogenesis, the proteolytic processing of DSPP is an activation step, essential for the development and maintenance of the periodontium.

Accumulating evidence suggest that the periodontal defects observed in *Dspp* deficient mice are due to the intrinsic defects in alveolar bone and cementum caused by loss of DSPP function, but are not secondary to the chronic periodontitis. First, *Dspp* is highly expressed in the alveolar bone and cementum [110, 113]; Second, our current study showed that transgenic expression of normal *Dspp* rescued the periodontal defects of *Dspp* deficient mice; Third, detailed analyses showed that the alveolar bone loss occurred independently from and even earlier than chronic periodontitis in these *Dspp* deficient mice (data not shown). However, inflammation may exacerbate the periodontal defects in *Dspp* deficient mice as chronic periodontitis itself also could cause alveolar bone loss and periodontal ligament destruction. Therefore, it remains to be determined whether treatment or prevention of the chronic periodontitis would relieve or rescue the periodontal defects seen in *Dspp* deficient mice.

The present study suggests that the function of DSPP may be mediated by its processed fragments. However, the proteolytic processing of DSPP gives rise to three fragments: DSP, DSP-PG and DPP, each of these may have a specific role in the periodontal tissues. Therefore, it is essential to find out the roles of each of these fragments in the alveolar bone and cementum. We recently found that the NH_2-terminal fragment of DSPP (DSP and DSP-PG) have an inhibitory effect on dentinogenesis [104].

Presumably, DSP and DSP-PG may have similar inhibitory roles in the alveolar bone and cementum. Considering the tooth and periodontal defects of *Dspp* deficient mice, it would be reasonable to point out that the DPP fragment may carry the stimulatory effects on dentinogenesis and periodontal development. In the future, it would be necessary to dissect out that the inhibitory effects are mediated by DSP or DSP-PG or both of them, and to determine whether the stimulatory effects are mediated by the DPP.

CHAPTER III

OVEREXPRESSING THE NH 2-TERMINAL FRAGMENT OF DENTIN SIALOPHOSPHOPROTEIN (DSPP) AGGRAVATES THE PERIODONTAL DEFECTS IN DSPP KNOCKOUT MICE

Synopsis

Previous studies have shown that dentin sialophosphoprotein (DSPP) is not only essential to the formation and mineralization of dentin but also plays an important role in forming and maintaining a healthy periodontium. Under physiological conditions, DSPP is proteolytically processed into the NH_2-terminal and COOH-terminal fragments, and these fragments are believed to perform different functions in the mineralized tissues. Previous studies in our group have demonstrated that the NH_2-terminal fragment of DSPP inhibits the formation and mineralization of dentin, while the role of this fragment in periodontium is unclear. We analyzed the periodontal tissues of the transgenic mice overexpressing the NH_2-terminal fragment of DSPP in the *Dspp* knockout background (referred to as "*Dspp* KO/DSP Tg" mice), in comparison with wild type mice and *Dspp*

---

*Reprinted with permission from "Overexpressing the NH2-terminal fragment of dentin sialophosphoprotein (DSPP) aggravates the periodontal defects in *Dspp* knockout mice" by MP Gibson, P Jani, X Wang, Y Lu, C Qin, 2014. Journal of Oral Biosciences, Volume 56, Issue 4, November 2014, Pages 143-148, Copyright 2014 by Journal of Oral Biosciences.

knockout mice. *Dspp* KO/DSP Tg mice exhibited a greater reduction of the alveolar bone, more remarkably altered canalicular systems around the osteocytes, less cementum, more radical migration of the epithelial attachment towards the apical direction, and more severe inflammation in molar furcation region, than in the *Dspp* knockout mice. Thus, overexpressing the NH_2-terminal fragment of DSPP worsened the periodontal defects in *Dspp* knockout mice, indicating that the NH_2-terminal fragment of DSPP may exert an inhibitory role in the formation and mineralization of hard tissues in the periodontium.

Introduction

Dentin sialophosphoprotein (DSPP) discovered by cDNA cloning using an odontoblast library was intitailly thought to be dentin-specific [37, 47]. Later on, its expression was also found in the long bone, alveolar bone and cementum [48, 115]. Genetic studies have shown an association of DSPP mutations with dentinogenesis imperfecta (DGI) in humans [41-44]. Gene ablation studies revealed that *Dspp* knockout (*Dspp* KO) mice have severe dental defects characterized by dentin hypomineralization, widened predentin zone and enlarged pulp chamber, resembling the tooth defects observed in human DGI [57]. These *in vivo* studies have confirmed the critical role of DSPP in dentinogenesis. A recent study by our group has shown that *Dspp* KO mice develop periodontal diseases manifesting a reduction of alveolar bone, decreased deposition of cementum and altered morphology of osteocytes in the alveolar bone [102]. These recent findings indicate that in addition to its critical role in dentin formation, DSPP is also essential for the formation and maintenance of a healthy periodontium.

Physiologically, DSPP is proteolytically cleaved by astacin proteases into the NH_2-terminal and COOH-terminal fragments [47, 58, 59, 78]. The NH_2-terminal fragments of DSPP exist in the extracellular matrix (ECM) of rat/mouse dentin as two forms, dentin sialoprotein (DSP) and the proteoglycan form of this fragment (DSP-PG); the former has no glycosaminoglycan (GAG) chains while the latter has two GAG chains made of chondroitin-4-sulfate [64, 112]. The COOH-terminal fragment of DSPP is referred to as dentin phosphoprotein (DPP) [64]. Previous studies in our group have established that the posttranslational processing (cleavage) of mouse DSPP at the NH_2-terminus of Asp^{452} is an activation step essential to the formation and mineralization of dentin and alveolar bone [114, 116]. We have shown that the substitution of Asp^{452} by Ala^{452} prevents the cleavage of DSPP into fragments, which subsequently leads to defects in the mouse dentin and periodontium [114, 116].

The exact mechanisms of how the cleaved fragments of DSPP function in the dentin and periodontal tissues remain largely unknown. *In vitro* analyses have shown that DPP is a strong initiator and regulator for the formation and growth of hydroxyapatite crystals [73, 74], while DSP (the NH_2-terminal fragment of DSPP without the GAG chains) has no significant effects on the formation and growth of hydroxyapatite crystals [67]. Recent *in vivo* studies have demonstrated that overexpressing the NH_2-terminal fragment of DSPP (including both DSP and DSP-PG) worsened the dentin defects in *Dspp* KO mice [104], indicating that DSP and/or DSP-PG may inhibit the formation and mineralization of dentin. This investigation focuses on the specific roles of the NH_2-terminal fragments of DSPP in periodontium, by analyzing the alveolar bone, cementum

and periodontal ligaments in the mutant mice overexpressing the NH_2-terminal fragment of DSPP but lacking the endogenous *Dspp* gene. Our results showed that overexpressing the NH_2-terminal fragment of DSPP worsened the periodontal defects in *Dspp* KO mice.

Materials and methods

Generation of transgenic mice overexpressing the NH_2-terminal fragment of DSPP in the Dspp-knockout background (Dspp KO/DSP Tg mice)

Detailed procedures for the generation of transgenic mice overexpressing the NH_2-terminal fragment of DSPP driven by a type I collagen promoter have been described in our previous publication [104]; these transgenic mice are named "DSP Tg mice". We crossbred DSP Tg mice with *Dspp* KO mice obtained from the Mutant Mouse Regional Resource Center (MMRRC, UNC, Chapel Hill, NC), to generate a line of mutant mice that express the transgene encoding the NH_2-terminal fragment of DSPP but lack the endogenous *Dspp*; this line of mutant mice is referred to as "*Dspp* KO/DSP Tg" mice. Detailed information regarding the genotyping primers and the expression level of the transgene can be found in our precious report [104]. We employed histology, micro-computed tomography and scanning electron microscopy to assess the periodontal tissues of *Dspp* KO/DSP Tg mice, in comparison with those of the wild type (WT) and *Dspp* KO mice.

Histology (H&E staining)

For histology analyses, 3-month-old *Dspp* KO/DSP Tg, WT and *Dspp* KO mice

were perfused from the ascending aorta with 4% paraformaldehyde (Sigma Aldrich Corporation, St. Louis, MO) in 0.1 M phosphate buffer. The heads form the sacrificed animals were then fixed in 4% paraformaldehyde for 48 hours and then decalcified in 8% EDTA (pH 7.4) (Sigma Aldrich Corporation, St. Louis, MO) at 4°C for approximately 2 weeks. The dissected mandibles were embedded in paraffin, and serial sections of 5 μm were prepared from these paraffin blocks. The sections were stained with hematoxylin & eosin (H&E) and observed under an Olympus microscope (Olympus BX51, Olympus Corporation, Center Valley, PA USA).

Micro-computed tomography (μ-CT)

We dissected the mandibles from the 3-month-old and 6-month-old WT, *Dspp* KO, and *Dspp* KO/DSP Tg mice (3 mice for each age group; i.e., totally, 6 animals for each type of mice). The mandibles were analyzed using the μ-CT (μ-CT 35 imaging system, Scanco Medical, Basserdorf, Switzerland), as we previously described [114, 117]. We performed high-resolution scans (3.5 μm/slice) and three-dimensional reconstructions to assess the morphological characteristics of the mouse mandibles and to calculate the ratios of alveolar bone volume to total volume (BV/TV), among the three groups of mice at both ages. The BV/TV values were expressed as mean ±SD. Student's t-test was adopted in our statistical analyses to determine the significance levels of differences between two individual groups, using SPSS (SPSS v.17.0, IBM, Somers, NY).

Back scattered and resin-casted scanning electron microscopy (SEM)

For these experiments, the mandibles from 3-month-old mice (n = 3 for each type of mice) were dissected and fixed in 2% paraformaldehyde with 2.5% glutaraldehyde (Sigma Aldrich Corporation, St. Louis, MO) in 0.1 M cacodylate buffer solution (pH 7.4) at room temperature. The detailed protocols used for processing, polishing and coating samples for back scattered and resin-casted SEM (Philips XL30 FEI scanning electron microscope, Philips, Hillsboro, OR, USA) analyses have been described in previous studies [102, 114].

Results

Inflammatory infiltration and migration of epithelial attachment in the periodontium of Dspp KO/DSP Tg mice

Results from H&E staining demonstrated that when compared to the WT controls (Fig. 3-1 A), the furcation region of the mandibular molar in *Dspp* KO mice (Fig. 3-1 B) and *Dspp* KO/DSP Tg mice (Fig. 3-1 C) had obvious inflammatory infiltration. The inflammatory reaction appeared more prevalent and severe in the *Dspp* KO/DSP Tg (Fig. 3-1 C) than in the *Dspp* KO mice (Fig. 3-1 B).

In comparison with the WT mice (Fig. 3-2 A), both types of the mutant mice (Fig. 3-2 B, 3-2 C) showed the detachment and migration of the junctional epithelium, along with the disruption of periodontal ligaments in the interdental region between the mandibular first and second molars. The above defects in the *Dspp* KO/DSP Tg mice (Fig. 3-2 C) were much more severe than in the *Dspp* KO mice (Fig. 3-2 B).

Reduction of alveolar bone in Dspp KO/DSP Tg mice

Results from both H&E staining (Figs. 3-1, 3-2) and μ-CT analyses (Fig. 3-3) showed that the reduction of alveolar bone in the *Dspp* KO/DSP Tg mice was greater than in *Dspp* KO mice. In the H&E-stained sections, *Dspp* KO mice (Fig. 3-1 B) showed a moderate loss of alveolar bone in the furcation region of the first mandibular molar when compared to the WT control (Fig. 3-1 A), while the same region in the *Dspp* KO/DSP Tg mice (Fig. 3-1 C) was completely engulfed with the inflammatory cells and had only a few islands of bone left with the majority of the alveolar bone structures being destroyed.

When the alveolar bone volume fractions (BV/TV) were compared among the three types of mice (Fig. 3-3 A and B), the *Dspp* KO/DSP Tg mice had the least values of BV/TV in either the 3- or 6-month-old age groups. The differences in BV/TV values were statistically significant between the *Dspp* KO and *Dspp* KO/DSP Tg mice at both ages.

Loss of cellular cementum in Dspp KO/DSP Tg mice

Using backscattered and resin-casted SEM approaches (Fig. 3-4), we observed an overall reduction of cellular cementum in the mandibular first molars of the *Dspp* KO (Figs. 3-4 B and 3-4 E) and *Dspp* KO/DSP Tg mice (Figs. 3-4 C and 3-4 F). The periapical region of the mandibular first molars in the *Dspp* KO/DSP Tg mice (Figs. 3-4 C and 3-4 F) had the least amounts of cementum when compared to the WT control (Figs. 3-4 A and 3-4 D) or the *Dspp* KO mice (Figs. 3-4 B and 3-4 E).

Alteration of the osteocyte lacunae and canalicular system in the alveolar bone of Dspp KO/DSP Tg mice

The osteocyte lacunae in the alveolar bone of WT mice were well organized and evenly spaced with most of the canaliculi radiating in directions perpendicular to the long axis of the osteocyte bodies (Fig. 3-5 A). In contrast, the osteocyte lacunae in the alveolar bone of the *Dspp* KO mice appeared irregular with disorganized and fewer canaliculi (Fig. 3-5 B). The osteocyte lacunae in the alveolar bone of *Dspp* KO/DSP Tg mice were extremely disorganized and had very few osteocyte canaliculi (Fig. 3-5 C). The osteocyte canaliculi in the alveolar bone of the *Dspp* KO/DSP Tg mice (Fig. 3-5 C) also had a reduced extension into the surrounding bone compared to *Dspp* KO mice (Fig. 3-5 B). It was apparent that the defects of the osteocyte lacunae and the structures surrounding the lacunae in the alveolar bone of *Dspp* KO/DSP Tg mice were worse than those of the *Dspp* KO mice.

Discussion

DSPP is expressed in dentin, cementum, alveolar bone, long bone and several non-mineralized tissues [54, 64]. Previously, our group showed that the expression level of DSPP in the alveolar bone and cellular cementum is significantly higher than that in the long bone [64, 115]. In the periodontal structures, DSPP was found in the osteocytes of the alveolar bone, cementocytes of cellular cementum in the apical region as well as in the matrices surrounding these mineralized tissue-forming cells [115]. There are a number of reports regarding the biological roles of DSPP and the mechanistic aspects of this protein

in dentinogenesis [41-44, 57, 105, 114], whereas little information is available regarding the biological functions of this molecule in periodontium. Recent work from our group has shown that deletion of DSPP leads to periodontal disease in mice and has established the essential role of this molecule in maintaining the integrity of the periodontium [64]. The current study provides new knowledge about the molecular mechanisms by which DSPP functions in the periodontal tissues.

DSPP is present in the ECM of dentin as three forms found at significant levels [64]: 1) DSP (the NH_2-terminal fragment without GAG chains**,** containing little or no phosphorylation), 2) DSP-PG (the proteoglycan form of the NH_2-terminal fragment, possessing two GAG chains), and 3) DPP (the COOH-terminal fragment, very highly phosphorylated). Based on their differences in chemical property and tissue distribution profiles, these three molecular variants derived from the amino acid sequence of DSPP are believed to play different functions [64, 118]. In this study, we analyzed the specific role of the NH_2-terminal fragment of DSPP in periodontium, using transgenic mice overexpressing this fragment.

We found that overexpressing the NH_2-terminal fragment of DSPP aggravated the periodontal defects in *Dspp* KO mice; the periodontal deterioration in the *Dspp* KO/DSP Tg mice evident in the multipronged analyses included more severe inflammatory infiltration around the alveolar bone, more significantly reduced propagation of the osteocyte processes into surrounding alveolar bone, greater reduction of interradicular and interdental bone, greater loss of cellular cementum, and more radical migration of junctional epithelium towards the apex, in comparison with the *Dspp* KO mice. The

periodontal deteriorations in *Dspp* KO/DSP Tg mice were likely due to more severe defects in the alveolar bone and cementum, which lead to secondary effects (including inflammation) on the periodontal ligament and to the formation of deeper periodontal pockets. The exacerbated abnormality in the morphology of osteocytes and canaliculi in the alveolar bone of *Dspp* KO/DSP Tg mice indicate that the defect of the alveolar bone must be due to intrinsic factors of bone cells associated with the overexpression of the NH_2-terminal fragment of DSPP.

In a previous study, Suzuki et al [68] generated transgenic mice expressing the NH_2-terminal fragment of DSPP driven by the mouse *Dspp* promoter and showed that transgenic expression of this fragment partially rescued the tooth defects in *Dspp*-null mice. We think that the variance between our studies and the previous one may be attributed to the use of different promoters.

The NH_2-terminal fragments of DSPP exist as two forms: DSP and DSP-PG [64]. While the exact ratio of DSP to DSP-PG is unknown, it appears that DSP-PG is a major proteoglycan in the dentin matrix [61, 62, 64]. *In vitro* mineralization analyses showed that DSP has no significant effects on the formation and growth of hydroxyapatite crystals [67] while information regarding the biological roles of DSP-PG is lacking. In this study, overexpressing the NH_2-terminal fragment of DSPP in the type I collagen-expressing tissues (dentin, bone, cementum and periodontal ligaments) aggravated the periodontal defects of *Dspp* KO mice, indicating that the NH_2-terminal fragment of this protein may play an inhibitory role in the formation and mineralization of hard tissues in the periodontium. However, we do not know which of the two molecular species (i.e.,

DSP or DSP-PG) derived from the NH_2-terminal fragment of DSPP is responsible for the exacerbated phenotypic changes in the *Dspp* KO/DSP Tg mice. Future studies are warranted to define which of the two NH_2-terminal forms is exerting the inhibitory functions in the formation and mineralization of hard tissues in the periodontium.

CHAPTER IV

TRANSGENIC EXPRESSION OF *DSPP* PARTIALLY RESCUED THE LONG BONE DEFECTS OF *DMP1*-NULL MICE

Synopsis

Dentin matrix protein 1 (DMP1) and dentin sialophosphoprotein (DSPP) belong to the Small Integrin-Binding Ligand *N*-linked Glycoprotein (SIBLING) family. In addition to the features common to all SIBLING members, DMP1 and DSPP share several unique similarities in chemical structure, proteolytic activation and tissue localization. Mutations in, or deletion of *DMP1*, cause autosomal recessive hypophosphatemic rickets along with dental defects; *DSPP* mutations or its ablation are associated with dentinogenesis imperfecta. While the roles and functional mechanisms of DMP1 in osteogenesis have been extensively studied, those of DSPP in long bones have been studied only to a limited extent. Previous studies by our group revealed that transgenic expression of *Dspp* completely rescued the dentin defects of *Dmp1*-null (*Dmp1*$^{-/-}$) mice. In this investigation, we assessed the effects of transgenic *Dspp* on osteogenesis by analyzing the formation and mineralization of the long bones in *Dmp1*$^{-/-}$ mice that expresses a transgene encoding full-

---

*Reprinted with permission from "Transgenic expression of Dspp partially rescued the long bone defects of Dmp1-null mice" by PH Jani, MP Gibson, C Liu, H Zhang, X Wang, Y Lu, C Qin, 2016. Matrix Biology, Volumes 52–54, May–July 2016, Copyright 2016 by Matrix Biology.

length DSPP driven by a 3.6-kb rat *Col1a1* promoter (referred as "*Dmp1*$^{-/-}$;*Dspp*-Tg mice"). We characterized the long bones of the *Dmp1*$^{-/-}$;*Dspp*-Tg mice at different ages and compared them with those from *Dmp1*$^{-/-}$ and normal control mice. Our analyses showed that the long bones of *Dmp1*$^{-/-}$;*Dspp*-Tg mice had a significant increase in cortical bone thickness, bone volume and mineral density along with a remarkable restoration of trabecular thickness compared to those of the *Dmp1*$^{-/-}$ mice. The long bones of *Dmp1*$^{-/-}$;*Dspp*-Tg mice underwent a dramatic reduction in the amount of osteoid, significant improvement of the collagen fibrillar network, and better organization of the lacunocanalicular system, compared to the *Dmp1*$^{-/-}$ mice. The elevated levels of biglycan, bone sialoprotein and osteopontin in *Dmp1*$^{-/-}$ mice were also noticeably corrected by the transgenic expression of *Dspp*. These findings suggest that DSPP and DMP1 may function synergistically within the complex milieus of bone matrices.

Introduction

The organic components in the extracellular matrix (ECM) of bone are composed of collagen type I and a number of non-collagenous proteins (NCPs). One family of NCPs is the Small Integrin-Binding Ligand N-linked Glycoprotein (SIBLING) family, which consists of osteopontin (OPN), bone sialoprotein (BSP), dentin matrix protein 1 (DMP1), dentin sialophosphoprotein (DSPP) and matrix extracellular phosphoglycoprotein (MEPE) [35]. These SIBLING family members play important biological roles in the formation and mineralization of bone and dentin [35, 119-121], as evidenced by the

observations that mutations in or ablation of their genes are associated with developmental abnormalities in the two tissues [41, 42, 90].

DMP1, first cloned from a rat odontoblast cDNA library, has been identified in dentin, bone and cementum as well as in some non-mineralized tissues [29, 122, 123]. In the appendicular skeleton, DMP1 is expressed by osteocytes, osteoblasts and hypertrophic chondrocytes [124-126]. *Dmp1*-deficient mice displayed severe defects in the cartilage and bone, which resembled the manifestations of autosomal recessive hypophosphatemic rickets (ARHR), a human hereditary disease caused by mutations in the *DMP1* gene. This condition was characterized by the elevation of serum fibroblast growth factor 23 (FGF23) and a reduction of serum phosphorus, along with malformed and hypomineralized bone and dentin [91, 92]. Although DSPP was originally thought to be exclusively expressed by odontoblasts, the dentin-forming cells, later on its expression was detected in bone, cementum and certain non-mineralizing tissues including the salivary glands and kidneys [48, 54, 111, 127]. Our previous studies showed that the expression level of DSPP in the rat long bone is approximately $1/400^{th}$ of that in the rat dentin [48]. Mouse and human genetic studies have associated *DSPP* mutations or its ablation with dentinogenesis imperfecta, characterized by thinner dentin, enlarged pulp chamber and widened predentin [41, 42, 57, 108]. While *Dspp* knockout mice have severe defects in the formation and mineralization of dentin, the changes in the long bones of *Dspp*-deficient mice are mild [101].

Certain pieces of evidence suggest a possible functional relationship between DMP1 and DSPP [96, 122, 127]. The dentin defects in $Dmp1^{-/-}$ mice are similar to those

in *Dspp*$^{-/-}$ mice [57, 94] and the dentin of the *Dmp1*$^{-/-}$ mice has a reduced level of DSPP expression [94]. *In vitro* studies revealed that DMP1 localizes in the nucleus during the differentiation of odontoblasts and is bound to and activates the *Dspp* promoter in odontoblast cell lines [95]. While DMP1 has been shown to play a crucial role in osteogenesis [91, 100, 128] and chondrogenesis [90], *Dspp* ablation in mice or its mutations in human dentinogenesis imperfecta subjects do not cause severe defects in the long bone, although *Dspp*-knockout mice have obvious alveolar bone abnormalities [101, 102]. Previously, we showed that the transgenic expression of *Dspp* rescued the dentin and alveolar bone defects of *Dmp1*$^{-/-}$ mice [105]. To further elucidate the molecular mechanisms by which DMP1 interacts with DSPP in osteogenesis, we systematically characterized the long bones of *Dmp1*$^{-/-}$ mice that express a transgene encoding full-length DSPP driven by a type I collagen promoter to determine whether or how much the transgenic expression of *Dspp* would rescue the long bone defects of *Dmp1*-deficient mice.

Results

In this study, the mice heterozygous for *Dmp1* (*Dmp1*$^{+/-}$) were used as normal controls for comparison, as these mice do not manifest any developmental abnormalities compared to wild type mice [7, 10, 14].

Expression of Dspp in the long bones of normal control, Dmp1$^{-/-}$ and Dmp1$^{-/-}$;Dspp-Tg mice

In order to compare the DSPP expression in the long bones of normal control (*Dmp1*$^{+/-}$), *Dmp1*$^{-/-}$ and *Dmp1*$^{-/-}$;*Dspp*-Tg mice, real-time quantitative polymerase chain reaction (RT-qPCR), immunohistochemical (IHC) staining and *in situ* hybridization (ISH) were performed. RT-qPCR analyses (Fig. 4-1a) showed that the DSPP mRNA level in the long bone of *Dmp1*$^{-/-}$ mice was reduced by approximately one-third compared to the normal control, while the DSPP mRNA level in the long bone of the *Dmp1*$^{-/-}$;*Dspp*-Tg mice was approximately 20-fold greater than that of the normal control. IHC revealed that, compared to the normal control mice (Fig. 4-1b), the long bone of the *Dmp1*$^{-/-}$ mice (Fig. 4-1c) had weaker anti-DSP signals, while the long bone of the *Dmp1*$^{-/-}$;*Dspp*-Tg mice (Fig. 4-1d) demonstrated a much stronger anti-DSP immunoreactivity than either the normal control or the *Dmp1*$^{-/-}$ mice, consistent with the observations of the RT-qPCR analyses. *In situ* hybridization analyses showed that osteoblasts in the trabeculae immediately adjacent to the growth plate area had stronger signals for DSPP mRNA than the cortical bone in diaphysis regions. Compared to the normal controls (Fig. 4-1e), DSPP mRNA was downregulated in the *Dmp1*$^{-/-}$ mice (Fig. 4-1f). The *Dmp1*$^{-/-}$;*Dspp*-Tg mice (Fig. 4-1g) had much elevated level of DSPP mRNA in the same region. These data confirmed the high expression level of the transgenic *Dspp* in the long bone of *Dmp1*$^{-/-}$;*Dspp*-Tg mice.

Transgenic expression of Dspp lengthened the long bones of Dmp1$^{-/-}$ mice

Plain X-ray radiography showed that compared to the femurs of normal 3-month-old controls (*Dmp1*$^{+/-}$, Fig. 4-2a), the femurs of the *Dmp1*$^{-/-}$ mice (Fig. 4-2b) were shorter and had wider metaphyses. The femurs of *Dmp1*$^{-/-}$;*Dspp*-Tg mice (Fig. 4-2c) were longer than those of the *Dmp1*$^{-/-}$ mice, with the metaphyses of the former slightly narrower than the latter. The density of the cortical bone in *Dmp1*$^{-/-}$;*Dspp*-Tg mice also appeared higher than the *Dmp1*$^{-/-}$ mice, indicating a higher level of mineralization in the former than in the latter, which was further confirmed by micro-computed tomographic (μ-CT) analyses (see below). However, the femurs of the *Dmp1*$^{-/-}$*Dspp*-Tg mice were notably shorter than those of the normal controls. At 6 months of age, the femurs of the control mice (Fig. 4-2d) were long and thin with parallel cortical plates; the degree of difference in the femur length between the *Dmp1*$^{-/-}$ mice (Fig. 4-1e) and *Dmp1*$^{-/-}$;*Dspp*-Tg mice (Fig. 4-2f) was similar to the 3-month-old mice, with the proximal and distal metaphyses becoming much narrower in the latter than in the former mice. The density of the femurs in the 6-month-old *Dmp1*$^{-/-}$;*Dspp*-Tg mice, as reflected by radiopacity, was much higher than that of the *Dmp1*$^{-/-}$ mice at the same age, indicating that as the animal aged, the improvement of mineralization by the transgenic *Dspp* further advanced. The quantitative analyses of the changes in femur length (Fig. 4-2g) showed that at 3 months of age, the average femur lengths of the normal control, *Dmp1*$^{-/-}$ and *Dmp1*$^{-/-}$;*Dspp*-Tg mice were 15.6 mm, 11 mm and 12.9 mm, respectively. At 6 months of age, the average femur lengths of the normal control, *Dmp1*$^{-/-}$ and *Dmp1*$^{-/-}$;*Dspp*-Tg mice were 17.6 mm, 13.5 mm and 15 mm, respectively. The femur lengths were reduced to 70% of normal in the *Dmp1*$^{-/-}$ mice,

which increased to 82% of the normal in *Dmp1*$^{-/-}$;*Dspp*-Tg mice at 3 months, an 11% increase in length. At 6 months of age, the femur length increased by 8% in *Dmp1*$^{-/-}$;*Dspp*-Tg mice compared to the *Dmp1*$^{-/-}$ mice. At either age point, the femur length differences between *Dmp1*$^{-/-}$;*Dspp*-Tg and *Dmp1*$^{-/-}$ mice were statistically significant ($P < 0.05$, $n = 5$). The tails of the *Dmp1*$^{-/-}$;*Dspp*-Tg mice were also longer than the those of *Dmp1*$^{-/-}$ mice but were shorter than the normal controls (data not shown).

Transgenic expression of Dspp partially rescued the cortical bone defects in Dmp1*$^{-/-}$ *mice

The three-dimensional imaging evaluation from the low resolution micro-computed tomographic (μ-CT) scans of whole femurs showed that the femurs of the normal control mice had no apparent surface porosities (Fig. 4-3a); the femurs of the *Dmp1*$^{-/-}$ (Fig. 4-3b) and *Dmp1*$^{-/-}$;*Dspp*-Tg mice (Fig. 4-3c) had reduced length and demonstrated a lower mineral content as reflected by the surface porosities at 3 months of age. Although noticeably more porous than the normal controls (Fig. 4-3d), the femurs of *Dmp1*$^{-/-}$;*Dspp*-Tg mice (Fig. 4-3f) had an obvious decrease in porosity at 6 months compared to the *Dmp1*$^{-/-}$ (Fig. 4-3e) mice. In contrast to the smooth and well-organized femurs of the normal control mice (Fig. 4-3g and j), the longitudinal view of the femurs revealed that at both 3 and 6 months of age, those of the *Dmp1*$^{-/-}$ (Fig. 4-3h and k) and *Dmp1*$^{-/-}$;*Dspp*-Tg mice (Fig. 4-3i and l) had inner surface porosities and structural disorganization of the cortical bone.

High-resolution μ-CT scans of the cortical bone in the midshaft region of the femoral diaphysis were done for detailed imaging and quantitative analyses. At either 3 or 6 months of age, the cortical layer of the *Dmp1*$^{-/-}$ mouse femurs (Fig. 4-4b and h) was dramatically thinner than the normal control mice (Fig. 4-4a and g). At 6 months, the cortical thickness of *Dmp1*$^{-/-}$;*Dspp*-Tg mouse femurs (Fig. 4-4c and i) was similar to the normal controls. The quantification of the cortical thickness for 3-month-old (Fig. 4-4d) and 6-month-old (Fig. 4-4j) mice showed that the cortical thickness in the *Dmp1*$^{-/-}$;*Dspp*-Tg mice was restored to nearly the normal level at both ages. The bone volume fraction, expressed as the ratio of bone volume to the total volume (BV/TV), had significantly improved in the femurs of the *Dmp1*$^{-/-}$;*Dspp*-Tg mice at 3 and 6 months of age compared to the *Dmp1*$^{-/-}$ mouse femurs, although the BV/TV ratios in both types of mice were lower than in the normal controls (Fig. 4-4e and k). When the BV/TV of the normal control mice was taken as 1, the BV/TV ratio of *Dmp1*$^{-/-}$ mice was lower than of the normal mice by 23% at 3 months, while that of the *Dmp1*$^{-/-}$;*Dspp*-Tg mice was lower than normal by 13%. At 6 months, the BV/TV ratio of *Dmp1*$^{-/-}$ mice was lower than for the normal mice by 23%, while that of the *Dmp1*$^{-/-}$;*Dspp*-Tg mice was lower by 8%. Based on these data, we calculated that the transgenic expression of *Dspp* rescued the BV/TV reduction of *Dmp1*$^{-/-}$ mice by 42% at 3 months and 63% at 6 months. There was a significant increase in the apparent density and material density of the cortical bone in the *Dmp1*$^{-/-}$;*Dspp*-Tg mouse femurs compared to those of the *Dmp1*$^{-/-}$ mice at 3 months of age (Fig. 4-4f and l). Our calculations revealed that the transgenic expression of *Dspp* rescued the apparent density reduction in the femurs of *Dmp1*$^{-/-}$ mice by 30% at 3 months and 45% at 6 months; it

corrected the material density reduction of *Dmp1*$^{-/-}$ mice by 34% at 3 months and 32% at 6 months. Nevertheless, both the apparent density and material density of the *Dmp1*$^{-/-}$*;Dspp*-Tg mice were still significantly lower than the normal control mice at either time point. These findings indicated that the transgenic expression of *Dspp* significantly increased the bone volume and mineral density of cortical bone of *Dmp1*$^{-/-}$ mice.

The trabecular thickness but not the trabecular number was significantly rescued by the transgenic expression of Dspp

To analyze the trabeculae in these mice, we performed high-resolution μ-CT scans of the femoral distal metaphysis regions. At 3 and 6 months, the trabecular images showed a drastic reduction in trabecular bone in the *Dmp1*$^{-/-}$ mice (Fig. 4-5b and h) compared to the control mice (Fig. 4-5a and g), which was marginally improved in the *Dmp1*$^{-/-}$;*Dspp*-Tg mice (Fig. 4-5c and i). The quantitative analyses revealed that the number of trabeculae in the *Dmp1*$^{-/-}$ mice was lower than for the normal control mice by 58% at 3 months and 53% at 6 months, while that of the *Dmp1*$^{-/-}$;*Dspp*-Tg mice was lower by 53% at 3 months and 42% at 6 months (Fig. 4-5d and j). We calculated that the transgenic expression of *Dspp* rescued the trabecular number reduction of *Dmp1*$^{-/-}$ mice by 8% at 3 months and 21% at 6 months. The trabecular bone thickness in the *Dmp1*$^{-/-}$ mice was greater than for the normal control mice by 40% at 3 months and 24% at 6 months, while that in the *Dmp1*$^{-/-}$;*Dspp*-Tg mice increased by 7% at 3 months and 2% at 6 months (Fig. 4-5e and k) compared to the normal control. At 6 months, the transgenic expression of *Dspp* near completely rescued the trabecular thickening defects of the *Dmp1*$^{-/-}$ mice. The trabecular

separation (spacing) in the *Dmp1*$^{-/-}$ mice was greater than in the normal control mice by 149% at 3 months and 87% at 6 months, while that in the *Dmp1*$^{-/-}$;*Dspp*-Tg mice had increased by 106% at 3 months and 57% at 6 months (Fig. 4-5f and l). For a detailed comparison of the bone parameters, see Tables 1 and 2 (Appendix B) The relatively lower level of rescue for trabecular spacing might be attributed to the limited correction of the trabecular bone numbers as described above (Fig. 4-5d and j).

Transgenic expression of Dspp significantly improved the morphology and ultrastructure of the long bone in Dmp1*$^{-/-}$ *mice

Hematoxylin and eosin (H&E) staining of femurs from 3-month-old mice showed that in comparison with the normal control mice (Fig. 4-6a), the femurs of the *Dmp1*$^{-/-}$ mice (Fig. 4-6b) were shorter and wider, along with presence of irregular trabeculae. There was a remarkably improved development of the trabecular bone network in the *Dmp1*$^{-/-}$;*Dspp*-Tg mice (Fig. 4-6c) compared to the *Dmp1*$^{-/-}$ mice. The overly-widened growth plate (red arrows) in the *Dmp1*$^{-/-}$ mice was reversed to a nearly normal thickness in the *Dmp1*$^{-/-}$;*Dspp*-Tg mice. The reduced thickness of the cortical bone in the *Dmp1*$^{-/-}$ mice (Fig. 4-6e) was also reversed in the *Dmp1*$^{-/-}$;*Dspp*-Tg mice (Fig. 4-6f) to a level similar to that of the normal control mice (Fig. 4-6d). Also, the cortical bone of *Dmp1*$^{-/-}$ mice (Fig. 4-6e) had numerous areas that were hypomineralized or osteoid-like (arrow heads). To assess the collagen structure of the cortical bone, we performed Picrosirius red staining and visualized the collagen fibers under polarized light. When examined under polarized light, the larger collagen fibers were bright yellow or orange, and the thinner ones,

including reticular fibers, were green. Compared to the normal control mice (Fig. 4-6g), the collagen fiber network in the cortical bone of the *Dmp1*$^{-/-}$ mice (Fig. 4-6h) appeared disorganized and sparse. The collagen fiber organization in the femoral cortical bone *of the Dmp1*$^{-/-}$;*Dspp*-Tg mice (Fig. 4-6i) had remarkably improved, although it was not as well oriented and dense as in the normal control mice. The results of histological evaluation provided further support to the conclusion drawn from the μ-CT data regarding the restoration of cortical bone thickness and structural organization.

To further confirm the partial rescue of the *Dmp1*-deficient defects by the *Dspp* transgene, we analyzed the osteocyte lacunocanalicular system of the femurs using the resin-casted scanning electron microscopy (SEM) approach. The osteocyte lacunae (red arrows) in the femurs of the normal control mice (Fig. 4-7a) were spindle-shaped, while the osteocyte lacunae in the *Dmp1*$^{-/-}$mice (Fig. 4-7b) appeared enlarged, which was probably due to an accumulation of osteoid in the bone of these mice. The lacunae in the *Dmp1*$^{-/-}$;*Dspp*-Tg mice (Fig. 4-7c) were smaller than those in the *Dmp1*$^{-/-}$mice but larger than in the normal controls. Acid-etched SEM imaging showed that the osteocytes in the *Dmp1*$^{-/-}$mice (Fig. 4-7e) exhibited a marked decrease in the number of canaliculi (red asterisks). The canaliculi in the long bones of the *Dmp1*$^{-/-}$;*Dspp*-Tg mice (Fig. 4-7f) were more numerous than in the *Dmp1*$^{-/-}$mice, but were not as well oriented as in the normal control mice (Fig. 4-7d). Fluorescein isothiocyanate (FITC) is a fluorescent stain that binds to the osteocytes and canaliculi but not to the mineralized matrix. Thus, it helps to visualize the unaltered cellular structure of osteocytes. The FITC staining showed well-organized and evenly spaced osteocytes with well oriented canaliculi in the normal control

mice (Fig. 4-7g). The osteocytes in the *Dmp1*$^{-/-}$mice (Fig. 4-7h) were round to ovoid and had a marked reduction in the number of canaliculi. The *Dmp1*$^{-/-}$;*Dspp*-Tg mice (Fig. 4-7i) exhibited smaller osteocytes than the *Dmp1*$^{-/-}$mice with a significant rise in the number of canaliculi although they were not as well oriented as in the normal controls. Thus, the *Dspp* transgene partially corrected the lacunocanalicular defects of the *Dmp1*-deficient mice.

The transgenic expression of Dspp partially corrected the altered levels of certain ECM molecules

Immunohistochemistry (IHC) results confirmed the presence of DMP1 signals around the osteocyte lacunae and in the bone ECM of the normal control mice (Fig. 4-8a) and its loss in *Dmp1*$^{-/-}$ mice (Fig. 8b) and *Dmp1*$^{-/-}$;*Dspp*-Tg mice (Fig. 4-8c). Biglycan is present in the unmineralized matrix (osteoid), and anti-biglycan IHC is often used to reveal osteoid [129]. The anti-biglycan IHC analyses showed remarkably increased biglycan in the matrix of the cortical bone of *Dmp1*$^{-/-}$ mice (Fig. 4-8e). The matrix of the *Dmp1*$^{-/-}$;*Dspp*-Tg mice (Fig. 4-8f) had much less biglycan (osteoid) than the *Dmp1*$^{-/-}$ mice, but more than the normal control mice (Fig. 4-8d). These findings substantiated the improved mineralization of the *Dmp1*$^{-/-}$;*Dspp*-Tg mouse long bones. The levels of BSP, OPN and MEPE were higher in the long bones of the *Dmp1*$^{-/-}$ mice (Fig. 4-8h,k and n) while the levels of these proteins in the long bones of the *Dmp1*$^{-/-}$;*Dspp*-Tg mice (Fig. 4-8i, l and o) were only slightly more elevated than those of the normal control mice (Fig. 4-8g, j and m). Compared to the normal control mice (Fig. 4-8p), the FGF23 level was elevated in the

Dmp1$^{-/-}$ mice (Fig. 4-8q), and the FGF23 level in the *Dmp1*$^{-/-}$;*Dspp*-Tg mice (Fig. 4-8r) was slightly lower than in the *Dmp1*$^{-/-}$ mice, and higher than in the normal control.

The RT-qPCR analyses showed that the BSP mRNA level (Fig. 4-9a) was elevated by 9 folds while that of the OPN (Fig. 4-9b) increased to 11 folds in *Dmp1*$^{-/-}$ mice compared to that of the normal control. The mRNA levels of both BSP and OPN in the *Dmp1*$^{-/-}$;*Dspp*-Tg mice were reduced to close to normal. The mRNA level of MEPE (Fig. 4-9c), which increased to about 5 folds in *Dmp1*$^{-/-}$ mice, was restored to normal in the *Dmp1*$^{-/-}$;*Dspp*-Tg mice. Similarly, the collagen Type 1 alpha 1 (Col1a1) expression (Fig. 4-9d) was reduced almost to the normal level in *Dmp1*$^{-/-}$;*Dspp*-Tg mice.

The i*n situ* hybridization analyses demonstrated relatively strong signals for DMP1, BSP, OPN and Col1a1 mRNAs in osteoblasts (arrows in Fig. 4-10) of the newly formed bone immediately subjacent to the epiphyseal growth plates in the normal mice. There was a complete lack of DMP1 mRNA in the *Dmp1*$^{-/-}$ (Fig. 4-10b) and *Dmp1*$^{-/-}$;*Dspp*-Tg mice (Fig. 4-10c), consistent with the immunohistochemistry results. In agreement with the immunohistochemistry and RT-qPCR data, the *in situ* hybridization analyses showed that compared to the normal controls (Fig. 4-10d and g), the BSP and OPN mRNA levels were higher in the *Dmp1*$^{-/-}$ mice (Fig. 4-10e and h), whereas the levels of these molecules in the *Dmp1*$^{-/-}$;*Dspp*-Tg mice (Fig. 4-10f and i) were similar to those of the normal mice. The Col1a1 mRNA level was also higher in the *Dmp1*$^{-/-}$ mice (Fig. 4-10k) than in the normal controls (Fig. 4-10j), while the Col1a1 level in *Dmp1*$^{-/-}$;*Dspp*-Tg mice (Fig. 4-10l) was similar to the normal controls.

Discussion

DMP1 and DSPP share several unique similarities [48, 112, 121]. Both are cleaved by bone morphogenetic protein 1/tolloid-like metalloproteinases into their NH_2-terminal and COOH-terminal fragments [75, 77, 123, 130, 131]. Their NH_2-terminal fragments mainly exist as proteoglycans [61, 64, 99], whereas their COOH-terminal fragments are highly phosphorylated and promote mineralization [73, 132]. They show similar localization patterns in bone and tooth [133, 134]. Additionally, *Dmp1*-null mice and *Dspp*-null mice manifest similar dentin defects [57, 94]. These striking similarities between DMP1 and DSPP indicate that these two molecules may have synergistic or redundant roles in the formation and mineralization of hard tissues.

While the role of DMP1 in osteogenesis has been extensively studied, the function of DSPP has been studied only to a limited extent. The loss of *Dspp* in mice leads to an age-related mineralization defect; however, the abnormalities in the long bone of the *Dspp*-deficient mice are mild [101]. Recently, we showed that the transgenic expression of DSPP completely rescued the dentin and alveolar bone defects of *Dmp1*$^{-/-}$ mice but failed to correct the elevated level of serum FGF23 and the reduction of serum phosphorus level in the *Dmp1*-deficient animals [105]. The *in vitro* luciferase assay studies by our group and others revealed that DMP1 enhanced the promoter activity of the *Dspp* gene in odontoblast-like cells or C3H10T1/2 mesenchymal cells transfected with DMP1-expressing constructs [95, 105]. These findings indicate that DSPP may be a downstream target of DMP1 during the formation of dentin and alveolar bone.

In this study, we observed that the transgenic expression of *Dspp* led to the significant rescue of the long bone defects in *Dmp1*-null mice. While the introduction of transgenic *Dspp* into the *Dmp1*-deficient background led to a remarkable correction of the long bone defects caused by *Dmp1* ablation, the impact of transgenic *Dspp* on different bone parameters reflecting various aspects of bone quality were divergent. The transgenic expression of DSPP rescued the bone volume reduction and hypomineralization defects in the cortical bone to a much greater extent than the correction of the trabecular number loss in the metaphysis region of *Dmp1*-deficient femurs. DMP1 plays broader roles than DSPP; the former is involved in gene regulation, FGF23 dynamics and phosphorus metabolism, in addition to mineralization-promoting effect, while the latter primarily participates in the matrix mineralization aspect of dentinogenesis and osteogenesis. The trabecular bone number is the most important indicator regarding the healthy status of trabeculae. The trabecular bones in the metaphysis region undergo faster remodeling and have a greater turnover rate than the cortical bone. Thus the formation of trabecular bones in this region may be more vulnerable to alterations of factors such as a reduction of the serum phosphorus level than is the cortical bone, which may be partially responsible for the observation that the rescue of trabecular number loss was not as significant as that of the cortical bones in the *Dmp1*$^{-/-}$;*Dspp*-Tg mice.

In addition to the cortical and trabecular bone changes, the partial restoration of the osteocyte defects by the *Dspp* transgenic expression was also significant. The number and orientation of canaliculi and the osteocyte morphology in the *Dmp1*$^{-/-}$;*Dspp*-Tg mice showed a remarkable improvement over the *Dmp1*$^{-/-}$ mice. Our immunohistochemistry,

RT-qPCR and *in situ* hybridization analyses of BSP, OPN and MEPE showed that all these molecular markers were elevated in the *Dmp1*$^{-/-}$ mice, but returned to levels close to normal in *Dmp1*$^{-/-}$;*Dspp*-Tg mice, suggesting that the osyeocyte maturation may have been rescued to a certain extent.

Both DMP1 and DSPP are acidic proteins that can attract Ca^{2+} and promote the formation and growth of hydroxyapatite (HA) crystals on the collagen matrix, facilitating the conversion of osteoid to bone and predentin to dentin [29, 121, 127, 128, 132, 135]. We speculate that DSPP's role in promoting the deposition of HA crystals as a redundant partner of DMP1 is the principal factor contributing to the improved quality of the long bone in *Dmp1*$^{-/-}$;*Dspp*-Tg mice.

Previously, we showed that the transgenic expression of DSPP completely rescued the alveolar bone defects in *Dmp1*-null mice [105], while in this study, the same transgene partially rescued the long bone defects of the *Dmp1*$^{-/-}$ mice. The differences in the extent of the improvement between the alveolar bone and the long bone could be attributed to the following aspects. 1) The forming alveolar bone cells originate from the neural crest, which is from the ectoderm, while the osteoblasts of the long bone are from the mesoderm. 2) The DSPP expression level in alveolar bone is much higher than in the long bone [48, 136]. 3) The alveolar bone defects in *Dspp*-null mice [102] are much more severe than the long bone defects [101], suggesting that DSPP's role in alveolar bone formation is more important than in the long bone. Clearly, future studies are warranted to elucidate the mechanisms by which the DMP1 and DSPP function differently in the formation of alveolar bone and long bone.

DSPP is proteolytically processed into NH_2-terminal and COOH-terminal fragments. *In vitro* studies have revealed that the COOH-terminal fragment of DSPP promotes the formation and growth of HA crystals [74, 135]. *In vivo* studies by our group showed that transgenic expression of *Dspp* NH_2-terminal fragment failed to rescue the dentin and alveolar bone defects in *Dspp*-null mice [137]. Future studies are warranted to define which of the individual fragments derived from DSPP is responsible for correcting the long bone defects of *Dmp1*-null mice.

In summary, the transgenic expression of DSPP partially, but not completely, rescued the long bone defects of *Dmp1*-null mice, without a correction of serum FGF23 elevation and serum phosphorus reduction. DMP1 and DSPP are likely to have redundant roles in promoting the deposition of HA crystals during osteogenesis, which may be responsible for the significant improvement of long bone quality in *Dmp1*$^{-/-}$;*Dspp*-Tg mice.

Materials and methods

Generation of Dmp1$^{-/-}$*;Dspp-Tg mice*

The generation of mice expressing a transgene encoding the full-length form of DSPP has been described in our previous reports [77]. In these transgenic mice, the DSPP transgene is downstream to the 3.6-kb rat *Col 1a1* promoter that drives the expression of the transgene in type I collagen-expressing tissues, including bone. The transgenic mouse line showing the highest level of DSPP mRNA [35] in the long bone in the wild type background was crossbred with the *Dmp1*$^{-/-}$ mice [90, 94] to create mice that express the

transgenic *Dspp* but lack *Dmp1*; these mice were referred to as "*Dmp1*$^{-/-}$;*Dspp*-Tg mice". The genotyping approach and primers for identifying the *Dmp1*-null alleles and *Dspp* transgene were described previously [105]. The animal protocols related to this study were approved by the Animal Welfare Committee of Texas A&M University Baylor College of Dentistry (Dallas, TX, USA). The mice heterozygous for *Dmp1* (Dmp1$^{+/-}$) of corresponding ages were used as normal controls for all experiments as these mice do not manifest any developmental abnormalities compared to the wild type mice [7, 10, 14].

Real Time Quantitative Polymerase Chain reaction (RT-qPCR)

The RT-qPCR analyses were performed to measure the mRNA levels of DSPP, BSP, OPN, MEPE and COL1a1 in the mouse long bone. Total RNA was extracted from the femurs of the 12-week-old mice of each group, treated with DNase I (Promega, Madison, WI), and purified with the RNeasy Mini Kit (Qiagen, Inc., Valencia, CA). The RNA (1 µg/ml per sample) was transcribed into cDNA by SuperScript III reverse transcriptase (Invitrogen, San Diego, CA). Specific primers and conditions used for the RT-qPCR analyses are listed in Table 3 (Appendix B). The housekeeping gene, glyceraldehyde-3-phosphate dehydrogenase (GAPDH), was used as the internal control. The RT-qPCR reactions were performed using the Brilliant SYBR Green QPCR Master Mix (Applied Biosystems; Foster City, CA) and the CFX-96 Real-Time PCR Detection System (Bio-Rad; Hercules, CA). The mean values from triplicate analyses were then calculated and compared.

Plain X-ray radiography and Micro-computed tomography (μ-CT)

The femurs from the hind limbs of 3- and 6-month-old male mice were dissected and analyzed with a Faxitron MX-20 specimen radiography system (Faxitron X-ray Corp., Buffalo Grove, IL). The measurement tool of the Faxitron software was used to measure the femur lengths using five femurs from five mice in each group (n = 5). The mean and standard deviation values from five measurements were used for quantitative comparison. For the μ-CT analyses, the femurs were scanned using a μ-CT 35 imaging system (Scanco Medical, Basserdorf, Switzerland). The μ-CT analyses included: 1) a low-resolution scan (7.2 μm slice increment) of the whole femur from the 3-month-old and 6-month-old male mice for an overall assessment of the shape and structure; 2) a high-resolution scan (3.4 μm slice increment) of the femoral midshaft region (midway between the two epiphyses along the cranio-caudal axis, 200 slices) for analysis of the cortical bone in the 3-month-old and 6-month-old male mice; 3) a high-resolution scan (3.4 μm slice increment) of the femoral metaphysis region proximal to the distal growth plate for evaluation of the trabecular bones in the 3- and 6-month-old male mice. For trabecular bone analyses, we selected a cylinder area in the center of the metaphysis region with a radius of 100 μm and a length of 1400 μm (400 slices); the cortical shell was excluded in these trabecular bone analyses. The cortical thickness was measured using the Scanco software, and the averages were obtained from five femurs of five mice in each group (n = 5). Every 20^{th} slice from the high-resolution scans of the femoral midshaft region of each sample were analyzed for cortical thickness. The data acquired from the high-resolution scans were used for quantitative analyses. The quantitative μ-CT parameters obtained and analyzed using the

Scanco software included: ratio of bone volume to total volume (BV/TV), apparent density, material density, trabecular number (Tb.N), trabecular thickness (Tb.Th), and trabecular separation (Tb.Sp). Six femurs from six mice in each group were used for quantitative analyses of BV/TV, apparent density, material density, Tb.N, Tb.Th, and Tb.Sp.

Tissue preparation and histological evaluation

Under anesthesia, the *Dmp1*$^{+/-}$, *Dmp1*$^{-/-}$ and *Dmp1*$^{-/-}$;*Dspp*-Tg mice at postnatal 6 weeks and 3 months were perfused from the ascending aorta with 4% paraformaldehyde in 0.1 M phosphate-buffered saline. The femurs were dissected and further soaked in the same fixative for 48 h, followed by demineralization in 14% EDTA (pH 7.4) at 4°C for 2 weeks. The tissues were processed for paraffin embedding, and serial 5-μm sections were prepared. The sections were stained with hematoxylin and eosin (H&E) for routine histology analyses; these paraffin sections were also used for immunohistochemistry and *In situ* hybridization analyses (see later). Picrosirius Red staining [138] was performed to assess the morphology and organization of the collagen fibrils.

Scanning Electron Microscopy (SEM)

The tibias of 3-month-old mice from each group were dissected and fixed in 2% paraformaldehyde and 2.5% glutaraldehyde in 0.1 m cacodylate buffer solution (pH 7.4) at room temperature. Four hours later, the samples were immersed in 0.1 m cacodylate solution. The samples were then dehydrated in ascending concentrations of ethanol and

embedded in methyl-methacrylate (MMA) resin. Microcloths with Metadi Supreme polycrystalline diamond suspensions of decreasing sizes (Buehler, Lake Bluff, IL) were used to polish the sample surfaces. The samples were coated with carbon for backscattered SEM analyses. For the resin-casted SEM, the samples were acid-etched with 37% phosphoric acid for 2–10 seconds and washed with 5.25% sodium hypochlorite for 5 minutes. The samples were then coated with gold and palladium for secondary electron image analyses. A JEOL JSM-6300 scanning electron microscope (JEOL Limited, Tokyo, Japan) was used to perform the analyses as reported previously [91].

Fluorescein Isothiocyanate (FITC) staining

FITC, a small molecular dye, fills in the osteocyte lacunae and canaliculi, but does not stain the mineralized matrix. Thus, the dye provides a visual representation of the organization of the octeocytes and their lacunocanalicular system under a confocal microscope [139]. The tibias from each group of 3-month-old mice were dissected and dehydrated through a series of ethanol solutions from 70–100% and acetone solution, followed by 1% FITC stain (Sigma-Aldrich, St. Louis, MO) overnight, with additional dehydration and MMA embedding as described above. A cross section (500 μm thick) from the tibial midshaft region was cut with a diamond-bladed saw (Buehler), and the plastic sections were then sanded and ground to a final thickness of 30-50 μm for confocal imaging using the Leica SP2 confocal microscope (Leica TCS, Germany).

Immunohistochemistry (IHC) and generation of monoclonal anti-FGF23 antibody

For the immunohistochemistry analyses, anti-DSP-2C12.3 monoclonal antibody [115] was used at a concentration of 2.05 μg/ml. Anti-DMP1 monoclonal antibody that recognizes the C-terminal region of DMP1 [134, 136] was used at a concentration of 4.7 μg/ml. Anti-biglycan polyclonal antibody LF-159 [140] was used at a dilution of 1:1000. Anti-BSP monoclonal antibody 10D9.2 [118] was used at a concentration of 4.5 μg/ml. Polyclonal anti-OPN antibody [141] was used at a dilution of 1:400. Anti-MEPE polyclonal antibody (Santa Cruz Biotechnology, Inc., Santa Cruz, CA) was used at a concentration of 2.1 μg/ml.

Recently, we generated anti-FGF23 monoclonal antibodies which recognize both human and mouse FGF23. Briefly, five BALB/c mice were immunized with the full-length human recombinant FGF23 using a Bac-to-Bac baculovirus expression system (Invitrogen) as we previously reported [142], and the immunization boosting was given every 3 weeks for a total of four times (Creative Biolabs, Shirley, NY). The titers of serum anti-FGF23 antibodies were determined with an enzyme-linked immunosorbent assay. One of the five mice that showed the highest titer for the anti-FGF23 activity was given a final boosting and sacrificed for cell fusion; the splenocytes from this mouse were fused with FO murine myeloma cells. The fusion cells showing positive reactions to FGF23 were screened with the Omni Hybridoma Platform (Creative Biolabs) and cloned. After testing 207 single clones, we obtained 15 positive clones. Western immunoblotting analyses in our laboratory revealed that the cultural media (supernatants) from three positive clones (hybridoma cell lines) including Clone 79 showed strong reactions to both

human and mouse FGF23. Clone 79 with the IgG isotype was expanded in syngeneic mice; the ascites were collected from these mice and the "anti-FGF23-79 antibody" was isolated from the ascites by HiTrap rProtein A FF (Creative Biolabs). We further confirmed the immunoreactivity of purified anti-FGF23-79 antibody to both human and mouse recombinant FGF23 by Western immunoblotting analyses. Our IHC analyses with long bone samples from *Dmp1*$^{+/-}$ and *Dmp1*$^{-/-}$ mice revealed that anti-FGF23-79 antibody gave rise to highly specific signals in the osteocyte lacunae and the matrices around osteocytes, and the anti-FGF23 immunoreactivity was remarkably stronger in the *Dmp1*$^{-/-}$ mouse bone than in the *Dmp1*$^{+/-}$ mouse bone. The anti-FGF23-79 antibody at 2.75 μg/ml concentration was used for IHC analyses in the current study.

All the IHC experiments were carried out using the mouse on mouse kit for monoclonal antibodies and the ABC kit for polyclonal antibodies (Vector Laboratories, Burlingame, CA). The 3, 3′-diaminobenzidine (DAB) kit (Vector Laboratories) was used for color development according to the manufacturer's instructions.

In situ hybridization

In situ hybridization was performed to assess the mRNA levels of DSPP, DMP1, BSP, OPN and COL1a1 in the femurs of 6-week-old mice for each group. Detailed information regarding the RNA probes for DSPP [127], DMP1 [127], BSP [143], OPN [143] and COL1a1 [91] has been described previously. The RNA probes were labeled with digoxigenin using a RNA labeling kit (Roche, Indianapolis, IN) and were detected by an enzyme-linked immunoassay with a specific anti-digoxigenin-alkaline phosphatase

antibody conjugate and alkaline phosphatase substrate (Roche), following the manufacturer's instructions. Nuclear fast red was used for counterstaining.

Statistical analysis

The data analyses were performed with a one-way analysis of variance for multiple group comparisons. If significant differences were found with the one-way analysis of variance, the Bonferroni method was used to determine which groups were significantly different from others. The quantified results were expressed as the mean ± S.D. $P \leq 0.05$ was considered to be statistically significant.

CHAPTER V

CONCLUSION

A multitude of studies have focused on the mineral-matrix relationship in bones and teeth. Dentin and bone are complex structures that consist of hydroxyapatite crystals deposited in an orchestrated manner on an organic matrix scaffold. In organic phase of ECM of these hard tissues, Noncollagenous proteins (NCPs) are found tightly associated with collagen. Among the NCPs, the SIBLING family of proteins are the most widely studied. DSPP, a member of the SIBLING family, is the most abundant NCP present in the ECM of dentin. In dentin and bone, DSPP is mainly present as the processed amino (NH2) terminal (including DSP and DSP-PG) and carboxy (COOH) terminal fragment, DPP. Despite of being derived from the same gene and protein precursor, their biochemical properties of DSP and DPP are very different. DSP is rich in sialic acid, is a glycoprotein and has few or no phosphate groups [37, 144]. It shares overall characteristics with the other sialoproteins, Osteopontin and Bone sialoprotein. DPP is the most abundant NCP in the ECM of dentin, accounting for as much as 50% of the NCPs [69]. DPP contains a large number of aspartic acid (Asp) and serine (Ser) residues [24, 70]. The repeating sequences of aspartic acid and phosphorylated serine make DPP highly acidic and negative which fits well with its function in the hydroxyapatite crystal growth and formation.

There are a total of 36 novel DSPP mutations reported so far that cause inherited dentin defects [46]. These mutations are transmitted in an autosomal dominant pattern and fall into two groups. In both cases, the mutant protein is retained in the rough endoplasmic

reticulum (rER) and hence fails to effectively traffic out of the cell [145]. *Dspp* null mice display severe tooth defects due to widened predentin and dentin hypomineralization [57], which closely mimic the signs of human DGI type III. Expression of DSPP in odontoblasts is reported to be higher during primary dentinogenesis than during secondary dentinogenesis, suggesting DSPP plays more significant role during odontoblast differentiation and primary dentinogenesis [146].

Along with its established role in tooth formation, DSPP has also been identified in bone, cementum and several non-mineralized tissues. Its expression in alveolar bone and cementum is remarkably higher than in the long bone [110]. DSP and DPP, the two cleaved fragments of DSPP, are the active forms essential for its function during dentinogenesis [114]. In the first study, we analyzed the periodontium of mice expressing the mutated DSPP transgene [114] to examine whether mutated DSPP (in which Aspartic acid, was replaced by Alanine at position 452) or normal-DSPP could rescue the phenotypes observed in alveolar bone and cementum of *Dspp*-KO mice. Transgenic expression of normal DSPP was able to rescue the alveolar and cementum phenotypes in *Dspp*-KO mice, but the mutated DSPP transgene failed to do so. Thus, during dentinogenesis, the cleavage of DSPP is an activation step, essential for the development and maintenance of the periodontium. This study suggests that the function of DSPP may be mediated by its processed fragments. However, the proteolytic processing of DSPP gives rise to three fragments: DSP, DSP-PG and DPP, each of these may have a specific role in the periodontal tissues. The N-terminal fragment of DSPP (DSP and DSP-PG) may

have an inhibitory effect on dentinogenesis [87]. It is therefore necessary to find out the roles played by each of these fragments in hard tissues.

The phenotype of *Dspp*-KO mice helps us understand the significance of DSPP, however, the individual roles of DSP or DPP in dentin mineralization remain elusive. In the periodontal structures, DSPP was found in the osteocytes of the alveolar bone, cementocytes of cellular cementum in the apical region as well as in the matrices surrounding these mineralized tissue-forming cells [110]. DSPP has been shown to play an essential role in periodontal tissue formation [102]. *Dspp*-KO mice had severe alveolar bone loss with reduced cementum deposition and altered osteocyte morphology. Transgenic mice, in which only DSP is expressed in a *Dspp*-KO background have been generated utilizing the *Col1a1* promoter[104]. In the second study, we analyzed the specific role of the NH2-terminal fragment of DSPP in periodontium, using transgenic mice overexpressing this fragment. We found that, in comparison to *Dspp*-KO mice, mice overexpressing the NH_2-terminal fragment of DSPP had severe inflammatory infiltration around the alveolar bone, significantly reduced osteocyte processes, greater reduction of interradicular and interdental bone, greater loss of cellular cementum, and more severe migration of junctional epithelium towards the apex. A recent report has demonstrated that DSP can act as a ligand and binds to integrin β6 [147]. Immunoprecipitation assays revealed that integrin β6 was bound by the 112 amino acid residues aa183-295 of DSP, protein-protein interaction assays indicated that only 36 amino acid residues of the DSP domain aa183-219 could bind to integrin β6. The NH2-terminal fragments of DSPP exist as two forms: DSP and DSP-PG [64]. The exact ratio of DSP to DSP-PG is unknown,

however, it is reported that DSP-PG is a major proteoglycan in the dentin matrix [61, 62, 64]. In this study, the worsening of periodontal defects of *Dspp*-KO mice overexpressing the NH2 terminal fragment, indicates that the NH2-terminal fragment of this protein may play an inhibitory role in the formation and mineralization of hard tissues in the periodontium. However, future studies are warranted to define which of the two NH2-terminal forms is exerting these inhibitory functions.

Dspp-KO mice displayed only subtle changes in the long bone, most likely because of its lower expression in bone as compared to dentin [101]. DPP is clearly important for undifferentiated mesenchymal and osteoblastic cells to differentiate into mature odontoblasts and/or osteoblasts [148]. By activation of the MAPK pathway recombinant DPP is able to induce osteogenic differentiation in osteoblastic cells and mesenchymal stem cells [149, 150]. In the same study, DPP stimulated phosphorylation of Smad-1 and induced expression of osteoblastic and odontoblastic differentiation markers. This suggests that DPP activates Smad-1 via integrin signaling independently of BMP signaling [151].

Function of DSPP in osteogenesis has been studied only to a limited extent. Transgenic expression of DSPP completely rescued the dentin and alveolar bone defects of *Dmp1*-null mice but failed to correct their altered serum FGF23 and phosphate levels [105]. *Dmp1* enhanced the promoter activity of the *Dspp* gene in odontoblast-like cells or mesenchymal cells *in vitro* [95, 105]. This means that DSPP may be a downstream target of DMP1 during the formation of dentin and alveolar bone.

In our third study, we observed that the transgenic expression of DSPP led to the significant rescue of the long bone defects in *Dmp1*-null mice. While the introduction of transgenic DSPP into the *Dmp1*-deficient background led to a remarkable correction of the long bone defects caused by *Dmp1* deletion, the impact of transgenic DSPP on different bone parameters was different. The transgenic expression of DSPP rescued the bone hypomineralization defects in the cortical bone to a much greater extent than the correction of the trabecular bone defects in *Dmp1*-deficient mice. DMP1 has been shown to play broader in gene regulation, phosphate metabolism, in addition to mineralization-promoting effect, while DSPP has only been reported to participate in mineralization aspect of dentinogenesis and osteogenesis. In addition to the cortical and trabecular bone changes, the partial restoration of the osteocyte defects by the DSPP transgenic expression was also significant. A recent report showed recombinant DSP upregulates type I collagen and DSPP expression in non-odontogenic osteoblasts, induces bone formation in *ex vivo* bone culture, at least in part by stimulating osteoblast cell growth and differentiation levels, thereby providing a mechanism for DSP induced anabolic effects on bone [152].

A vital number of questions regarding DSPP still need to be addressed. The role of the proteoglycan form of N-terminal fragment (DSP-PG) is yet to be elucidated. Does the N-terminal fragment facilitate DSPP protein folding and/or secretion? Why are these biochemically and functionally diverse fragments transcribed from the same gene. Minute quantity of full-length DSPP has been isolated from bone and dentin recently, however it's unclear if it is the remainder of the uncleaved fragments or if it plays a specific function [153, 154]. Regulatory mechanisms for the gene expression of DSPP Still need to be

further studied. Also, DMP-1 directly induced DSPP gene expression and DSPP overexpression compensated for lack of DMP1 in mice and rescued the dentin defects completely and long bone defects partially [89, 95, 105]. Thus, DMP1 and DSPP may have synergistic roles not only during dentinogenesis, but also during osteogenesis. In order to answer these questions, studies on intracellular transport of DSPP, its precursor synthesis, and transport to ECM via the ER and golgi apparatus need to be studied in detail. A complete understanding of these mechanisms can help us elaborate the basic understanding of mineralization process during dentinogenesis and osteogenesis and can lead to development of new biomedical applications for alleviating mineralized tissue diseases.

REFERENCES

[1] Mann S, Heywood B, Rajam S, Wade V. Molecular recognition in biomineralization. Mechanisms and phylogeny of mineralization in biological systems: Springer; 1991. p. 47-55.

[2] Lowenstam HA. Minerals formed by organisms. Science. 1981;211:1126-31.

[3] Glimcher MJ. Molecular biology of mineralized tissues with particular reference to bone. Reviews of Modern Physics. 1959;31:359-93.

[4] Hall BK, Miyake T. The membranous skeleton: the role of cell condensations in vertebrate skeletogenesis. Anatomy and Embryology. 1992;186:107-24.

[5] Mundlos S, Olsen BR. Heritable diseases of the skeleton. Part I: Molecular insights into skeletal development-transcription factors and signaling pathways. The FASEB Journal. 1997;11:125-32.

[6] Tencate AR, Mills C. The development of the periodontium: The origin of alveolar bone. The Anatomical Record. 1972;173:69-77.

[7] Thesleff I, Hurmerinta K. Tissue interactions in tooth development. Differentiation. 1981;18:75-88.

[8] Mina M, Kollar EJ. The induction of odontogenesis in non-dental mesenchyme combined with early murine mandibular arch epithelium. Archives of Oral Biology. 1987;32:123-7.

[9] Tucker AS, Sharpe PT. Molecular genetics of tooth morphogenesis and patterning: The right shape in the right place. Journal of Dental Research. 1999;78:826-34.

[10] Satokata I, Maas R. Msx1 deficient mice exhibit cleft palate and abnormalities of craniofacial and tooth development. Nature Genetics. 1994;6:348-56.

[11] Peters H, Neubuser A, Kratochwil K, Balling R. Pax9-deficient mice lack pharyngeal pouch derivatives and teeth and exhibit craniofacial and limb abnormalities. Genes & Development. 1998;12:2735-47.

[12] Vaahtokari A, Åberg T, Jernvall J, Keränen S, Thesleff I. The enamel knot as a signaling center in the developing mouse tooth. Mechanisms of Development. 1996;54:39-43.

[13] Ruch JV, Lesot H, Karcher-Djuricic V, Meyer JM, Olive M. Facts and hypotheses concerning the control of odontoblast differentiation. Differentiation. 1982;21:7-12.

[14] Thesleff I, Keranen S, Jernvall J. Enamel knots as signaling centers linking tooth morphogenesis and odontoblast differentiation. Advances in Dental Research. 2001;15:14-8.

[15] Karcher-Djuricic V, Staubli A, Meyer J-M, Ruch J-V. Acellular dental matrices promote functional differentiation of ameloblasts. Differentiation. 1985;29:169-75.

[16] Diep L, Matalova E, Mitsiadis TA, Tucker AS. Contribution of the tooth bud mesenchyme to alveolar bone. Journal of Experimental Zoology Part B: Molecular and Developmental Evolution. 2009;312B:510-7.

[17] Tucker A, Sharpe P. The cutting-edge of mammalian development; how the embryo makes teeth. Nature Reviews Genetics. 2004;5:499-508.

[18] Tummers M. Root or crown: a developmental choice orchestrated by the differential regulation of the epithelial stem cell niche in the tooth of two rodent species. Development. 2003;130:1049-57.

[19] Cho M-I, Garant PR. Development and general structure of the periodontium. Periodontology 2000. 2000;24:9-27.

[20] Diekwisch T. Pathways and fate of migratory cells during late tooth organogenesis. Connective Tissue Research. 2002;43:246-56.

[21] Lekic P, McCulloch CAG. Periodontal ligament cell populations: The central role of fibroblasts in creating a unique tissue. The Anatomical Record. 1996;245:327-41.

[22] Seyer J, Slavkin H. The comparative molecular biology of extracellular matrices. Academic Press, New York; 1972.

[23] Veis A, Perry A. The phosphoprotein of the dentin matrix. Biochemistry. 1967;6:2409-16.

[24] Lee SL, Veis A, Glonek T. Dentin phosphoprotein: an extracellular calcium-binding protein. Biochemistry. 1977;16:2971-9.

[25] Dimuzio MT, Veis A. Phosphophoryns—major noncollagenous proteins of rat incisor dentin. Calcified Tissue Research. 1978;25:169-78.

[26] Zanetti M, Bernard B, Jontell M, Linde A. Ca2+-binding studies of the phosphoprotein from rat-incisor dentine. European Journal of Biochemistry. 1981;113:541-5.

[27] Linde A. Dentin matrix proteins: Composition and possible functions in calcification.The Anatomical Record. 1989;224:154-66.

[28] Marsh ME. Binding of calcium and phosphate ions to dentin phosphophoryn. Biochemistry. 1989;28:346-52.

[29] George A, Sabsay B, Simonian PA, Veis A. Characterization of a novel dentin matrix acidic phosphoprotein. Implications for induction of biomineralization. Journal of Biological Chemistry. 1993;268:12624-30.

[30] Butler WT. Dentin matrix proteins and dentinogenesis. Connective Tissue Research. 1995;33:59-65.

[31] Butler WT, Ritchie H. The nature and functional significance of dentin extracellular matrix proteins. International Journal of Developmental Biology. 1995;39:169-79.

[32] Bronckers A, Lyaruu D, Wöltgens J. Immunohistochemistry of extracellular matrix proteins during various stages of dentinogenesis. Connective Tissue Research. 1989;22:691-6.

[33] Nagata K, Huang YH, Ohsaki Y, Kukita T, Nakata M, Kurisu K. Demonstration of type III collagen in the dentin of mice. Matrix. 1992;12:448-55.

[34] Butler WT, Mikulski A, Urist MR, Bridges G, Uyeno S. Noncollagenous proteins of a rat dentin matrix possessing bone morphogenetic activity. Journal of Dental Research. 1977;56:228-32.

[35] Fisher LW, Fedarko NS. Six genes expressed in bones and teeth encode the current members of the SIBLING family of proteins. Connective Tissue Research. 2003;44:33-40.

[36] Fisher LW, Torchia DA, Fohr B, Young MF, Fedarko NS. Flexible structures of SIBLING proteins, Bone sialoprotein, and Osteopontin. Biochemical and Biophysical Research Communications. 2001;280:460-5.

[37] Butler WT. Dentin matrix proteins. European Journal of Oral Sciences. 1998;106:204-10.

[38] Shields ED, Bixler D, el-Kafrawy AM. A proposed classification for heritable human dentine defects with a description of a new entity. Archives of Oral Biology. 1973;18:543-53.

[39] MacDougall M, Simmons D, Luan X, Gu TT, DuPont BR. Assignment of dentin sialophosphoprotein (DSPP) to the critical DGI2 locus on human chromosome 4 band q21.3 by in situ hybridization. Cytogenetic and Genome Research. 1997;79:121-2.

[40] MacDougall M. Refined mapping of the human dentin sialophosphoprotein (DSPP) gene within the critical dentinogenesis imperfecta type II and dentin dysplasia type II loci. European Journal of Oral Sciences. 1998;106:227-33.

[41] Xiao S, Yu C, Chou X, Yuan W, Wang Y, Bu L, Fu G, Qian M, Yang J, Shi Y, Hu L, Han B, Wang Z, Huang W, Liu J, Chen Z, Zhao G, Kong X. Dentinogenesis imperfecta 1 with or without progressive hearing loss is associated with distinct mutations in DSPP. Nature Genetics. 2001;27:201-4.

[42] Zhang XH, Zhao J, Li CF, Gao S, Qiu CC, Liu P, Wu GY, Qiang BQ, Lo WHY, Shen Y. DSPP mutation in dentinogenesis imperfecta Shields type II. Nature Genetics. 2001;27:151-2.

[43] Rajpar MH, Koch MJ, Davies RM, Mellody KT, Kielty CM, Dixon MJ. Mutation of the signal peptide region of the bicistronic gene DSPP affects translocation to the endoplasmic reticulum and results in defective dentine biomineralization. Human Molecular Genetics. 2002;11:2559-65.

[44] Kim JW, Nam SH, Jang KT, Lee SH, Kim CC, Hahn SH, Hu JCC, Simmer JP. A novel splice acceptor mutation in the DSPP gene causing dentinogenesis imperfecta type II. Human Genetics. 2004;115.

[45] Kim J-W, Hu JC-C, Lee J-I, Moon S-K, Kim Y-J, Jang K-T, Lee S-H, Kim C-C, Hahn S-H, Simmer JP. Mutational hot spot in the DSPP gene causing dentinogenesis imperfecta type II. Human Genetics. 2004;116:186-91.

[46] Yang J, Kawasaki K, Lee M, Reid BM, Nunez SM, Choi M, Seymen F, Koruyucu M, Kasimoglu Y, Estrella-Yuson N, Lin BPJ, Simmer JP, Hu JCC. The dentin phosphoprotein repeat region and inherited defects of dentin. Molecular Genetics & Genomic Medicine. 2016;4:28-38.

[47] MacDougall M, Simmons D, Luan X, Nydegger J, Feng J, Gu TT. Dentin phosphoprotein and Dentin sialoprotein are cleavage products expressed from a single transcript coded by a gene on human chromosome 4: Dentin phosphoprotein DNA sequence determination. Journal of Biological Chemistry. 1997;272:835-42.

[48] Qin C, Brunn JC, Cadena E, Ridall A, Tsujigiwa H, Nagatsuka H, Nagai N, Butler WT. The expression of dentin sialophosphoprotein gene in bone. Journal of Dental Research. 2002;81:392-4.

[49] Qin C, Brunn JC, Cadena E, Ridall A, Butler WT. Dentin sialoprotein in bone and dentin sialophosphoprotein gene expressed by osteoblasts. Connective Tissue Research. 2003;44:179-83.

[50] Ogbureke KUE, Fisher LW. Expression of SIBLINGs and their partner MMPs in salivary glands. Journal of Dental Research. 2004;83:664-70.

[51] Ogbureke KUE, Fisher LW. Renal expression of SIBLING proteins and their partner matrix metalloproteinases (MMPs). Kidney International. 2005;68:155-66.

[52] Alvares K, Kanwar YS, Veis A. Expression and potential role of dentin phosphophoryn (DPP) in mouse embryonic tissues involved in epithelial–mesenchymal interactions and branching morphogenesis. Developmental Dynamics. 2006;235:2980-90.

[53] Ogbureke KUE, Fisher LW. SIBLING expression patterns in duct epithelia reflect the degree of metabolic activity. Journal of Histochemistry & Cytochemistry. 2007;55:403-9.

[54] Prasad M, Zhu Q, Sun Y, Wang X, Kulkarni A, Boskey A, Feng JQ, Qin C. Expression of dentin sialophosphoprotein in non-mineralized tissues. Journal of Histochemistry & Cytochemistry. 2011;59:1009-21.

[55] Zhang R, Chen F-M, Zhao S-L, Xiao M-Z, Smith AJ, Feng JQ. Expression of dentine sialophosphoprotein in mouse nasal cartilage. Archives of Oral Biology. 2012;57:607-13.

[56] Liu Q, Gibson MP, Sun H, Qin C. Dentin sialophosphoprotein (DSPP) plays an essential role in the postnatal development and maintenance of mouse mandibular condylar cartilage. Journal of Histochemistry & Cytochemistry. 2013;61:749-58.

[57] Sreenath T, Thyagarajan T, Hall B, Longenecker G, D'Souza R, Hong S, Wright JT, MacDougall M, Sauk J, Kulkarni AB. Dentin sialophosphoprotein knockout mouse teeth display widened predentin zone and develop defective dentin mineralization similar to human dentinogenesis imperfecta type III. Journal of Biological Chemistry. 2003;278:24874-80.

[58] Gu K, Chang S, Ritchie HH, Clarkson BH, Rutherford RB. Molecular cloning of a human dentin sialophosphoprotein gene. European Journal of Oral Sciences. 2000;108:35-42.

[59] Ritchie HH, Wang L-H, Knudtson K. A novel rat 523 amino acid phosphophoryn: nucleotide sequence and genomic organization. Biochimica et Biophysica Acta (BBA) - Gene Structure and Expression. 2001;1520:212-22.

[60] Feng JQ, Luan X, Wallace J, Jing D, Ohshima T, Kulkarni AB, D'Souza RN, Kozak CA, MacDougall M. Genomic organization, chromosomal mapping, and promoter analysis of the mouse dentin sialophosphoprotein (dspp) gene, which codes for both dentin sialoprotein and dentin phosphoprotein. Journal of Biological Chemistry. 1998;273:9457-64.

[61] Qin C, Brunn JC, Baba O, Wygant JN, McIntyre BW, Butler WT. Dentin sialoprotein isoforms: detection and characterization of a high molecular weight dentin sialoprotein. European Journal of Oral Sciences. 2003;111:235-42.

[62] Yamakoshi Y, Hu JC, Fukae M, Iwata T, Kim JW, Zhang H, Simmer JP. Porcine dentin sialoprotein is a proteoglycan with glycosaminoglycan chains containing chondroitin 6-sulfate. The Journal of Biological Chemistry. 2005;280:1552-60.

[63] Sugars RV, Olsson M-L, Waddington R, Wendel M. Substitution of bovine dentine sialoprotein with chondroitin sulfate glycosaminoglycan chains. European Journal of Oral Sciences. 2006;114:89-92.

[64] Zhu Q, Sun Y, Prasad M, Wang X, Yamoah AK, Li Y, Feng J, Qin C. Glycosaminoglycan chain of dentin sialoprotein proteoglycan. Journal of Dental Research. 2010;89:808-12.

[65] Yamakoshi Y, Hu JCC, Fukae M, Iwata T, Kim JW, Zhang H, Simmer JP. Porcine dentin sialoprotein is a proteoglycan with glycosaminoglycan chains containing chondroitin 6-sulfate. Journal of Biological Chemistry. 2004;280:1552-60.

[66] Yamakoshi Y, Hu JC-C, Iwata T, Kobayashi K, Fukae M, Simmer JP. dentin sialophosphoprotein is processed by MMP-2 and MMP-20 in vitro and in vivo. Journal of Biological Chemistry. 2006;281:38235-43.

[67] Boskey A, Spevak L, Tan M, Doty SB, Butler WT. Dentin sialoprotein (DSP) has limited effects on in vitro apatite formation and growth. Calcified Tissue International. 2000;67:472-8.

[68] Suzuki S, Sreenath T, Haruyama N, Honeycutt C, Terse A, Cho A, Kohler T, Müller R, Goldberg M, Kulkarni AB. Dentin sialoprotein and dentin phosphoprotein have distinct roles in dentin mineralization. Matrix Biology. 2009;28:221-9.

[69] MacDougall M, Zeichner-David M, Slavkin HC. Production and characterization of antibodies against murine dentine phosphoprotein. Journal of Biochemistry. 1985;232:493-500.

[70] Butler WT, Bhown M, DiMuzio MT, Cothran WC, Linde A. Multiple forms of rat dentin phosphoproteins. Archives of Biochemistry and Biophysics. 1983;225:178-86.

[71] Jonsson M, Fredriksson S, Jontell M, Linde A. Isoelectric focusing of the phosphoprotein of rat-incisor dentin in ampholine and acid pH gradients. Journal of Chromatography A. 1978;157:235-42.

[72] Dickson IR, Dimuzio MT, Volpin D, Ananthanarayanan S, Veis A. The extraction of phosphoproteins from bovine dentin. Calcified Tissue Research. 1975;19:51-61.

[73] Boskey AL, Maresca M, Doty S, Sabsay B, Veis A. Concentration-dependent effects of dentin phosphophoryn in the regulation of in vitro hydroxyapatite formation and growth. Bone and Mineral. 1990;11:55-65.

[74] Saito T, Arsenault AL, Yamauchi M, Kuboki Y, Crenshaw MA. Mineral induction by immobilized phosphoproteins. Bone. 1997;21:305-11.

[75] Sun Y, Lu Y, Chen S, Prasad M, Wang X, Zhu Q, Zhang J, Ball H, Feng J, Butler WT, Qin C. Key Proteolytic Cleavage Site and Full-length Form of DSPP. Journal of Dental Research. 2010;89:498-503.

[76] von Marschall Z, Fisher LW. Dentin sialophosphoprotein (DSPP) is cleaved into its two natural dentin matrix products by three isoforms of bone morphogenetic protein-1 (BMP1). Matrix Biology. 2010;29:295-303.

[77] Zhu Q, Prasad M, Kong H, Lu Y, Sun Y, Wang X, Yamoah A, Feng JQ, Qin C. Partial Blocking of Mouse DSPP processing by substitution of Gly451–Asp452 bond suggests the presence of secondary cleavage site(s). Connective Tissue Research. 2012;53:307-12.

[78] Tsuchiya S, Simmer JP, Hu JC, Richardson AS, Yamakoshi F, Yamakoshi Y. Astacin proteases cleave dentin sialophosphoprotein (Dspp) to generate dentin phosphoprotein (Dpp). Journal of Bone and Mineral Research. 2011;26:220-8.

[79] Witkop C. Hereditary defects in enamel and dentin. Human Heredity. 1957;7:236-9.

[80] Aplin HM, Hirst KL, Crosby AH, Dixon MJ. Mapping of the human dentin matrix acidic phosphoprotein gene (DMP1) to the dentinogenesis imperfecta type II critical region at chromosome 4q21. Genomics. 1995;30:347-9.

[81] Hart PS, Hart TC. Disorders of human dentin. Cells Tissues Organs. 2007;186:70-7.

[82] Barron MJ, McDonnell ST, MacKie I, Dixon MJ. Hereditary dentine disorders: dentinogenesis imperfecta and dentine dysplasia. Orphanet Journal of Rare Diseases. 2008;3:31.

[83] Witkop Jr CJ. Hereditary defects of dentin. Dental Clinics of North America. 1975;19:25-45.

[84] Plotkin H. Syndromes with congenital brittle bones. BMC Pediatrics. 2004;4:16.

[85] Roberts HC, Moseley R, Sloan AJ, Youde SJ, Waddington RJ. Lipopolysaccharide alters decorin and biglycan synthesis in rat alveolar bone osteoblasts: consequences for bone repair during periodontal disease. European Journal of Oral Sciences. 2008;116:207-16.

[86] Saxén L, Nevanlinna HR. Autosomal recessive inheritance of juvenile periodontitis: test of a hypothesis. Clinical Genetics. 1984;25:332-5.

[87] Marazita ML, Burmeister JA, Gunsolley JC, Koertge TE, Lake K, Schenkein HA. Evidence for autosomal dominant inheritance and race-specific heterogeneity in early-onset periodontitis. Journal of Periodontology. 1994;65:623-30.

[88] Narayanan K, Ramachandran A, Hao J, He G, Park KW, Cho M, George A. Dual Functional Roles of Dentin Matrix Protein 1: Implications in biomineralization and gene transcription by activation of intracellular Ca2+ store. Journal of Biological Chemistry. 2003;278:17500-8.

[89] Lu Y, Ye L, Yu S, Zhang S, Xie Y, McKee MD, Li YC, Kong J, Eick JD, Dallas SL, Feng JQ. Rescue of odontogenesis in Dmp1-deficient mice by targeted re-expression of DMP1 reveals roles for DMP1 in early odontogenesis and dentin apposition in vivo. Developmental Biology. 2007;303:191-201.

[90] Ye L, Mishina Y, Chen D, Huang H, Dallas SL, Dallas MR, Sivakumar P, Kunieda T, Tsutsui TW, Boskey A, Bonewald LF, Feng JQ. Dmp1-deficient mice display severe defects in cartilage formation responsible for a chondrodysplasia-like phenotype. The Journal of Biological Chemistry. 2005;280:6197-203.

[91] Feng JQ, Ward LM, Liu S, Lu Y, Xie Y, Yuan B, Yu X, Rauch F, Davis SI, Zhang S, Rios H, Drezner MK, Quarles LD, Bonewald LF, White KE. Loss of DMP1 causes rickets and osteomalacia and identifies a role for osteocytes in mineral metabolism. Nature Genetics. 2006;38:1310-5.

[92] Farrow EG, Davis SI, Ward LM, Summers LJ, Bubbear JS, Keen R, Stamp TCB, Baker LRI, Bonewald LF, White KE. Molecular analysis of DMP1 mutants causing autosomal recessive hypophosphatemic rickets. Bone. 2009;44:287-94.

[93] Lu Y, Qin C, Xie Y, Bonewald LF, Feng JQ. Studies of the DMP1 57-kDa functional domain both in vivo and in vitro. Cells Tissues Organs. 2009;189:175-85.

[94] Ye L, MacDougall M, Zhang S, Xie Y, Zhang J, Li Z, Lu Y, Mishina Y, Feng JQ. Deletion of dentin matrix protein-1 leads to a partial failure of maturation of predentin into dentin, hypomineralization, and expanded cavities of pulp and root canal during postnatal tooth development. Journal of Biological Chemistry. 2004;279:19141-8.

[95] Narayanan K, Gajjeraman S, Ramachandran A, Hao J, George A. Dentin matrix protein 1 regulates dentin sialophosphoprotein gene transcription during early odontoblast differentiation. Journal of Biological Chemistry. 2006;281:19064-71.

[96] Fisher LW. DMP1 and DSPP: Evidence for duplication and convergent evolution of two sibling proteins. Cells Tissues Organs. 2011;194:113-8.

[97] McKnight DA, Fisher LW. Molecular evolution of dentin phosphoprotein among toothed and toothless animals. BMC Evolutionary Biology. 2009;9:1-16.

[98] Huq NL, Cross KJ, Talbo GH, Riley PF, Loganathan A, Crossley MA, Perich JW, Reynolds EC. N-terminal sequence analysis of bovine dentin phosphophoryn after conversion of phosphoseryl to S-propylcysteinyl residues. Journal of Dental Research. 2000;79:1914-9.

[99] Qin C, Huang B, Wygant JN, McIntyre BW, McDonald CH, Cook RG, Butler WT. A chondroitin sulfate chain attached to the bone dentin matrix protein 1 NH2-terminal fragment. The Journal of Biological Chemistry. 2006;281:8034-40.

[100] Ling Y, Rios HF, Myers ER, Lu Y, Feng JQ, Boskey AL. DMP1 depletion decreases bone mineralization in vivo: An FTIR imaging analysis. Journal of Bone and Mineral Research. 2005;20:2169-77.

[101] Verdelis K, Ling Y, Sreenath T, Haruyama N, MacDougall M, van der Meulen MCH, Lukashova L, Spevak L, Kulkarni AB, Boskey AL. DSPP effects on in vivo bone mineralization. Bone. 2008;43:983-90.

[102] Gibson MP, Zhu Q, Liu Q, D'Souza RN, Feng JQ, Qin C. Loss of dentin sialophosphoprotein leads to periodontal diseases in mice. Journal of Periodontal Research. 2013;48:221-7.

[103] Zhu Q, Prasad M, Kong H, Lu Y, Sun Y, Wang X, Yamoah A, Feng JQ, Qin C. Partial blocking of mouse DSPP processing by substitution of Gly451–Asp452 bond suggests the presence of secondary cleavage site(s). Connective Tissue Research. 2011;53:307-12.

[104] Gibson MP, Liu Q, Zhu Q, Lu Y, Jani P, Wang X, Liu Y, Paine ML, Snead ML, Feng JQ, Qin C. Role of the NH 2 -terminal fragment of dentin sialophosphoprotein in dentinogenesis. European Journal of Oral Sciences. 2013;121:76-85.

[105] Gibson MP, Zhu Q, Wang S, Liu Q, Liu Y, Wang X, Yuan B, Ruest LB, Feng JQ, D'Souza RN, Qin C, Lu Y. The rescue of dentin matrix protein 1 (DMP1)-deficient tooth defects by the transgenic expression of dentin sialophosphoprotein (DSPP) indicates that Dspp is a downstream effector molecule of Dmp1 in dentinogenesis. Journal of Biological Chemistry. 2013;288:7204-14.

[106] Dong J, Gu T, Jeffords L, MacDougall M. Dentin phosphoprotein compound mutation in dentin sialophosphoprotein causes dentinogenesis imperfecta type III. American Journal of Medical Genetics. 2005;132A:305-9.

[107] Holappa H, Nieminen P, Tolva L, Lukinmaa P-L, Alaluusua S. Splicing site mutations in dentin sialophosphoprotein causing dentinogenesis imperfecta type II. European Journal of Oral Sciences. 2006;114:381-4.

[108] Kim JW, Simmer JP. Hereditary dentin defects. Journal of Dental Research. 2007;86:392-9.

[109] Qin C, Brunn J, Cadena E, Ridall A, Butler W. Dentin sialoprotein in bone and dentin sialophosphoprotein gene expressed by osteoblasts. Connective Tissue Research. 2003;44:179-83.

[110] Baba O, Qin C, Brunn JC, Jones JE, Wygant JN, McIntyre BW, Butler WT. Detection of dentin sialoprotein in rat periodontium. European Journal of Oral Sciences. 2004;112:163-70.

[111] Ogbureke KUE, Fisher LW. SIBLING expression patterns in duct epithelia reflect the degree of metabolic activity. Journal of Histochemistry and Cytochemistry. 2006;55:403-9.

[112] Prasad M, Butler WT, Qin C. Dentin sialophosphoprotein in biomineralization. Connective Tissue Research. 2010;51:404-17.

[113] Gibson MP, Zhu Q, Liu Q, D'Souza RN, Feng JQ, Qin C. Loss of dentin sialophosphoprotein leads to periodontal diseases in mice. Journal of Periodontal Research. 2012;48:221-7.

[114] Zhu Q, Gibson MP, Liu Q, Liu Y, Lu Y, Wang X, Feng JQ, Qin C. Proteolytic processing of dentin sialophosphoprotein (DSPP) is essential to dentinogenesis. Journal of Biological Chemistry. 2012;287:30426-35.

[115] Baba O, Qin C, Brunn JC, Jones JE, Wygant JN, McIntyre BW, Butler WT. Detection of dentin sialoprotein in rat periodontium. European Journal of Oral Sciences. 2004;112:163-70.

[116] Gibson MP, Jani P, Liu Y, Wang X, Lu Y, Feng JQ, Qin C. Failure to process dentin sialophosphoprotein into fragments leads to periodontal defects in mice. European Journal of Oral Sciences. 2013;121:545-50.

[117] Sun Y, Lu Y, Chen L, Gao T, D'Souza R, Feng JQ, Qin C. DMP1 processing is essential to dentin and jaw formation. Journal of Dental Research. 2011;90:619-24.

[118] Huang B, Sun Y, Maciejewska I, Qin D, Peng T, McIntyre B, Wygant J, Butler WT, Qin C. Distribution of SIBLING proteins in the organic and inorganic phases of rat dentin and bone. European Journal of Oral Sciences. 2008;116:104-12.

[119] Rowe PSN. The chicken or the egg: PHEX, FGF23 and SIBLINGs unscrambled. Cell Biochemistry and Function. 2012;30:355-75.

[120] Jain A, Karadag A, Fohr B, Fisher LW, Fedarko NS. Three SIBLINGs (small integrin-binding ligand, N-linked glycoproteins) enhance factor H's cofactor activity enabling MCP-like cellular evasion of complement-mediated attack. The Journal of Biological Chemistry. 2002;277:13700-8.

[121] Qin C, Baba O, Butler WT. Post-translational modifications of SIBLING proteins and their roles in osteogenesis and dentinogenesis. Critical Reviews in Oral Biology & Medicine. 2004;15:126-36.

[122] D'Souza RN, Cavender A, Sunavala G, Alvarez J, Ohshima T, Kulkarni AB, MacDougall M. Gene expression patterns of murine dentin matrix protein 1 (Dmp1) and dentin sialophosphoprotein (DSPP) suggest distinct developmental functions in vivo. Journal of Bone and Mineral Research. 1997;12:2040-9.

[123] Sun Y, Chen L, Ma S, Zhou J, Zhang H, Feng JQ, Qin C. Roles of DMP1 processing in osteogenesis, dentinogenesis and chondrogenesis. Cells Tissues Organs. 2011;194:199-204.

[124] Toyosawa S, Shintani S, Fujiwara T, Ooshima T, Sato A, Ijuhin N, Komori T. Dentin matrix protein 1 is predominantly expressed in chicken and rat osteocytes but not in osteoblasts. Journal of Bone and Mineral Research. 2001;16:2017-26.

[125] Feng JQ, Zhang J, Dallas SL, Lu Y, Chen S, Tan X, Owen M, Harris SE, Macdougall M. Dentin matrix protein 1, a target molecule for Cbfa1 in bone, is a unique bone marker gene. Journal of Bone and Mineral Research. 2002;17:1822-31.

[126] Feng JQ, Huang H, Lu Y, Ye L, Xie Y, Tsutsui TW, Kunieda T, Castranio T, Scott G, Bonewald LB, Mishina Y. The dentin matrix protein 1 (Dmp1) is specifically expressed in mineralized, but not soft, tissues during development. Journal of Dental Research. 2003;82:776-80.

[127] Baba O, Qin C, Brunn JC, Wygant JN, McIntyre BW, Butler WT. Colocalization of dentin matrix protein 1 and dentin sialoprotein at late stages of rat molar development. Matrix Biology. 2004;23:371-9.

[128] Qin C, D'Souza R, Feng JQ. Dentin matrix protein 1 (DMP1): New and important roles for biomineralization and phosphate homeostasis. Journal of Dental Research. 2007;86:1134-41.

[129] Bianco P, Fisher LW, Young MF, Termine JD, Robey PG. Expression and localization of the two small proteoglycans biglycan and decorin in developing human skeletal and non-skeletal tissues. The Journal of Histochemistry and Cytochemistry. 1990;38:1549-63.

[130] Qin C, Brunn JC, Cook RG, Orkiszewski RS, Malone JP, Veis A, Butler WT. Evidence for the proteolytic processing of Dentin Matrix Protein 1: Identification and characterization of processed fragments and cleavage sites. Journal of Biological Chemistry. 2003;278:34700-8.

[131] Steiglitz BM, Ayala M, Narayanan K, George A, Greenspan DS. Bone morphogenetic protein-1/tolloid-like proteinases process dentin matrix protein-1. Journal of Biological Chemistry. 2004;279:980-6.

[132] Tartaix PH, Doulaverakis M, George A, Fisher LW, Butler WT, Qin C, Salih E, Tan M, Fujimoto Y, Spevak L, Boskey AL. In vitro effects of dentin matrix protein-1 on hydroxyapatite formation provide insights into in vivo functions. The Journal of Biological Chemistry. 2004;279:18115-20.

[133] Maciejewska I, Cowan C, Svoboda K, Butler WT, D'Souza R, Qin C. The NH2-terminal and COOH-terminal fragments of dentin matrix protein 1 (DMP1) localize differently in the compartments of dentin and growth plate of bone. Journal of Histochemistry & Cytochemistry. 2009;57:155-66.

[134] Sun Y, Gandhi V, Prasad M, Yu W, Wang X, Zhu Q, Feng JQ, Hinton RJ, Qin C. Distribution of Small Integrin-Binding LIgand, N-linked Glycoproteins (SIBLING) in the condylar cartilage of rat mandible. International Journal of Oral and Maxillofacial Surgery. 2010;39:272-81.

[135] Zurick KM, Qin C, Bernards MT. Mineralization induction effects of osteopontin, bone sialoprotein, and dentin phosphoprotein on a biomimetic collagen substrate. Journal of Biomedical Materials Research Part A. 2013;101A:1571-81.

[136] Zhang B, Sun Y, Chen L, Guan C, Guo L, Qin C. Expression and distribution of SIBLING proteins in the predentin/dentin and mandible of hyp mice. Oral Diseases. 2010;16:453-64.

[137] Gibson MP, Jani P, Wang X, Lu Y, Qin C. Overexpressing the NH2-terminal fragment of dentin sialophosphoprotein (DSPP) aggravates the periodontal defects in Dspp knockout mice. Journal of Oral Biosciences. 2014;56:143-8.

[138] Junqueira LCU, Bignolas G, Brentani RR. Picrosirius staining plus polarization microscopy, a specific method for collagen detection in tissue sections. Journal of Histochemistry. 1979;11:447-55.

[139] Ciani C, Doty SB, Fritton SP. An effective histological staining process to visualize bone interstitial fluid space using confocal microscopy. Bone. 2009;44:1015-7.

[140] Fisher LW, Stubbs JT, 3rd, Young MF. Antisera and cDNA probes to human and certain animal model bone matrix noncollagenous proteins. Acta orthopaedica Scandinavica Supplementum. 1995;266:61-5.

[141] McFarland RJ, Garza S, Butler WT, HÖÖK M. The mutagenesis of the RGD sequence of recombinant osteopontin causes it to lose its cell adhesion ability. Annals of the New York Academy of Sciences. 1995;760:327-31.

[142] Wang X, Wang S, Li C, Gao T, Liu Y, Rangiani A, Sun Y, Hao J, George A, Lu Y, Groppe J, Yuan B, Feng JQ, Qin C. Inactivation of a novel FGF23 rRegulator, FAM20C, leads to hypophosphatemic rickets in mice. PLoS Genetics. 2012;8:e1002708.

[143] Lu Y, Yuan B, Qin C, Cao Z, Xie Y, Dallas SL, McKee MD, Drezner MK, Bonewald LF, Feng JQ. The biological function of DMP-1 in osteocyte maturation is mediated by its 57-kDa C-terminal fragment. Journal of Bone and Mineral Research. 2011;26:331-40.

[144] Butler WT, Bhown M, Brunn JC, D'Souza RN, Farach-Carson MC, Happonen R-P, Schrohenloher RE, Seyer JM, Somerman MJ, Foster RA, Tomana M, Van Dijk S. Isolation, characterization and immunolocalization of a 53-kDal dentin sialoprotein (DSP). Matrix. 1992;12:343-51.

[145] von Marschall Z, Mok S, Phillips MD, McKnight DA, Fisher LW. Rough endoplasmic reticulum trafficking errors by different classes of mutant dentin sialophosphoprotein (DSPP) cause dominant negative effects in both dentinogenesis imperfecta and dentin dysplasia by entrapping normal DSPP. Journal of Bone and Mineral Research. 2012;27:1309-21.

[146] Simon S, Smith AJ, Lumley PJ, Berdal A, Smith G, Finney S, Cooper PR. Molecular characterization of young and mature odontoblasts. Bone. 2009;45:693-703.

[147] Wan C, Yuan G, Luo D, Zhang L, Lin H, Liu H, Chen L, Yang G, Chen S, Chen Z. The dentin sialoprotein (DSP) domain regulates dental mesenchymal cell differentiation through a novel surface receptor. Scientific Reports. 2016;6:29666.

[148] Sfeir C, Lee D, Li J, Zhang X, Boskey AL, Kumta PN. Expression of phosphophoryn is sufficient for the induction of matrix mineralization by mammalian cells. The Journal of Biological Chemistry. 2011;286:20228-38.

[149] Jadlowiec J, Koch H, Zhang X, Campbell PG, Seyedain M, Sfeir C. Phosphophoryn regulates the gene expression and differentiation of NIH3T3, MC3T3-E1, and human mesenchymal stem cells via the integrin/MAPK signaling pathway. The Journal of Biological Chemistry. 2004;279:53323-30.

[150] Eapen A, Ramachandran A, George A. Dentin phosphoprotein (DPP) activates integrin-mediated anchorage-dependent signals in undifferentiated mesenchymal cells. Journal of Biological Chemistry. 2012;287:5211-24.

[151] Jadlowiec JA, Zhang X, Li J, Campbell PG, Sfeir C. Extracellular matrix-mediated signaling by dentin phosphophoryn involves activation of the Smad pathway independent of bone morphogenetic protein. The Journal of Biological Chemistry. 2006;281:5341-7.

[152] Jaha H, Husein D, Ohyama Y, Xu D, Suzuki S, Huang GTJ, Mochida Y. N-terminal Dentin Sialoprotein fragment induces type I collagen production and upregulates dentinogenesis marker expression in osteoblasts. Biochemistry and Biophysics Reports. 2016;6:190-6.

[153] Huang B, Maciejewska I, Sun Y, Peng T, Qin D, Lu Y, Bonewald L, Butler W, Feng J, Qin C. Identification of full-length dentin matrix protein 1 in dentin and bone. Calcified Tissue International. 2008;82:401-10.

[154] von Marschall Z, Fisher LW. Dentin matrix protein-1 isoforms promote differential cell attachment and migration. The Journal of Biological Chemistry. 2008;283:32730-40.

APPENDIX A

FIGURES

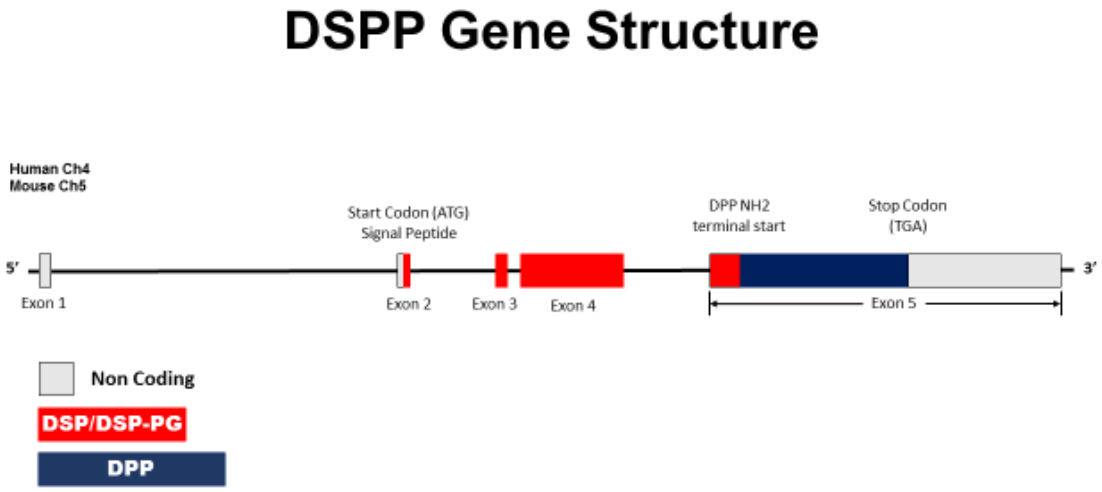

Figure 1-1 Deintin sialophosphoprotein gene structure: The Dentin sialophosphoprotein gene consiste of 5 exons and 4 introns. Exon 1 is non-coding. The second exon codes the signal peptide. The NH2-terminal fragment arises from the exons 2, 3, 4 and 5' end of exon 5. The C-terminal fragment is encoded from exon 5. DSP, Dentin Sialoprotein; DSP-PG, proteoglycan form of DSP; DPP, Dentin phosphoprotein.

Figure 1-2 Generation and characterization of the D452A-DSPP Tg mice: To examine the in vivo effects of the NH2-terminal fragment of DSPP on biomineralization we generated a strain of *Col 1a1*-VSV-DSP mice that express the NH2-terminal fragment of DSPP in the *Dspp*-KO background. In the transgenic mice, the DSP transgene is driven by a type I collagen promoter (*Col 1A1*). The rationale for using the *Col 1A1* promoter to drive the DSP transgene include: 1) this promoter works properly in driving the expression of genes that are active in bone and/or dentin; 2) a high expression level of the DSP transgene in the bone will allow us to study the role of this protein in osteogenesis since under physiological conditions the expression of DSPP (DSP) in bone is very low. The targeting vector used for the generation of the transgenic mice contains rat *Col 1A1* promoter plus intron of the rat *Col 1A1* gene, mouse *Dspp* signal peptide, three VSV epitopes and the cDNA sequence encoding the NH2-terminal portion of mouse DSPP.

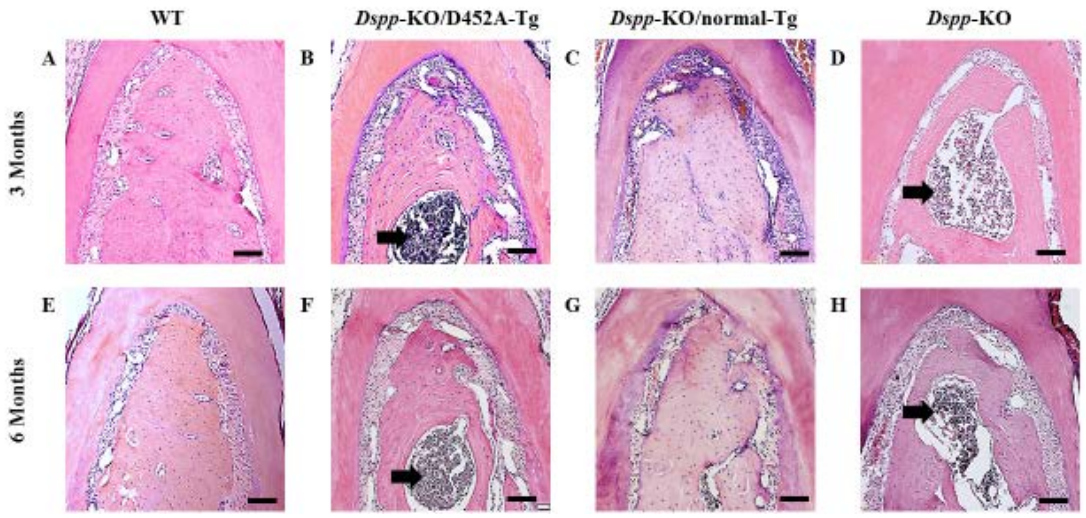

Figure 2-1 Failure to process DSPP into fragments leads to alveolar bone defects. H&E staining of alveolar bone at both 3- and 6-months of age, showed that the *Dspp*-KO (D and H) and *Dspp*-KO/D452A-Tg mice (B and F) had significant alveolar bone loss in the furcation region of the first mandibular molar with inflammation (black arrows), compared to the WT mice (A and E). The transgenic expression of normal DSPP (C and G, *Dspp*-KO/normal-Tg mice) completely rescued the alveolar bone defects of *Dspp*-KO mice; the alveolar bone *Dspp*-KO/normal-Tg mice (C and G) appeared similar to those of the WT mice (A and E). Bar: 100 μm

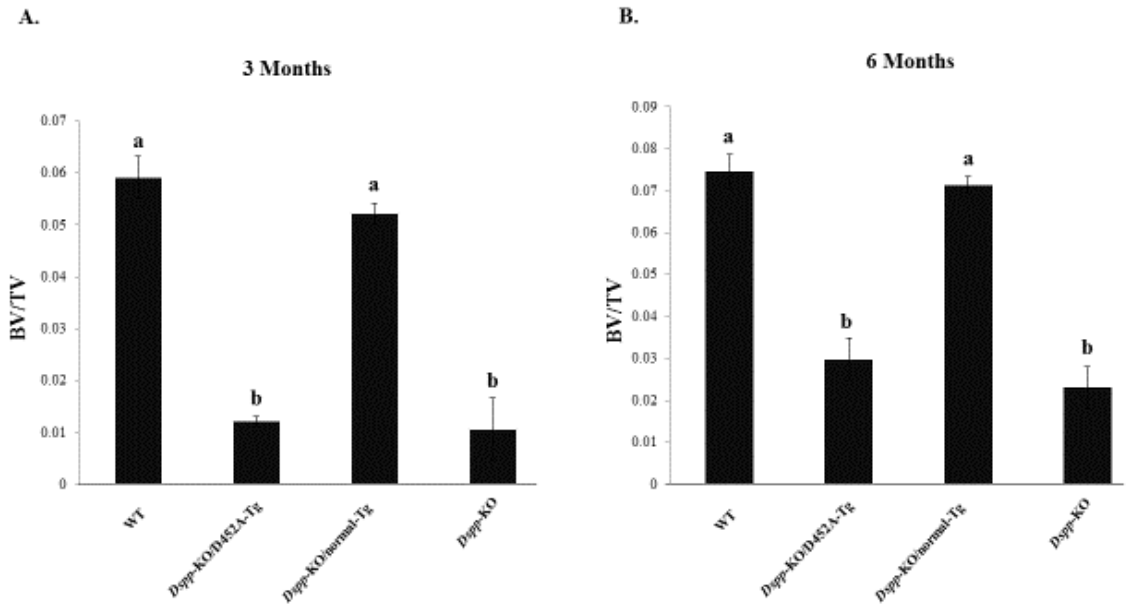

Figure 2-2 Quantitative μ-CT analyses. The quantitative μ-CT analyses of alveolar bone in the 3-month (A) and 6-month (B) old mice showed that transgenic expression of normal DSPP transgene was able to reverse the bone volume fraction of *Dspp*-KO mice at both ages to a level comparable to WT mice. There was no significant difference between the bone volume fraction of the WT and *Dspp*-KO/normal-Tg mice (a). The *Dspp*-KO/D452A-Tg mice showed no significant improvement over *Dspp*-KO mice at either age (b). $P < 0.05$ was considered significant; different letters above each bar indicate a significant difference (Student's *t*-test, $p < 0.05$); data represent mean ± SD and $n = 5$.

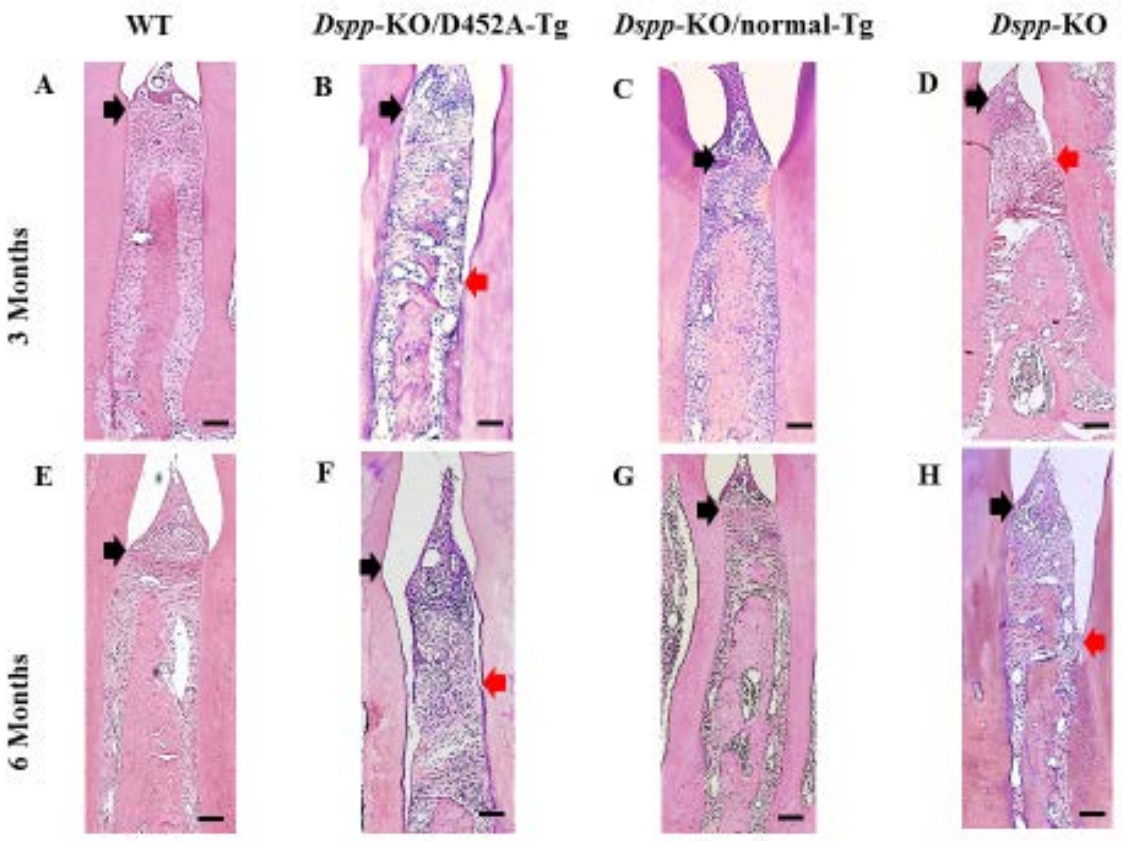

Figure 2-3 Failure to process DSPP into fragments leads to loss of epithelium attachment in the interdental region. At 3- and 6-months of age, H & E staining showed that the interdental epithelial attachment between the first and second mandibular molars of the WT (A and E) and *Dspp*-KO/normal-Tg mice (C and G) was at the cemento-enamel junction (CEJ) (indicated with a black arrow), whereas the *Dspp*-KO (D and H) and *Dspp*-KO/D452A-Tg mice (B and F) showed alveolar bone loss with an apically recessed epithelial attachment (black arrows denote the CEJ; red arrows indicate the actual epithelial attachment). Bar: 100 μm.

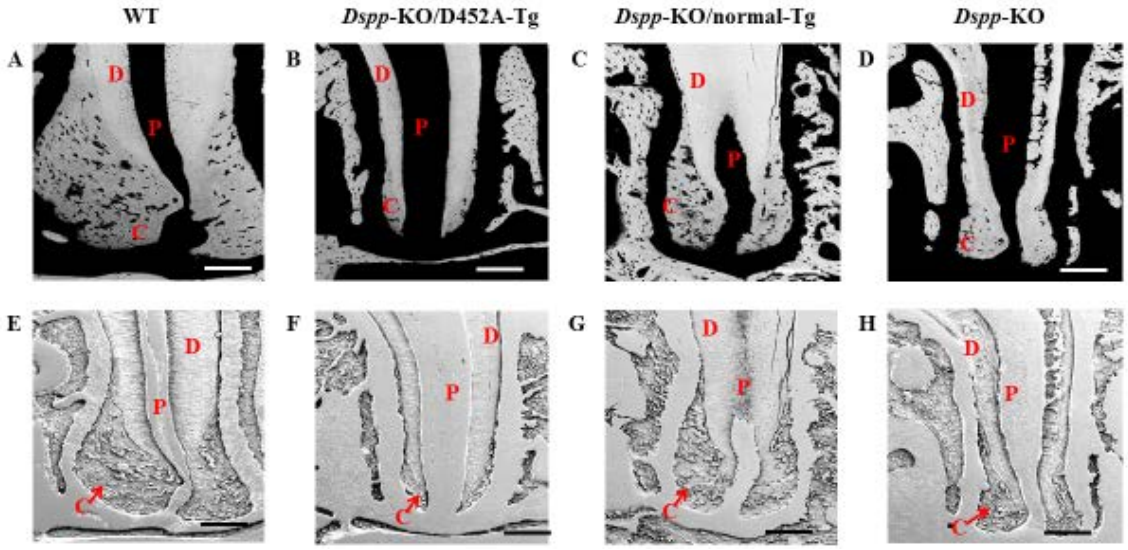

Figure 2-4 Failure to process DSPP into fragments leads to decreased cementum deposition. In these backscattered SEM (A-D) and resin-casted SEM (E-H) images, the dentin is denoted as "D"; pulp as "P" and cementum as "C". In the backscattered SEM images, the black areas represent unmineralized or hypomineralized areas. Therefore, the pulpal space appears as black (denoted as P); Cementum (C) is less mineralized than Dentin (D) and appears darker than dentin. The *Dspp*-KO (D) and *Dspp*-KO/D452A-Tg mice (B) showed increased black areas periapically indicating decreased cementum deposition compared to the WT (A) and *Dspp*-KO/normal-Tg mice (C). The resin-casted SEM gave a better visualization of the periapical region of cementum.. The WT (E) and *Dspp*-KO/normal-Tg mice (G) showed a thick layer of cementum deposition at the root apex whereas; *Dspp*-KO (H) and *Dspp*-KO/D452A-Tg mice (F) showed little or no cementum in the same region. Bar: 200 μm.

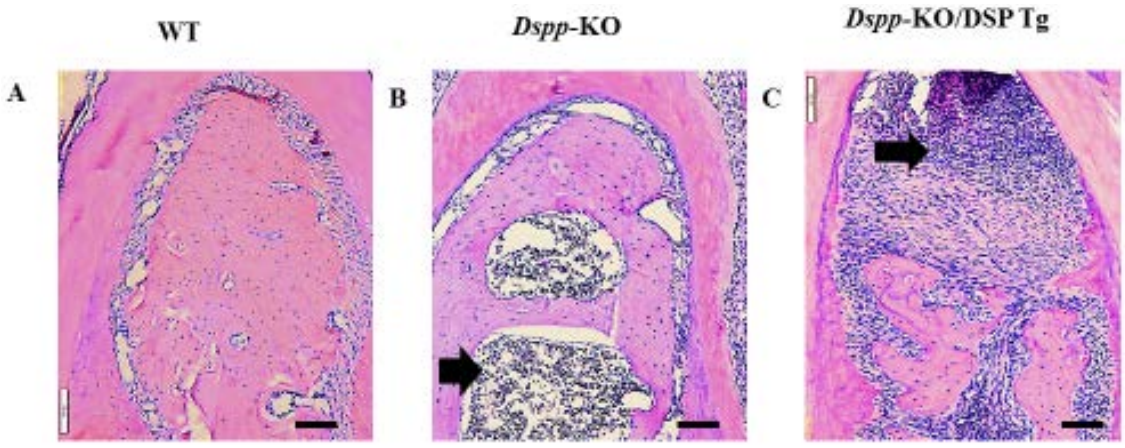

Figure 3-1 Inflammatory infiltration and furcation bone loss. H&E staining for the furcation regions of the first mandibular molars from 3-month-old WT (A), *Dspp* KO (B) and *Dspp* KO/DSP Tg (C) mice. While the inflammatory reaction (black arrows in B and C) was present in the molar furcation region of both *Dspp* KO and *Dspp* KO/DSP Tg mice, the inflammation in the latter mice was more remarkable than in the former. Note that there was very little alveolar bone left in the molar furcation region of *Dspp* KO/DSP Tg mice. Bar: 100 μm.

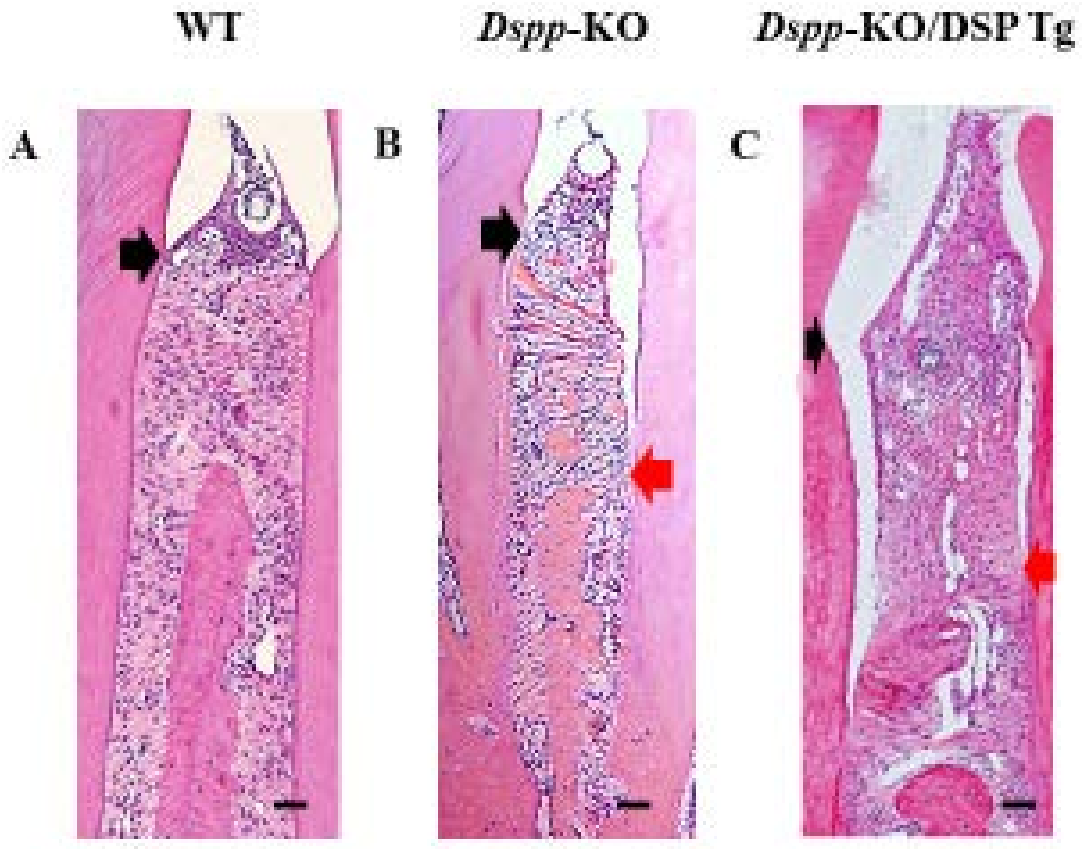

Figure 3-2 Migration of epithelial attachment in the periodontium. H&E staining for the interdental regions between the first and second molars of mandibles in the 3-month-old WT (A), *Dspp* KO (B) and *Dspp* KO/DSP Tg (C) mice. Black arrows indicate the cemento-enamel junctions. Blue arrows indicate the site of the epithelial attachment (bottom of the gingival sulcus). The reduction of the interdental alveolar bone in the *Dspp* KO/DSP Tg (C) was greater than in the *Dspp* KO mice. The epithelial attachment receded more apically in the *Dspp* KO/DSP Tg mice (C, indicated by blue arrow) than in the *Dspp* KO mice. Bar: 100 μm.

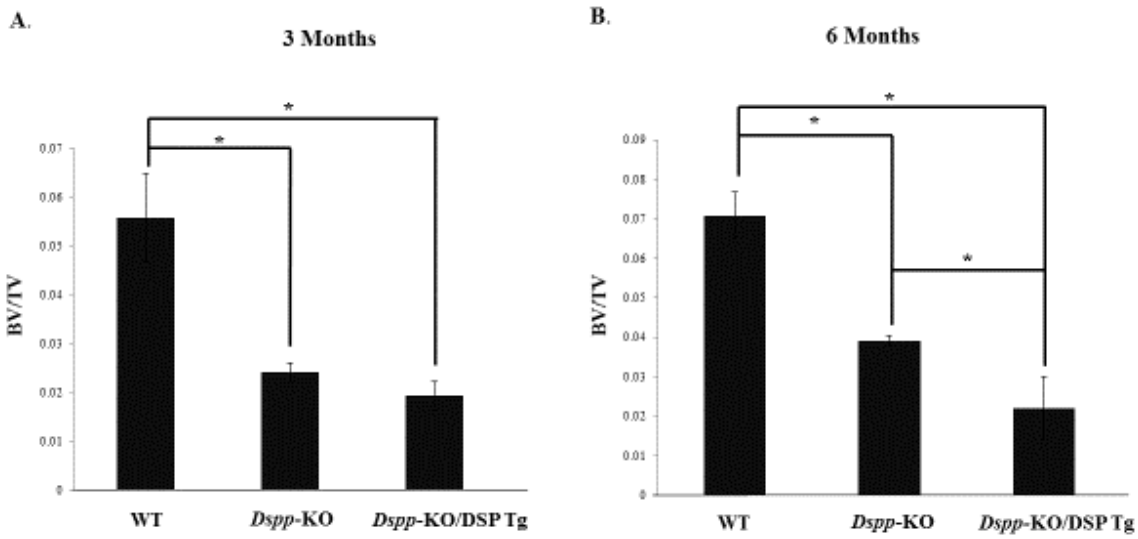

Figure 3-3 Quantitative analysis of reduction of alveolar bone. The quantitative μ-CT analyses of the interradicular alveolar bone in the 3-month-old (A) and 6-month-old (B) mice. Student's *t-test* was used to statistically compare the mean differences between two groups in each of the paired analyses. The differences in the bone volume fractions (BV/TV) between the *Dspp* KO and *Dspp* KO/DSP Tg mice at both ages were statistically significant. The data represent mean ± SD (n = 3). BV, bone volume; TV, total volume; *: $P \leq 0.05$.

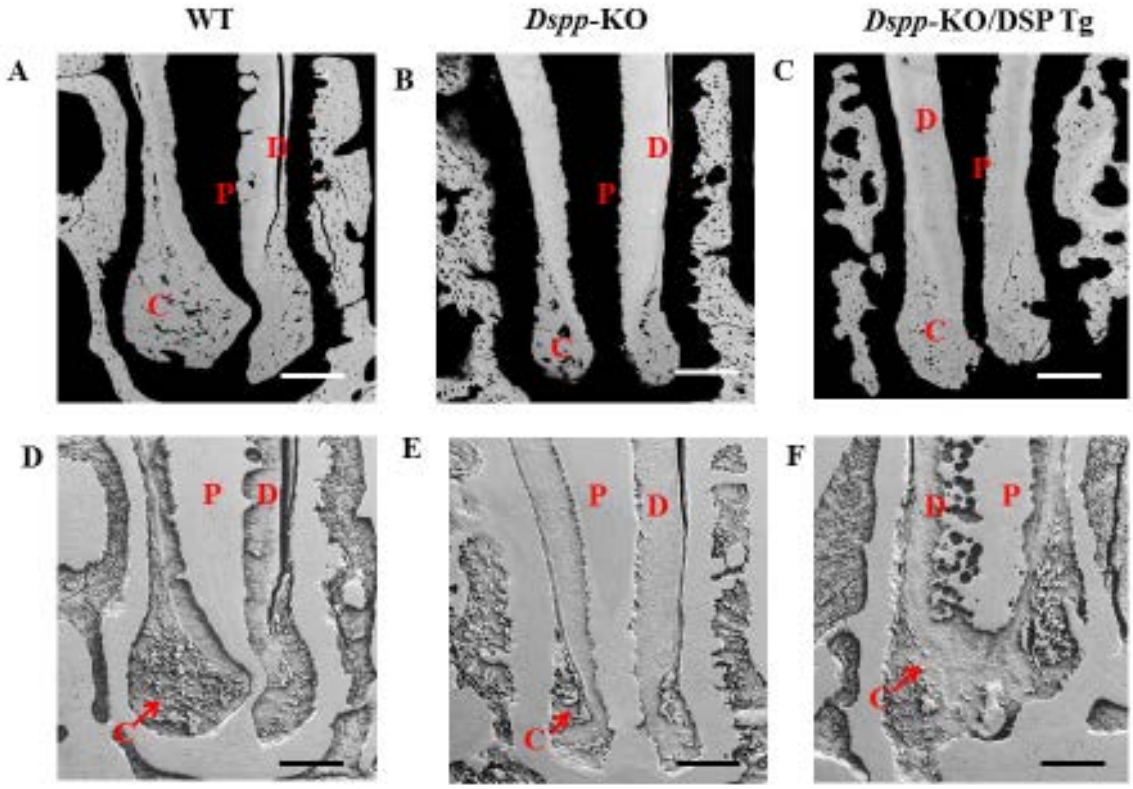

Figure 3-4 SEM imaging of cementum. Backscattered SEM (A-C) and resin-casted SEM analyses for the periapical regions of first molars in the mandibles of 3-month-old WT (A, D), *Dspp* KO (B, E) and *Dspp* KO/DSP Tg (C, F) mice. In these SEM images, the dentin is denoted as 'D', pulp as 'P', and cementum as 'C'. In the backscattered SEM images, the black areas represent unmineralized or hypomineralized areas, and thus, the dental pulp (P) appears black. Cementum (C) is less mineralized (appears darker) than dentin (D). In comparison with the WT mice (A), the periapical regions of *Dspp* KO (B) and *Dspp* KO/DSP Tg (C) mice had broader areas of blackness in the backscattered SEM images and contained smaller areas of cementum. Among the three types of mice, *Dspp* KO/DSP Tg mice had the least amounts of cellular cementum. The resin-casted SEM images (D-F) also revealed that among the three groups, the *Dspp* KO/DSP Tg mice (F) had the least amounts of cellular cementum in the periapical region. Bar: 200 μm.

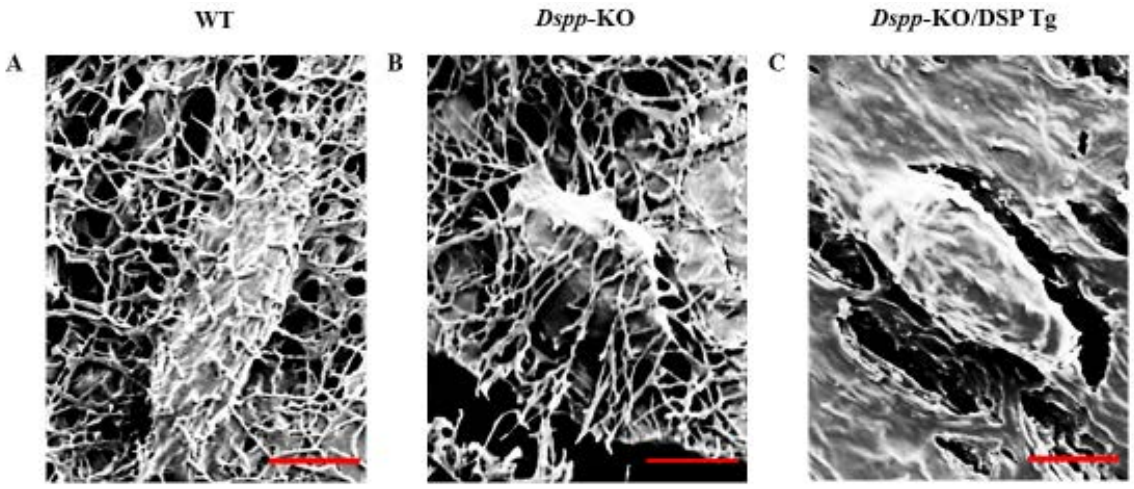

Figure 3-5 Alteration of the osteocyte morphology. Resin-casted SEM analyses of the osteocyte lacunae and canaliculi in the alveolar bone of 3-month-old WT (A), *Dspp* KO (B) and *Dspp* KO/DSP Tg (C) mice. In the WT mice the canaliculi radiated out in directions perpendicular to the long axis of the osteocyte bodies. In contrast, the osteocyte lacunae in the alveolar bone of the *Dspp* KO and *Dspp* KO/DSP Tg mice appeared irregular with disorganized and fewer canaliculi. The defects of the osteocyte lacunae and the structures surrounding the lacunae in the alveolar bone of *Dspp* KO/DSP Tg mice were apparently worse than those of the *Dspp* KO mice. Bar: 5 μm.

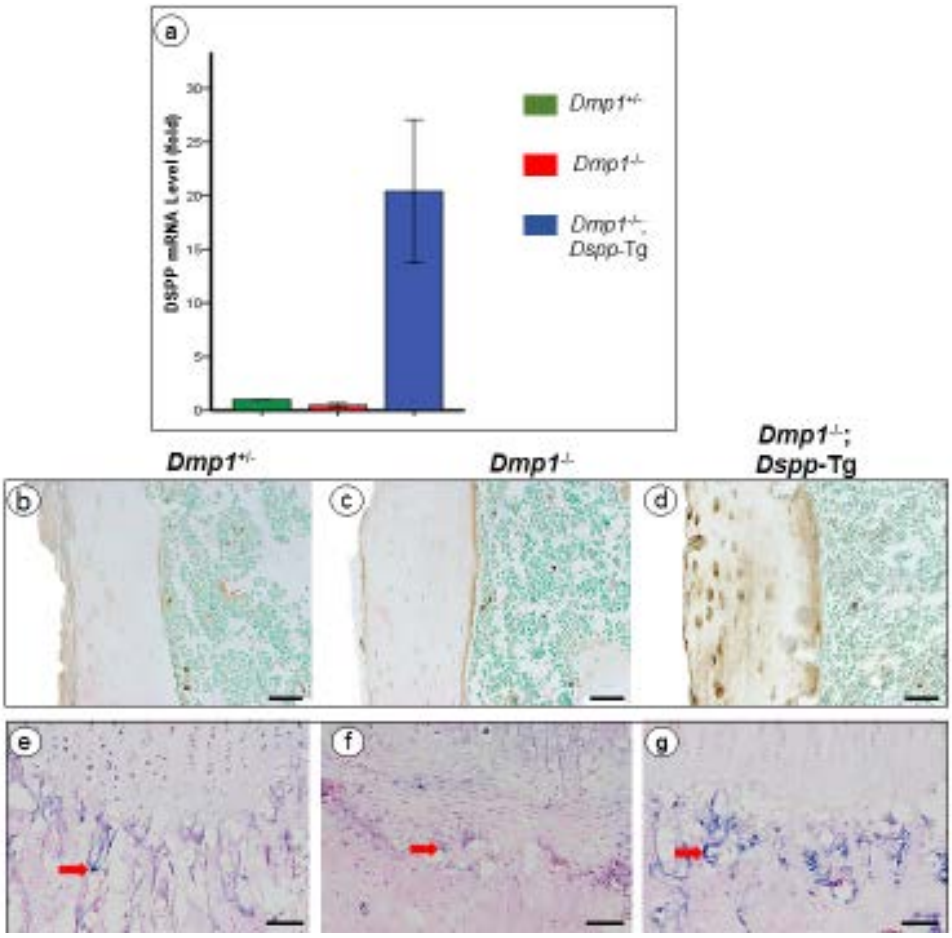

Figure 4-1 Expression of Dspp transgene. a, RT-qPCR analyses; b-d, immunohistochemistry staining using the anti-DSP antibody; e-g, i*n situ* hybridization analyses for DSPP mRNA. In the RT-qPCR analyses (a), we measured the mRNA levels of DSPP in the femurs of 3-month-old mice from each group. The DSPP mRNA level in the normal control (*Dmp1*$^{+/-}$) mice (green bar) was taken as 1. DSPP mRNA level in the *Dmp1*$^{-/-}$ mice (red bar) was 30% of the normal mice, while its level in the *Dmp1*$^{-/-}$;*Dspp*-Tg mice (blue bar) was 20 fold of the normal. The anti-DSP immunostaining exhibited signals for this protein around the osteocyte lacunae in the cortical bone in the mid-shaft region of the femurs of control mice (b). The anti-DSP signals were slightly weaker in the cortical bone of *Dmp1*$^{-/-}$ mice (c) than in the normal controls. The cortical bone of *Dmp1*$^{-/-}$;*Dspp*-Tg mice (d) demonstrated a higher level of anti-DSP immunoreactivity compared to the other two groups of mice. *In situ* hybridization analyses show the presence of DSPP mRNA (arrows) in the newly formed bone proximal to the epiphyseal growth plate of normal controls (e); DSPP mRNA level was lower in *Dmp1*$^{-/-}$ mice (f) than in the normal control. In the same region, *Dmp1*$^{-/-}$;*Dspp*-Tg mice (g) showed elevated level of DSPP mRNA confirming the higher expression levels of *Dspp* transgene in these mice. Scale bar: 50 μm in b-g.

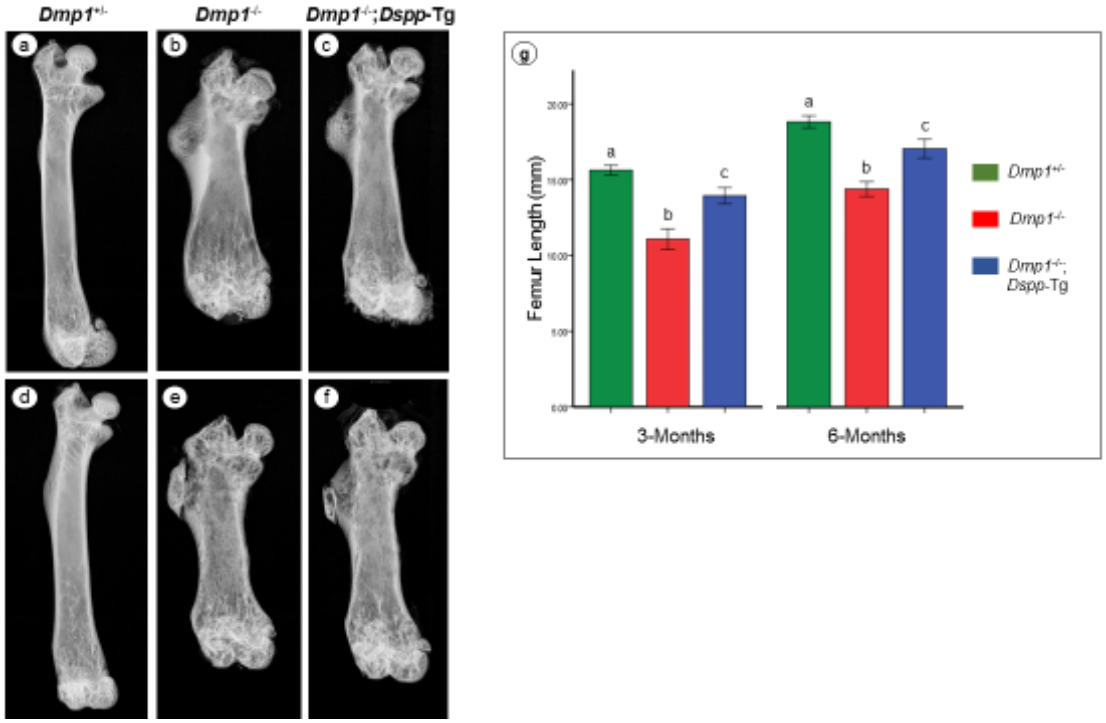

Figure 4-2 Plain X-ray radiography of femurs from the three groups of mice at the ages of 3 and 6 months. At 3 months, the femurs of the normal control (*Dmp1*$^{+/-}$) mice (a) had parallel and uniform cortical layers throughout the diaphysis of the bone and the metaphysis regions were slightly wider than the shaft. The femurs of the 3-month-old *Dmp1*$^{-/-}$ mice (b) and *Dmp1*$^{-/-}$;*Dspp*-Tg mice (c) were shorter and wider than those of the normal control, and showed significant outward protrusion (irregular enlargement) in the metaphysis regions, particularly in the distal metaphysis areas. At 6 months, the length difference between the normal control mice (d) and *Dmp1*$^{-/-}$ mice (e) became greater. Both the distal and proximal metaphysis regions of 6-month-old *Dmp1*$^{-/-}$ mice (e) and *Dmp1*$^{-/-}$;*Dspp*-Tg mice (f) showed apparent enlargement. At either 3 or 6 months, the femurs of *Dmp1*$^{-/-}$;*Dspp*-Tg mice (c, f) were longer than those of the *Dmp1*$^{-/-}$ mice (b, e). Quantitative analyses (g) showed the differences in average femur length between the *Dmp1*$^{-/-}$;*Dspp*-Tg and *Dmp1*$^{-/-}$ mice at 3 months (12.94 mm vs. 11.08 mm) and 6 months (15.1 mm vs. 13.5 mm) were statistically significant. $P < 0.05$ (Student's *t*-test) was considered significant. Data represent mean ± SD ($n = 5$). When the letters above two bars are different, the difference between the two groups was statistically significant ($P < 0.05$).

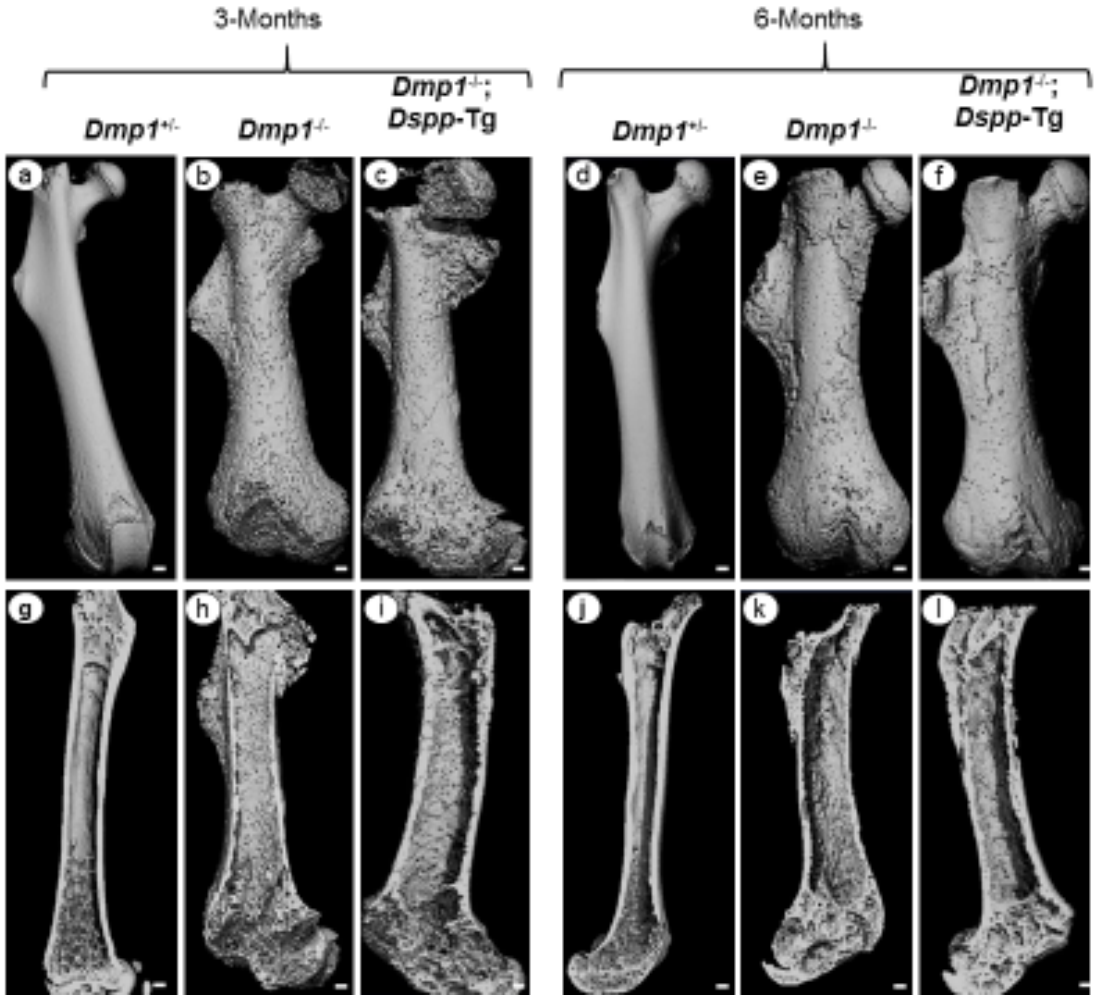

Figure 4-3 Micro-computed tomography (µ-CT) analyses of femurs from 3- and 6-month-old mice. a-f: full views of the femurs at lower resolution; g-l: longitudinal-section views of the femurs at lower resolution. Full views of the whole femurs revealed that at both ages, the femurs of the normal control mice (a, d) had a smooth surface while those of the *Dmp1*$^{-/-}$ (b, e) and *Dmp1*$^{-/-}$;*Dspp*-Tg (c, f) mice showed a porous appearance. Longitudinal-section views demonstrated that compared to the normal control (g, j), the inner surfaces of the femur shells of the *Dmp1*$^{-/-}$ (h, k) and *Dmp1*$^{-/-}$;*Dspp*-Tg (i, l) mice were rougher. At either 3 or 6 months, the bone in the *Dmp1*$^{-/-}$;*Dspp*-Tg mice appeared to have fewer surface porosities than in the *Dmp1*$^{-/-}$ mice in both the full and longitudinal-section views. Scale bar: a to l = 500 µm

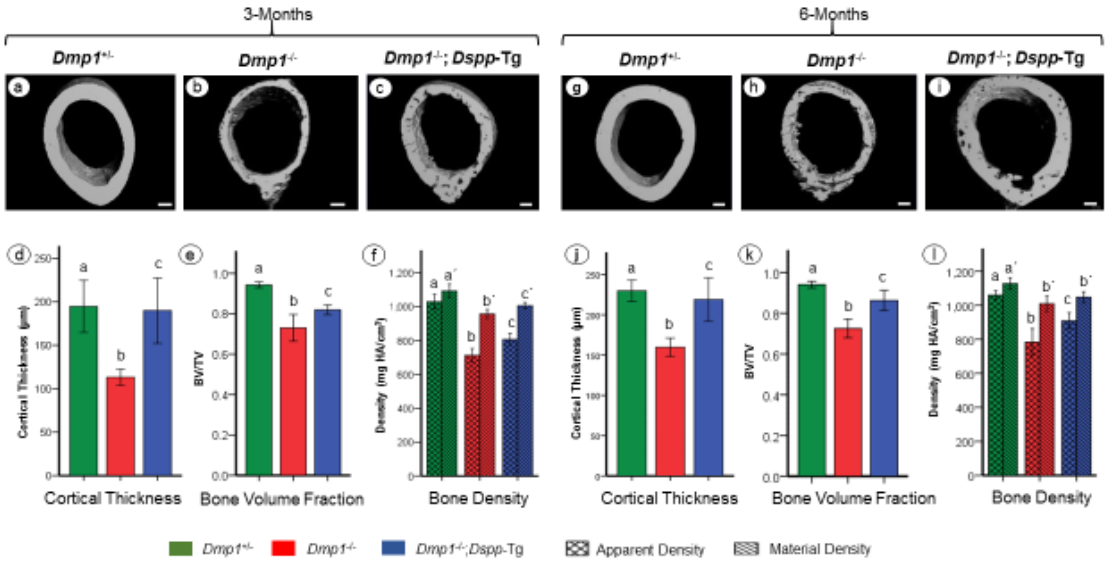

Figure 4-4 High resolution imaging and quantitative μ-CT analyses of cortical bone. a-c: high resolution views of the cortical mid-shaft regions of femurs at 3 months; g-i: high resolution views of the cortical mid-shaft regions of femurs at 6 months. At both ages, the cortical bone in the mid-shaft region was thinner in the *Dmp1*$^{-/-}$ mice (b, h) than in the normal controls (a, g), while the femur thickness of *Dmp1*$^{-/-}$;*Dspp*-Tg mice (c, i) was similar to that of *Dmp1*$^{+/-}$ mice. Scale bars: 100 μm in all images. The quantitative analyses of the cortical thickness validated the imaging result at 3 months (d) and 6 months (j) of ages; the cortical thickness in *Dmp1*$^{-/-}$;*Dspp*-Tg mice was restored to a level similar to that of the normal control. The bone volume fraction (BV/TV) in the diaphyseal mid-shaft region in the femurs of *Dmp1*$^{-/-}$;*Dspp*-Tg mice was significantly greater than in the *Dmp1*$^{-/-}$ mice; at 6 months, the improvement of BV/TV in the *Dmp1*$^{-/-}$;*Dspp*-Tg mice was more remarkable (e, k). The bone density represented by the density of total volume (Apparent Density) and density of bone volume (Material Density) was significantly reduced in *Dmp1*$^{-/-}$ mice compared to the normal controls at 3 months (f) and 6 months (l). The transgenic expression of *Dspp* significantly improved the apparent and material densities at 3 months. At 6 months, the apparent density of the *Dmp1*$^{-/-}$;*Dspp*-Tg mice was significantly higher than in *Dmp1*$^{-/-}$ mice, but the change in the material density was not statistically significant. $P < 0.05$ (Student's *t*-test) was considered significant. Data represent mean ± SD ($n = 5$ for d and j; n = 6 for e, f, k and l). Different letters above two bars indicate a significant difference ($P < 0.05$) between the two groups.

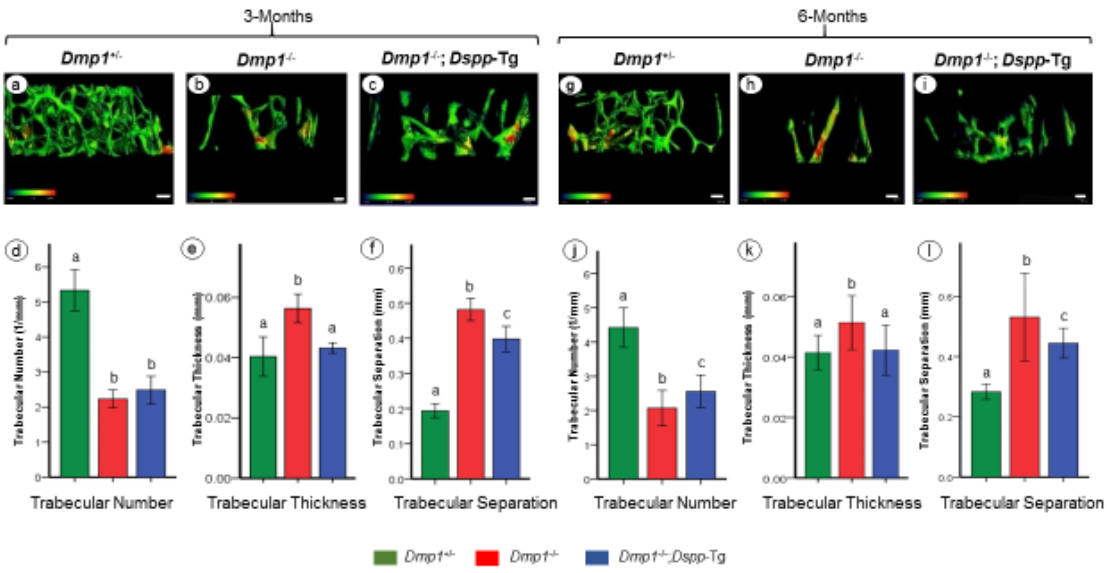

Figure 4-5 High resolution imaging and quantitative μ-CT analyses of trabecular bone. a-c: high resolution views of the distal metaphysis regions at 3 months; g-i: high resolution views of the distal metaphysis regions at 6 months. High resolution images of the distal metaphysis regions showed that in comparison with the normal controls (a, g), *Dmp1*$^{-/-}$ mice (b, h) and *Dmp1*$^{-/-}$;*Dspp*-Tg mice (c, i) had a remarkable reduction in trabecular bone number. Scale bars: 100 μm in all images. Colored scale bars indicate the trabecular thickness ranging from 0.00 mm (blue) to 0.07 mm (red). Quantitative analyses revealed that at 6 months (j), but not at 3 months (d), the trabecular number was significantly higher in the *Dmp1*$^{-/-}$;*Dspp*-Tg mice than in *Dmp1*$^{-/-}$ mice. The most remarkable change of trabeculae in *Dmp1*$^{-/-}$;*Dspp*-Tg mice was the restoration of trabecular thickness to nearly normal level at both ages (e, k). The spacing between the trabeculae in *Dmp1*$^{-/-}$;*Dspp*-Tg mice, at both 3 months (f) and 6 months (l), although not completely reduced to the normal level of control mice, was significantly lower than that of *Dmp1*$^{-/-}$ mice. $P < 0.05$ (Student's *t*-test) was considered significant. Data represent mean ± SD ($n = 6$ for d-l). Different letters above two bars indicate a significant difference ($P < 0.05$) between the two groups

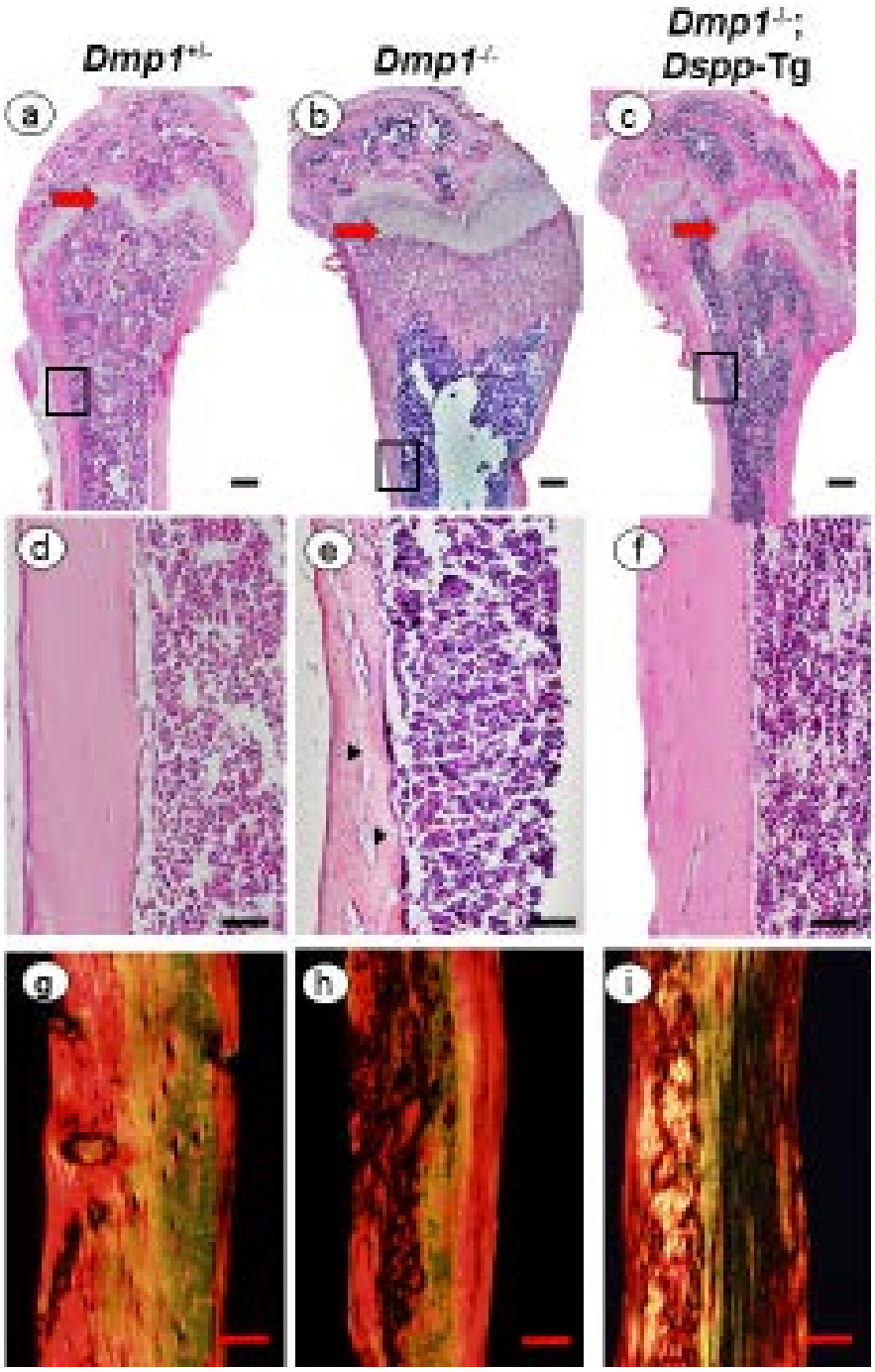

Figure 4-6 Histological analyses of the femurs from 3-month-old mice. a-f: H&E staining; the images in the middle row are higher magnification views of boxed areas in the upper row; g-i: Picrosirius red staining of the cortical bone in the mid-shaft region of the femurs. The growth plate (red arrows) was wider and cortical bone was thinner in the *Dmp1*$^{-/-}$ mice (b) than in the normal control (a) or *Dmp1*$^{-/-}$;*Dspp*-Tg mice (c). The cortical

Fig. 4-6 Continued:
bone in the *Dmp1*$^{-/-}$ mice (e) appeared to have more hypomineralized areas or osteoid areas (stained grey, indicated by arrowheads) than in the normal control (d) or the *Dmp1*$^{-/-}$;*Dspp*-Tg mice (f). Picrosirius red staining, which specifically stains collagen, showed that while the cortical bone of normal control mice (g) had well-organized fibrillary network with fewer large (yellow/orange) fibers and more reticular (green) fibers. The collagen network was highly disorganized in *Dmp1*$^{-/-}$ mice (h) with obvious reduction in the reticular fibers. *Dmp1*$^{-/-}$;*Dspp*-Tg mice (i) showed a notable improvement in collagen fibril organization. Scale bars: 500 μm in a-c; 100 μm in d-f; 50 μm in g-i

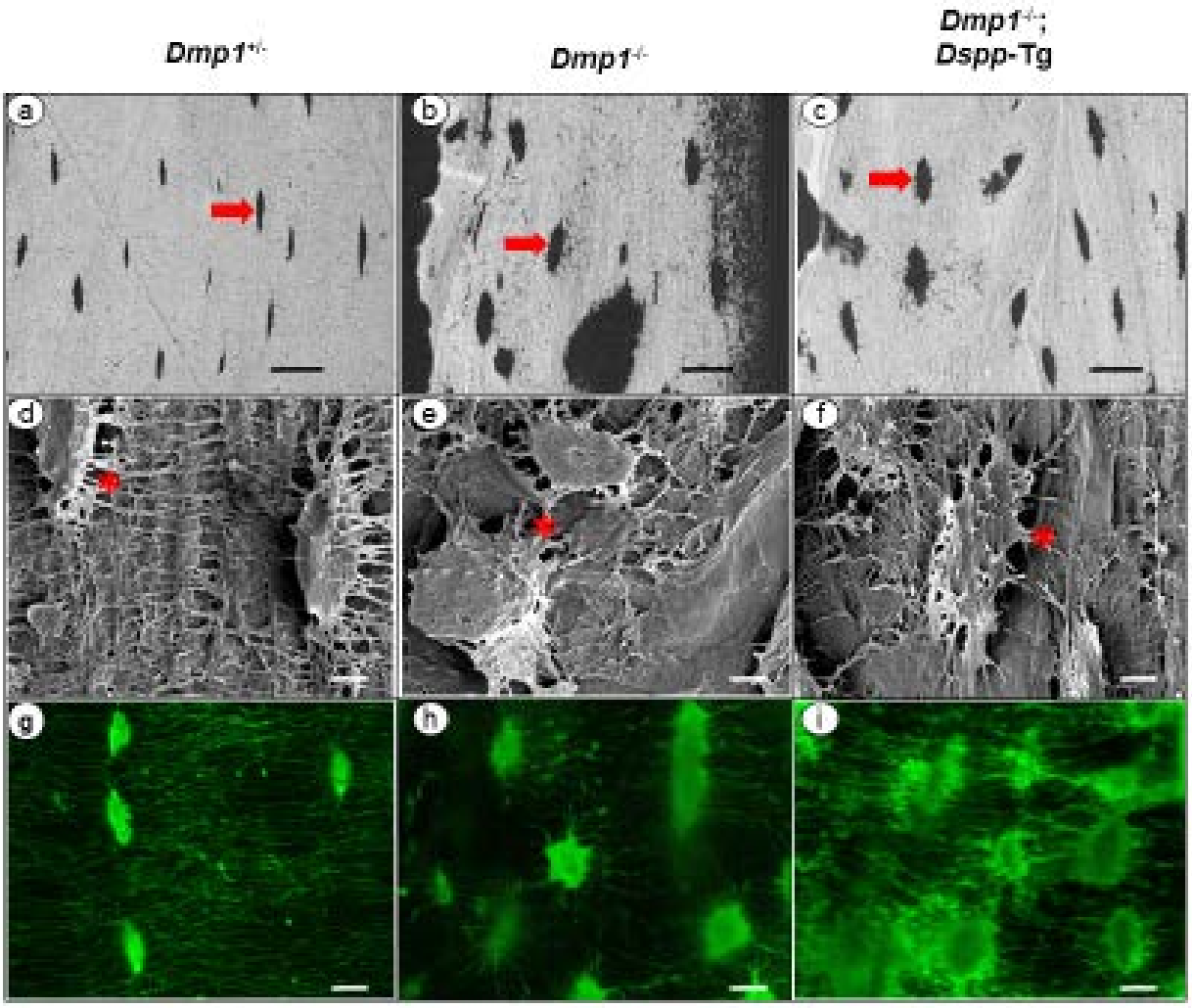

Figure 4-7 Scanning electron microscopy (SEM) analyses of the femurs from 3-month-old mice. a-c: Backscatered SEM imaging of cortical bone from midshaft region of tibia; d-f: acid-etched SEM imaging of cortical bone from midshaft region of tibia; g-i: FITC staining of cortical bone from the same region. The backscattered SEM imaging showed spindle-shaped osteocyte lacunae that were well organized and well oriented in the bone of normal control mice (a). The cortical bone of *Dmp1*$^{-/-}$ mice (b) and *Dmp1*$^{-/-}$;*Dspp*-Tg mice (c) showed fewer and disoriented osteocyte lacunae. The acid etched SEM analyses revealed that the osteocytes in the normal control mice (d) were narrow with many osteocyte processes in the canaliculi that were running perpendicular to the cell bodies. The osteocyte lacunae in *Dmp1*$^{-/-}$;*Dspp*-Tg mice (f) were slightly more enlarged and ovoid with fewer canaliculi than the in normal mice, but were smaller than the rounded lacunae in *Dmp1*$^{-/-}$ mice (e) that had lost nearly all of the canaliculi. FITC staining showed the lacunocanalicular system was well organized with numerous canaliculi in the normal control mice (g). *Dmp1*$^{-/-}$ mice (h) had a remarkable reduction in the number of canaliculi while the *Dmp1*$^{-/-}$;*Dspp*-Tg mice (i) showed a partial restoration in the number of canaliculi. Scale bars in a-c: 20 μm; in d-f: 5 μm; in g-i: 10 μm.

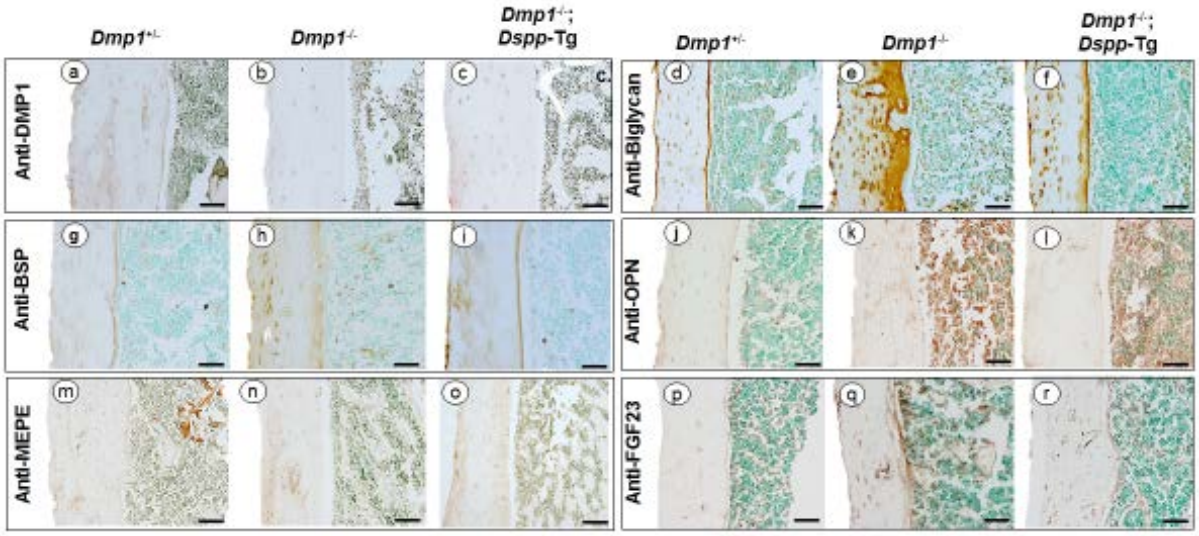

Figure 4-8 Immunohistochemical analyses of the femurs from 3-month-old mice. All of the images were from the mid-shaft region of the femurs. Immunohistochemistry against DMP1 (a-c) showed that the normal control mice (a) demonstrated positive anti-DMP1 signals in the cortical bone, which were relatively stronger around the osteocyte lacunae, whereas there was a complete loss of signals for this molecule in *Dmp1*$^{-/-}$ mice (b) and *Dmp1*$^{-/-}$;*Dspp*-Tg mice (c). Immunohistochemistry against biglycan (d-f), which often serves to reflect the amount of osteoid in the bone matrix, showed that compared to the normal control mice (d), the femurs of *Dmp1*$^{-/-}$ mice (e) had much more biglycan. The level of biglycan in *Dmp1*$^{-/-}$;*Dspp*-Tg mice (f) was remarkably lower than in the *Dmp1*$^{-/-}$ mice but slightly higher than in the normal control mice. The signals for BSP, OPN and MEPE were increased in *Dmp1*$^{-/-}$ mice (h, k, n), compared to the normal controls (g, j, m), while the levels of the these proteins in *Dmp1*$^{-/-}$;*Dspp*-Tg mice (i, l, o) were comparable to the normal control mice. FGF23 level was increased in *Dmp1*$^{-/-}$ mice (q), compared to the normal control mice (p). FGF23 level was slightly reduced in *Dmp1*$^{-/-}$;*Dspp*-Tg mice (r) compared to the *Dmp1*$^{-/-}$ mice. Scale bars: 50 μm in all images.

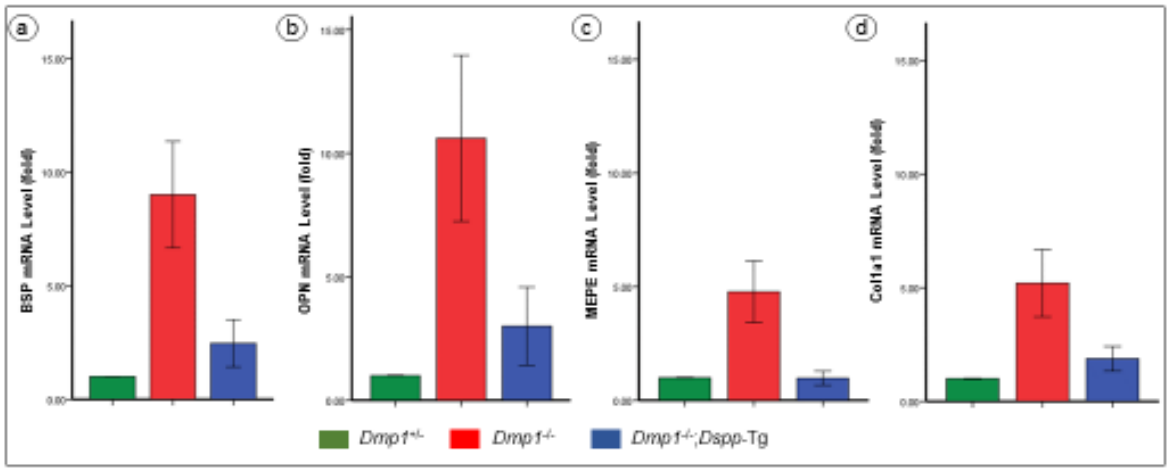

Figure 4-9 Real Time Quantitative PCR (RT-qPCR) analyses. RT-qPCR analyses of RNA samples from the femurs of 3-month-old mice showed that compared to the normal control, *Dmp1*$^{-/-}$ mice had an approximately 9 fold increase of BSP mRNA level (a); in *Dmp1*$^{-/-}$;*Dspp*-Tg mice, BSP mRNA level was about 2 fold of the normal. The changes of OPN mRNA levels (b) showed a similar pattern. The mRNA level of MEPE (c) in *Dmp1*$^{-/-}$ mice was 5 fold over normal, while it was restored completely back to normal in *Dmp1*$^{-/-}$;*Dspp*-Tg mice. Col1a1 mRNA levels (d) were restored close to normal in *Dmp1*$^{-/-}$;*Dspp*-Tg mice.

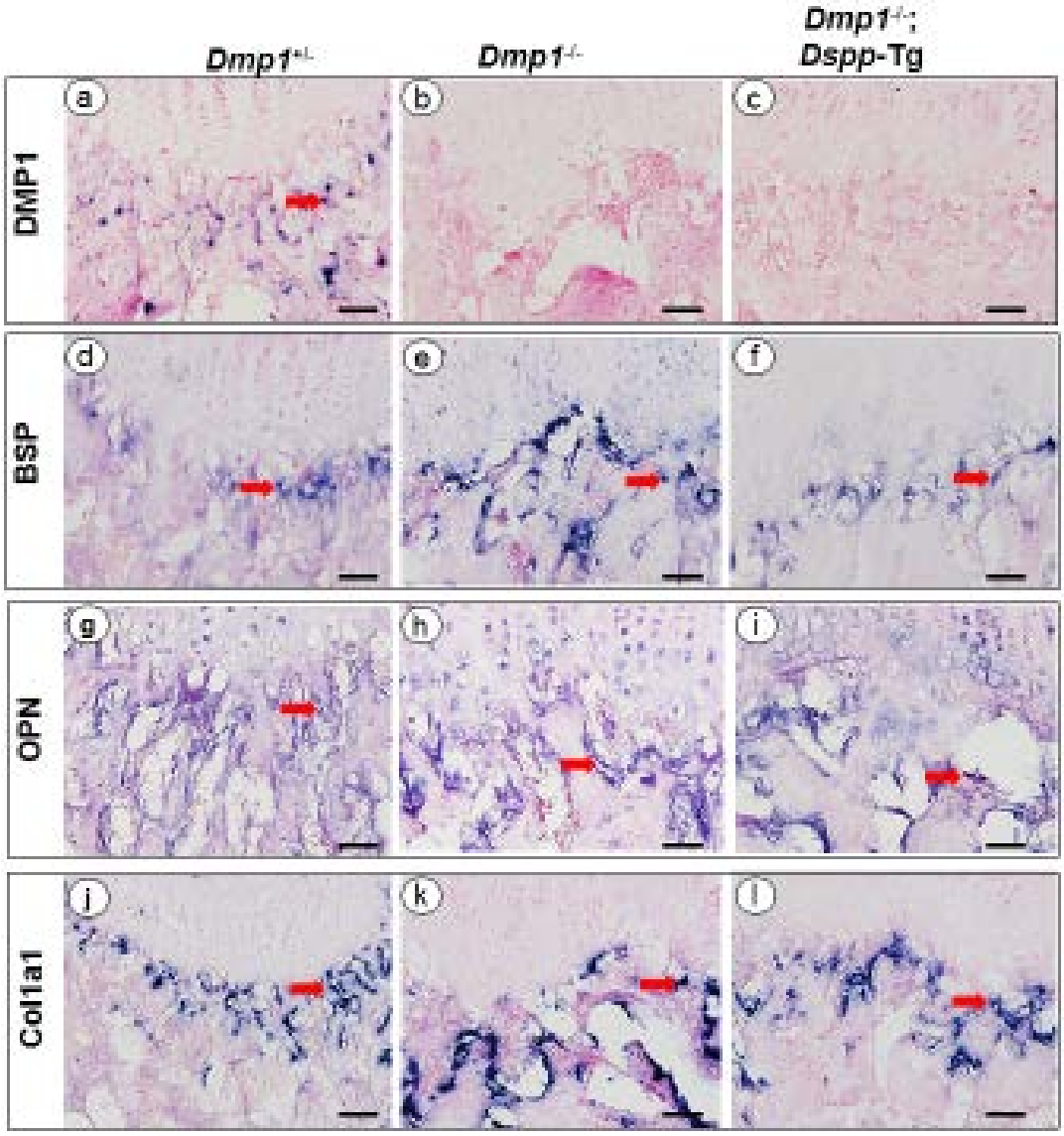

Figure 4-10 In Situ hybridization analyses. *In situ* hybridization showed the presence of DMP1 mRNA in the osteoblasts (arrows) of newly formed trabecular bone immediately subjacent to the growth plate in the normal control mice (a). The *Dmp1*$^{-/-}$ mice (b) and *Dmp1*$^{-/-}$;*Dspp*-Tg mice (c) had a complete lack of signals for DMP1. The same region of *Dmp1*$^{-/-}$ mouse femurs (e, h) had elevated levels of BSP and OPN mRNA, compared to the normal control (d, g). The BSP and OPN mRNA levels in *Dmp1*$^{-/-}$;*Dspp*-Tg mice (f, i) were similar to the normal controls. Col1a1 mRNA level was higher in *Dmp1*$^{-/-}$ mice (k), which was also reduced in *Dmp1*$^{-/-}$;*Dspp*-Tg mice (l), to a level similar to the *Dmp1*$^{+/-}$ mice (j). Scale bar: 50 μm in all images.

APPENDIX B

TABLES

Table 1. Bone parameters at 3 months

	Dmp1+/-	*Dmp1*-/-	*Dmp1*-/-;Dspp-Tg
BV/TV	.94250	.72962	.81946
Std. Deviation	.0161	.073	.026
Material Density (mgHA/cm^3)	1092.82	957.53	1006.40
Std. Deviation	40.75	26.37	18.55
Apparent Density (mgHA/cm^3)	1029.71	712.41	806.81
Std. Deviation	43.38	39.64	36.87
Trabecular Number	5.334	2.234	2.487
Std. Deviation	.5880	.2546	.3951
Trabecular Thickness (mm)	.040	.056	.043
Std. Deviation	.0065	.0047	.0017
Trabecular spacing (mm)	.1934	.4815	.3980
Std. Deviation	.019	.031	.036

Table 2. Bone parameters at 6 months

	Dmp1+/-	*Dmp1*-/-	*Dmp1*-/-;Dspp-Tg
BV/TV	.9405	.7254	.8630
Std. Deviation	.0158	.0453	.0494
Material Density (mgHA/cm^3)	1127.46	1009.05	1047.41
Std. Deviation	34.39	45.38	32.27
Apparent Density (mgHA/cm^3)	1059.88	783.71	908.83
Std. Deviation	25.88	79.18	47.11
Trabecular Number	4.421	2.070	2.554
Std. Deviation	.5794	.5167	.4778
Trabecular Thickness (mm)	.041	.051	.042
Std. Deviation	.0057	.0089	.0082
Trabecular spacing (mm)	.2833	.5310	.4442
Std. Deviation	.025	.146	.0495

Table 3. Primer sequences used for Real Time quantitative PCR

Gene	Primer sequences	Product size	T_m (°C)
Dspp	Forward: 5′-AACTCTGTGGCTGTGCCTCT-3′	171	59
	Reverse: 5′-TATTGACTCGGAGCCATTCC-3′		
Bsp	Forward: 5′-AAAGTGAAGGAAAGCGACGA-3′	215	52
	Reverse: 5′-GTTCCTTCTGCACCTGCTTC-3′		
Opn	Forward: 5′-TCTGATGAGACCGTCACTGC-3′	170	53
	Reverse: 5′-AGGTCCTCATCTGTGGCATC-3′		
Mepe	Forward: 5′-CTGTGGATCCTTGTGAGAAT-3′	199	55
	Reverse: 5′-TAGAGGATTTTGGCTTTCTG-3′		
Col1α1	Forward: 5′-CCTGACGCATGGCCAAGAAGA-3′	145	60
	Reverse: 5′-GCATTGCACGTCATCGCACA-3′		
Gapdh	Forward: 5′-CAAAGTTGTCATGGATGACC-3′	195	56
	Reverse: 5′-CCATGGAGAAGGCTGGGG-3′		

(Note: T_m – Melting Temperature)